

**TR 693- Development of Quality Standards for Inclusion of High Recycled
Asphalt Pavement Content in Asphalt Mixtures – Phase III**

FINAL REPORT

Hosin “David” Lee, Ph.D., P.E., Professor, Principal Investigator
Center for Computer-Aided Design
University of Iowa, Iowa City, IA 52242
E-mail: hlee@engineering.uiowa.edu

Ali Mokhtari, Graduate Research Assistant
Center for Computer-Aided Design
University of Iowa, Iowa City, IA 52242
E-mail: ali-mokhtari@uiowa.edu

Chris Williams, Ph.D., Professor, Co-Principal Investigator
Institute for Transportation
Iowa State University, Ames, IA 50010
E-mail: rwilliam@iastate.edu



June 2018

Disclaimer

The contents of this report reflect the views of the authors, who are responsible for the facts and the accuracy of the information presented herein. The opinions, findings, and conclusions expressed in this publication are those of the authors and not necessarily those of the sponsors.

The sponsors assume no liability for the contents or use of the information contained in this document. This report does not constitute a standard, specification, or regulation. The sponsors do not endorse products or manufacturers. Trademarks or manufacturers' names appear in this report only because they are considered essential to the objectives of the document.

Statement of Non-Discrimination

Federal and state laws prohibit employment and/or public accommodation discrimination on the basis of age, color, creed, disability, gender identity, national origin, pregnancy, race, religion, sex, sexual orientation or veteran's status. If you believe you have been discriminated against, please contact the Iowa Civil Rights Commission at 800-457-4416 or Iowa Department of Transportation's affirmative action officer. If you need accommodations because of a disability to access the Iowa Department of Transportation's services, contact the agency's affirmative action officer at 800-262-0003.

1. REPORT NO.		2. GOVERNMENT ACCESSION NO.		3. RECIPIENT'S CATALOG NO.	
4. TITLE AND SUBTITLE DEVELOPMENT OF QUALITY STANDARDS FOR INCLUSION OF HIGH RECYCLED ASPHALT PAVEMENT CONTENT IN ASPHALT MIXTURES – PHASE III				5. REPORT DATE May 2018	
				6. PERFORMING ORGANIZATION CODE	
7. AUTHOR(S) Hosin "David" Lee, Ali Mokhtari, Chris Williams				8. PERFORMING ORGANIZATION REPORT NO.	
9. PERFORMING ORGANIZATION NAME AND ADDRESS Center for Computer-Aided Design, 4601 SC University of Iowa Iowa City, IA 52242				10. WORK UNIT NO.	
				11. CONTRACT OR GRANT NO.	
12. SPONSORING AGENCY NAME AND ADDRESS Iowa Highway Research Board Iowa Department of Transportation 800 Lincoln Way, Ames, IA 50010				13. TYPE OF REPORT AND PERIOD COVERED Final Report	
				14. SPONSORING AGENCY CODE	
15. SUPPLEMENTARY NOTES					
16. ABSTRACT Federal, state and local public agencies encourage the use of recycled asphalt pavement (RAP) in constructing pavements to the maximum extent possible with an equal performance. According to the recent NAPA's report, average percent used in asphalt pavement was 21% based on total reported tons of RAP divided by reported total tons asphalt mixtures produced. 24% of RAP mixtures were estimated to be produced using softer binders whereas 7% of RAP mixtures produced using a rejuvenator. The main purpose of this research is to develop a scientific method to effectively identify the most appropriate rejuvenators for Iowa's high RAP mixtures. The specific objectives of this study are to provide the Iowa DOT with: 1) a screening method for approving rejuvenators in asphalt mixtures and 2) a method of field evaluation for HMA containing rejuvenators. The effects of different rejuvenators were evaluated through applying each product to aged asphalt binder and high-RAP mixtures. Fourier Transform Infrared (FTIR) test indicated all rejuvenators were effective in decreasing the aging level of hardened asphalt binder. Cryo-SEM technology was then utilized to measure cracking developed on the surfaces of both aged and rejuvenated asphalt binders when the temperature was lowered to -165 °C. Significantly less cracking was observed from the surface of rejuvenated asphalt compared to that of aged asphalt, which indicates an improved resistance to low-temperature cracking. All rejuvenators lowered both PG high-temperature and low-temperature limits of aged asphalt binder. The optimum dosage rate of each rejuvenator was identified using the Bending Beam Rheometer (BBR) test. G-R parameter was then calculated to determine the level of aging. All rejuvenators lowered the aging level to different extents but could not bring its properties to those of the original virgin binder. To evaluate the low-temperature cracking potential, Disk-Shaped Compact Tension (DCT) test was performed on the laboratory high-RAP mixtures with 27.6% and 70% of RAP materials (by binder replacement). In addition, cores and lab-compacted specimens from field loose mixtures were also tested using both DCT and Hamburg Wheel Tracking (HWT) devices. Based on the DCT test result, it was concluded that high-RAP mixtures with rejuvenators were more resistant to a low-temperature cracking than the high-RAP mixtures without it. However, based on HWT test results, a rejuvenator did not improve the moisture susceptibility and rutting potential. Overall, it can also be concluded that Rejuvenators "A" and "B" performed better than Rejuvenator "C" at their optimum dosage rates. Test sections using Rejuvenators "B" and "D" were successfully constructed in Crawford and O'Brien Counties in Iowa.					
17. KEY WORDS recycled asphalt pavement, high RAP content, rejuvenators, asphalt aging, Fourier transform infrared, cryo-SEM				18. DISTRIBUTION STATEMENT No restrictions.	
19. SECURITY CLASSIF. (of this report) None		20. SECURITY CLASSIF. (of this page) None		21. NO. OF PAGES 71	22. PRICE N/A

TECHNICAL ADVISORY COMMITTEE

Scott Schram, Iowa DOT, Scott.Schram@dot.iowa.gov

Jeffrey Schmitt, Iowa DOT, Jeffrey.schmitt@dot.iowa.gov

William Dotzler, Iowa DOT, william.dotzler@dot.iowa.gov

Bill Rosener, APAI, billr@apai.net

Larry Mattusch, APAI, lmatt2@mchsi.com

Andrew Cascione, Flint Hills Resources, andrew.cascione@fhr.com

John Hinrichsen, Hinrichsen.john@yahoo.com

Chuck Finnegan, L.L. Pelling, chuckf@llpelling.com

Erv Dukatz, Mathy Construction, edukatz@mathy.com

Ted Huisman, InTrans, thuis@iastate.edu

TABLE OF CONTENTS

ABSTRACT.....	1
1. INTRODUCTION.....	2
2. LITERATURE REVIEW	3
2.1 Asphalt Mixture Aging.....	4
2.2 Rejuvenators	6
3. ANALYTICAL EVALUATION OF REJUVENATOR’S DIFFUSION IN HARDENED ASPHALT..	10
3.1 Fourier Transform Infrared (FTIR) Spectroscopy.....	10
3.2 Cryo-Scanning Electron Microscopy	19
4. RHEOLOGICAL EVALUATION OF HARDENED ASPHALT WITH VARIOUS REJUVENATORS	32
4.1 Dynamic Shear Rheometer (DSR) Results.....	32
4.2 Block Cracking Test Results	33
4.3 Statistical Relationship between G-R Values and Carbonyl Index	35
4.4 Bending Beam Rheometer (BBR) Results	37
5. EVALUATION OF HIGH-RAP MIXTURES WITH VARIOUS REJUVENATORS.....	39
5.1 Mix Design	39
5.2 Disk-shaped Compact Tension (DCT) Test	40
6. CONSTRUCTION OF TEST SECTION AND TESTING OF FIELD SAMPLES	44
6.1 Test Section in Crawford County	44
6.1.1 HWT Test Results of Lab-compacted Field Mixtures.....	47
6.1.2 DCT Test Results of Cores and Lab-compacted Field Samples.....	48
6.1.3 Beam Fatigue Test for Crawford Mixtures.....	49
6.2 Test Section in O’Brien County	49
6.2.1 HWT Test Results of Lab-compacted Field Mixtures.....	54
6.2.2 DCT Test Results of Cores	56
6.2.3 DCT Test Results of Lab-compacted Field Samples.....	58
7. SUMMARY AND CONCLUSION	61
8. REFERENCES.....	63
APPENDIX A: DCT RESULTS FOR LAB-PRODUCED SAMPLES.....	66

LIST OF TABLES

Table 2-1 Physical Properties of Six Types of Rejuvenator (ASTM 4552)	3
Table 2-2 Rejuvenator Types (NCAT 2014)	4
Table 2-3 Dosage of rejuvenators in different mixtures (Mogawer et al. 2013)	4
Table 3-1 Rejuvenators with their original sources	11
Table 3-2 Sulfoxide and Carbonyl index values for each binder type.....	16
Table 4-1 DSR results for virgin, aged and rejuvenated binders.....	32
Table 4-2 Average m-values for virgin, aged and rejuvenated binders.....	37
Table 4-3 Average stiffnesses for virgin, aged and rejuvenated binders.....	37
Table 4-4 Optimum Dosages for virgin, aged and rejuvenated binders	38
Table 5-1 Volumetric Mix Design Results	40
Table 6-1 Crawford County Highway M-64 Project Mixture Gradation	44
Table 6-2 Crawford County Highway M-64 Project Mix Design Data.....	46
Table 6-3 Target vs. Actual Design Parameters of Crawford County Project.....	47
Table 6-4 Minimum Stripping Inflection Point (Iowa DOT)	48
Table 6-5 Beam Fatigue Results for Crawford County Project.....	49
Table 6-6 Aggregate Gradation for rejuvenator “D” Control Mixtures	50
Table 6-7 Target vs. Actual Design Parameters for Control Mixtures	51
Table 6-8 Aggregate Gradation for rejuvenator “D” Mixtures.....	51
Table 6-9 Target vs. Actual Design Parameters for rejuvenator “D” Mixtures.....	52
Table 6-10 Aggregate Gradation for Rejuvenator “B” Control Mixtures	52
Table 6-11 Target vs. Actual Design Parameters for Control Mixtures (November 17 th , 2017)	53
Table 6-12 Aggregate Gradation for Rejuvenator “B” Mixtures.....	53
Table 6-13 Target vs. Actual Design Parameters for Rejuvenator “B” Mixtures	54
Table 6-14 Density Results for Rejuvenator “D” and “B” field mixtures.....	54

LIST OF FIGURES

Figure 2-1 Effect of aging on binder film: (a) Compacted and (b) Loose mix (Reed, 2010).....	6
Figure 2-2 Mechanism of rejuvenator (Zaumanis et al. 2014)	7
Figure 2-3 Effect of rejuvenator contents on RAP binder (Tran et al. 2012)	7
Figure 2-4 Optimum rejuvenator dosage for different rejuvenators	8
Figure 2-5 Penetration of aged binder with different rejuvenators (Zaumanis et al. 2014).....	8
Figure 2-6 Topographic images of virgin and aged samples (Yu et al. 2014).....	9
Figure 3-1 Rejuvenators used for the study	11
Figure 3-2 FTIR test equipment used for this study	11
Figure 3-3 FTIR test results for aged and rejuvenated samples (i.e., C15: 15% Rejuvenator “C”; B10: 10% Rejuvenator “B”)	13
Figure 3-4 (a): Sulfoxide index; (b): Carbonyl index (i.e., C15: 15% Rejuvenator “C”; B10: 10% Rejuvenator “B”)	14
Figure 3-5 FTIR test results of aged and rejuvenated samples with rejuvenators (i.e., C8: 8% Rejuvenator “C”; B5: 5% Rejuvenator “B”; A7.5: 7.5% Rejuvenator “A”).....	15
Figure 3-6 FTIR spectrum area measurement	15
Figure 3-7 FTIR test results of the aged and rejuvenated samples for one dosage rate of rejuvenators (C16: 16% Rejuvenator “C”; B10: 10% Rejuvenator “B”; A15: 15% Rejuvenator “A”).....	17
Figure 3-8 Oxidation levels of eight different binder types.....	18
Figure 3-9 FTIR results of three rejuvenators.....	18
Figure 3-10 Tools used for the Cryo-SEM test.....	19
Figure 3-11 Cryo SEM images of (a): Aged and (b) 30% Rejuvenator “C”-restored asphalt.....	20
Figure 3-12 Cryo-SEM images of five asphalt samples	22
Figure 3-13 Comparison between Canny and Log methods to detect edges	23
Figure 3-14 Crack detection for aged and rejuvenated asphalt.....	25
Figure 3-15 Comparative plot of Fracture Indices for various asphalt types (i.e., C-15%: 15%Rejuvenator “C”; B-10%: 10% Rejuvenator “B”)	26
Figure 3-16 Cryo-SEM and binary crack-detected images for additional samples	30
Figure 3-17 Fracture index chart for all samples from the second-round tests	30
Figure 3-18 Fracture index chart for all samples from both first and second-round tests	31
Figure 4-1 G-R Parameter for virgin, aged and rejuvenated binder with Rejuvenator “C”	34
Figure 4-2 G-R Parameter for virgin, aged and rejuvenated binder with Rejuvenator “B”	34
Figure 4-3 G-R Parameter for virgin, aged and rejuvenated binder with Rejuvenator “A”	34
Figure 4-4 Comparative chart of G-R parameter for virgin, aged and all rejuvenated binders	35
Figure 4-5 Relationship between G-R values and Carbonyl indexes	36
Figure 4-6 Relationship between G-R values and Sulfoxide indexes.....	36
Figure 4-7 The optimum dosage of 6.9% was selected for the rejuvenator “B”.	37
Figure 4-7 Determining optimum dosage of rejuvenator "B"	38
Figure 5-1 Gradation for 27.6% RAP-included mixture	39
Figure 5-2 Gradation for 70% RAP-included mixture	40
Figure 5-3 RAP materials gradation	41
Figure 5-4 DCT test results.....	42
Figure 5-5 DCT results for 27.6% RAP lab-compacted mixtures	42

Figure 5-6 DCT results for 70% RAP lab-compacted mixtures	43
Figure 6-1 Layout of test section in Crawford County	45
Figure 6-2 Rejuvenator “D” test section in Crawford County.....	46
Figure 6-3 HWT Results for Crawford Control vs. Rejuvenator “D” Mixture	47
Figure 6-4 DCT Results for Crawford County	48
Figure 6-5 Test section in O’Brien County.....	50
Figure 6-6 HWT Results for O’Brien Rejuvenator “B” Control Mixture	55
Figure 6-7 HWT Results for O’Brien Rejuvenator “B” Mixture	55
Figure 6-8 Stripping observed after HWT test	56
Figure 6-9 DCT Results for Rejuvenator “D” Mixtures.....	57
Figure 6-10 DCT Results for Rejuvenator “B” Mixtures	57
Figure 6-11 Difference in lab samples and field cores thicknesses	58
Figure 6-12 DCT Results for Rejuvenator “B” Lab-compacted Field Samples	59
Figure 6-13 Energy Values for All Cores and Lab-compacted Samples.....	60
Figure A-1: DCT Results for 27.6% RAP Mixtures.....	66
Figure A-2: DCT Results for 70% RAP Mixtures.....	66

ABSTRACT

Federal, state and local public agencies encourage the use of recycled asphalt pavement (RAP) in constructing pavements to the maximum extent possible with an equal performance. According to the recent NAPA's report, average percent used in asphalt pavement was 21% based on total reported tons of RAP divided by reported total tons asphalt mixtures produced. 24% of RAP mixtures were estimated to be produced using softer binders whereas 7% of RAP mixtures produced using a rejuvenator.

The main purpose of this research is to develop a scientific method to effectively identify the most appropriate rejuvenators for Iowa's high RAP mixtures. The specific objectives of this study are to provide the Iowa DOT with: 1) a screening method for approving rejuvenators in asphalt mixtures and 2) a method of field evaluation for HMA containing rejuvenators. The effects of different rejuvenators were evaluated through applying each product to aged asphalt binder and high-RAP mixtures. Fourier Transform Infrared (FTIR) test indicated all rejuvenators were effective in decreasing the aging level of hardened asphalt binder. Cryo-SEM technology was then utilized to measure cracking developed on the surfaces of both aged and rejuvenated asphalt binders when the temperature was lowered to -165 °C. Significantly less cracking was observed from the surface of rejuvenated asphalt compared to that of aged asphalt, which indicates an improved resistance to low-temperature cracking. All rejuvenators lowered both PG high-temperature and low-temperature limits of aged asphalt binder. The optimum dosage rate of each rejuvenator was identified using the Bending Beam Rheometer (BBR) test. G-R parameter was then calculated to determine the level of aging. All rejuvenators lowered the aging level to different extents but could not bring its properties to those of the original virgin binder.

To evaluate the low-temperature cracking potential, Disk-Shaped Compact Tension (DCT) test was performed on the laboratory high-RAP mixtures with 27.6% and 70% of RAP materials (by binder replacement). In addition, cores and lab-compacted specimens from field loose mixtures were also tested using both DCT and Hamburg Wheel Tracking (HWT). Based on the DCT test result, it was concluded that high-RAP mixtures with rejuvenators were more resistant to a low-temperature cracking than the high-RAP mixtures without it. However, based on HWT test results, a rejuvenator did not improve the moisture susceptibility and rutting potential. Overall, it can also be concluded that Rejuvenators "A" and "B" performed better than Rejuvenator "C" at their optimum dosage rates. Test sections using Rejuvenators "B" and "D" were successfully constructed in Crawford and O'Brien Counties in Iowa.

1 INTRODUCTION

The use of high RAP mixes is increasing due to both economic and environmental reasons. However, a high RAP mix can cause asphalt mixtures to stiffen due to the hardening effect of the aged binder in RAP materials. During the aging process of asphalt, the amount of asphaltene increases as the maltene changes to the asphaltene. Thus, there will be less maltene to disperse the asphaltene in the aged binder structure. As a result, the aged binder becomes more brittle and less ductile, which could negatively affect the performance of the high RAP mixes in the field.

Low temperature cracking potential is a primary concern with high RAP mixtures, which is caused by the aging of asphalt through the oxidation. To minimize a low temperature cracking, various rejuvenators have been utilized in the past instead of bumping down a PG grade of the specified virgin asphalt for high RAP mixes. However, in some cases, the premature failures such as rutting have been observed from the high RAP mixtures with rejuvenators.

The term “rejuvenation” can be defined as a restoration of the original condition. Aging process of asphalt is a combination of reversible and permanent changes. Reversible changes are referred to as molecular association like wax crystallization whereas permanent changes occur as a result of physical changes like loss of lighter molecules or chemical changes like oxidation. Oxidation is a chemical reaction between asphalt and oxygen such that carbon and sulfur atoms increase within asphalt molecules. Oxidation is considered as a dominant cause when it comes to long-term asphalt aging phenomenon.

The main purpose of this research is to develop a scientific method to effectively identify the most appropriate rejuvenators for Iowa’s high RAP mixtures. The specific objectives of this study are to provide the Iowa DOT with: 1) a screening method for approving rejuvenator products in asphalt mixtures on a project basis and 2) a method of field evaluation for HMA containing rejuvenators. To achieve these objectives, the following tasks have been performed: 1) evaluate the effectiveness of various rejuvenators to soften aged binders by employing analytical technologies to examine different rejuvenators in the laboratory-aged asphalt, 2) perform rheological binder tests to determine the effects of rejuvenators on aged binder properties, 3) perform mechanistic mixture tests to assess the effect of rejuvenators on high RAP mixtures, 4) build test sections with selected rejuvenators and 5) perform laboratory tests of field loose mixtures and cores. The outcome of this research is to help pavement engineers specify the most appropriate rejuvenator for the given condition by understanding complex chemical and physical interactions between aged binder and rejuvenators.

2 LITERATURE REVIEW

ASTM classifies rejuvenators into six groups as shown in Table 2-1. It should be noted that the main criterion for classifying rejuvenators is viscosity at 60 °C. To determine the percentage of a rejuvenator required to meet the target viscosity or PG temperature, the ASTM D4887 specification recommends the use of a viscosity blending chart or a PG temperature blending chart, respectively (ASTM 4887). For example, the City of Columbus, Ohio, provides a specification for a rejuvenator as a petroleum resin base oil emulsified with water and its chemical compositions should be obtained by SARA analysis (ASTM Method D-2006-70) as percentages of Polar Compounds (PC); First Acidaffins (A1); Second Acidaffins (A2); and Saturated Hydrocarbons (S). The specification requires the Maltene distribution ratio of (PC + A1)/ (S + A2) to fall between 0.3 and 0.6. In addition, the PC/S ratio should be at least 0.5 and saturated hydrocarbons (S) should be between 21 and 28 percent (City of Columbus 2006).

Table 2-1 summarizes five categories of rejuvenators along with typical examples and descriptions (NCAT, 2014). Mogawer et al. (2013) reported that the manufacturer of each rejuvenator recommended that, for the 40% RAP mixtures, the dosage of the rejuvenator should be 0.5% by weight of the total RAP or 9.28% of replaced binder. Amounts of rejuvenators are summarized in Table 2-3 by percentages of replaced binder, recycled material and total mix for each mixture type (Mogawer et al., 2013).

Table 2-1 Physical Properties of Six Types of Rejuvenator (ASTM 4552)

Test	ASTM Test Method	RA 1		RA 5		RA 25		RA 75		RA 250		RA 500	
		Min	Max	Min	Max	Min	Max	Min	Max	Min	Max	Min	Max
Viscosity • 60 °C [140 °F], mm ² /s	D2170 or D2171	50	175	176	900	901	4500	4501	12500	12501	37500	37501	60000
Flash Point, COC, °C [°F]	D92	219 [425]	...	219 [425]	...	219 [425]	...	219 [425]	...	219 [425]	...	219 [425]	...
Saturates, wt, %	D2007	...	30	...	30	...	30	...	30	...	30	...	30
Tests on Residue from RTFO or TFO oven 163 °C [325 °F]	D2872 or D1754												
Viscosity Ratio ^A	"	...	3	...	3	...	3	...	3	...	3	...	3
Wt Change, ±, %	"	...	4	...	4	...	3	...	3	...	3	...	3
Specific Gravity	D70 or D1298	Report		Report		Report		Report		Report		Report	

^AViscosity Ratio = $\frac{\text{Viscosity of Residue from RTFO or TFO Oven Test-60 °C [140 °F], cSt}}{\text{Original Viscosity-60 °C [140 °F], cSt}}$

Table 2-2 Rejuvenator Types (NCAT 2014)

Category	Examples	Description
Paraffinic Oils	Waste Engine Oil (WEO) Waste Engine Oil Bottoms (WEOB) Valero VP 165 [®] Storbit [®]	Refined used lubricating oils
Aromatic Extracts	Hydrolene [®] Reclamite [®] Cyclogen L [®] ValAro 130A [®]	Refined crude oil products with polar aromatic oil components
Naphthenic Oils	SonneWarmix RJ [™] Ergon HyPrene [®]	Engineered hydrocarbons for asphalt modification
Triglycerides & Fatty Acids	Waste Vegetable Oil Waste Vegetable Grease Brown Grease	Derived from vegetable oils, Has other key chemical elements in addition to triglycerides and fatty acids
Tall Oils	Sylvaroad [™] RP 1000 Hydrogreen [®]	Paper industry byproducts, Same chemical family as liquid antistrip agents and emulsifiers

Table 2-3 Dosage of rejuvenators in different mixtures (Mogawer et al. 2013)

Mixture	Total Binder (%)	Replaced Binder (%)	Rej by Replaced Binder (%)	Rej by Recycled Material (%)	Rej by Total Mix (%)
40% RAP*	6	2.16	9.28	0.50	0.200
5% RAS**	6	0.89	9.28	1.64	0.082
5%RAS+35% RAP	6	2.77	9.28	0.64	0.257
*RAP Binder Content: 5.39%					
**RAS Binder Content: 17.7%					

2.1 Asphalt Mixture Aging

Due to the complex field conditions, asphalt binder aging factors are usually evaluated in the controlled laboratory environment. To simulate the aging process of asphalt mixtures in the field, various laboratory aging equipment have been used such as ovens, rolling thin film oven (RTFO) and pressure aging vessel (PAV) on loose mixtures and compacted specimens (Zhu 2015). Loose asphalt mixtures can be aged before being compacted. The main advantages of this approach are: 1) uniform aging due to the heat and air circulating through the loose mixture and 2) the increased rate of aging due to a larger binder surface area being exposed to the heat and air. However, aged loose mixtures can be difficult to compact due to the higher stiffness. The aged loose mixtures were often used for extracting the aged binder from the mixtures.

Van den Bergh (2009) conducted loose mixture aging process to simulate the long-term mixture aging. The mixtures were first short-term aged at 130°C for three hours and then long-term aged at 90°C for an extended time. The extracted binders from aged loose mixture were compared against the binders from seven- to ten-year-old pavement field sections. Mollenhauer and Mouillet (2011) compared the test results of lab-aged binders against the 11- to 12-year-old field mixtures. The aged loose mixtures in the PAV oven for 20 hours exhibited a comparable aging level to those aged in the oven at 85 °C for nine days. Partl et al. (2013) proposed a short-term aging procedure of aging in the oven at 135 °C for four hours and a long-term aging procedure of aging in the oven at 85 °C for 1, 2, 5, 7 and 9 days.

Another approach in aging asphalt mixtures is to perform the aging process on the compacted mixtures, which can simulate an actual field aging process during the service life. The AASHTO R30 standard recommends a short-term aging in the oven at 135 °C for four hours followed by a long-term aging process at 85 °C ± 3 °C for 120 ± 0.5 hours, which would represent five to ten years of aging in the field. Some limitations on this AASHTO R30 aging method include:

- It specifies only one temperature for the aging process
- It can only simulate the aging in the field for up to 10 years
- It does not consider the effect of the amount of air voids in the mixtures.
- It does not consider different size and shapes of specimens

Van den Bergh (2011) recommended a long-term aging process in the oven at 110-120 °C for 16 hours and Nicholls (2006) recommended 48 hours aging in the oven at 60 °C. Hayicha et al. (2003) proposed a long-term aging in the oven at 60 °C for 20 days. During the SHRP-A-390 project, for a short-term aging, a duration of four hours in the oven at 135 °C on loose mixtures was proposed and, for a long-term aging, the compacted mixtures were proposed to be aged in the oven at 85 °C for 2, 4, 8 days which would represent four, eight and sixteen years of field aging, respectively.

Reed (2010) compared characteristics of lab-aged loose mixtures against the compacted mixtures. Both loose and compacted specimens were long-term aged in the oven at 85 °C for 5 and 14 days. They reported that more efforts were needed for compacting aged loose mixtures and it caused an excessive degradation in the aggregate structure and negatively affected the mixture properties. As illustrated in Figure 2-1, the aged loose mixtures exhibited less cohesion between aggregate particles because the binders were aged more than the compacted mixtures. Bell (1994) recommended that specimens should be compacted at the equi-viscous temperature based on the viscosity of the short-term aged mix.

As discussed earlier, different levels of aging can be obtained by varying the temperature of and the duration in oven. For this study, to simulate a short-term aging condition, the RTFO test following AASHTO T240-94 was performed on virgin asphalt. To simulate a long-term aging

condition, the short-term aged asphalt was then subjected to PAV test for 20 hours following AASHTO R 28. For mixture aging, 5 days aging in oven at temperature 85 °C is considered.

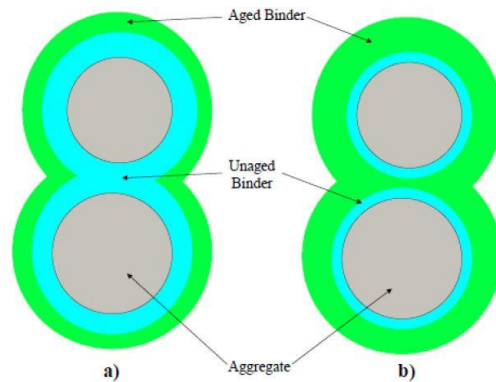


Figure 2-1 Effect of aging on binder film: (a) Compacted and (b) Loose mix (Reed, 2010)

2.2 Rejuvenators

The main function of a rejuvenator is to replenish the reduced amount of the maltene which occurred either by oxidation, evaporation, or absorption into aggregates. Rejuvenators can be made from lubricating oil extract or extender oil. However, certain types of saturates in rejuvenators may not be compatible with the asphaltene in the aged binder. Therefore, two fundamental characteristics of a rejuvenator considered for high RAP mixes are: 1) the diffusion of a rejuvenator into the aged binder and 2) the dispersion of a rejuvenator within a high RAP matrix (Corbett 1975, Petersen 1984).

A diffusion process of a rejuvenator into the aged binder would progress during mixing and construction process but it would stop after a certain period of time. The diffusion rate would be influenced by the viscosity of the maltene in the aged binder and it would increase by increasing the amount of diluent oil fractions. However, a considerable period of time is required for absorption of the fluxing oil by the asphalt in the pavement surface exposed to the traffic (Oliver 1974).

A mechanism of diffusion of modifiers into aged asphalt is defined as the following four-step process (Carpenter and Wolosick 1980):

1. A very low viscosity layer is formed surrounding the RAP by a rejuvenator.
2. The rejuvenator begins to penetrate into the aged binder and makes it softer.
3. Penetration continues as the inner layer viscosity decreases whereas the outer layer viscosity increases.
4. Balance in viscosity is reached after a certain amount of time.

The diffusion steps are illustrated in Figure 2-2 (Zaumanis et al. 2014). Feng et al. (2011) reported that the diffusion level of rejuvenators into the binder was improved by increasing temperature and time duration. The diffusion of the rejuvenators into the binder was quantified by

measuring the penetration and chemical components of rejuvenator-coated aged binder. García et al. (2010) presented the new idea of using encapsulated rejuvenators which will break and release rejuvenator when the stress applied on those capsules exceeds their strength.

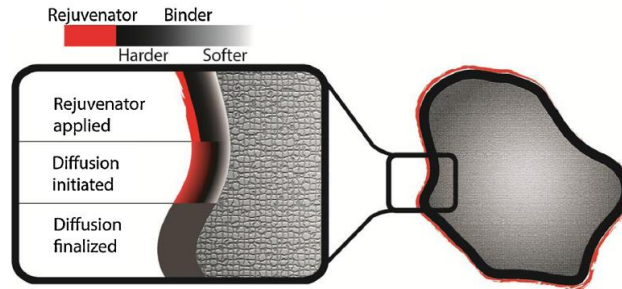
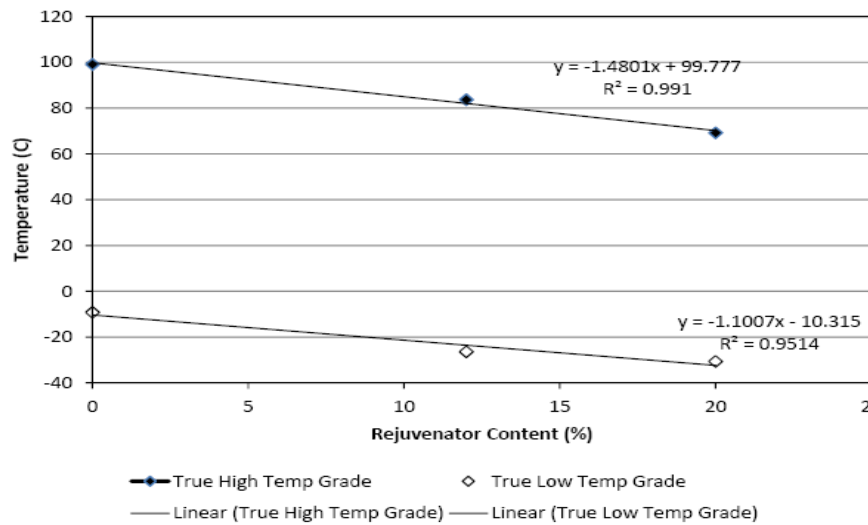


Figure 2-2 Mechanism of rejuvenator (Zaumanis et al. 2014)

As shown in Figure 2-3, Tran et al. (2012) identified the effect of rejuvenator on performance of the aged binder extracted from RAP materials and its optimum dosage needed to restore the original properties of the aged binder. Although the rejuvenators increased the low temperature cracking resistance, they decreased the rutting resistance (Shen et al. 2007). Im et al. (2014) reported that the rejuvenators increased a cracking resistance while decreasing the stiffness of asphalt mixtures. In addition, the rejuvenators decreased the moisture sensitivity and rutting depth of high RAP mixtures.



Property	Rejuvenator Content		
	0	12	20
High Temp DSR	99.1	83.6	69.2
Intermediate Temp DSR	33.1	22.1	18.0
Bending Beam Rheometer - S	-24.2	-30.7	-30.6
Bending Beam Rheometer - m	-9.2	-26.4	-31.2
True Grade	99.1 - 9.2	83.6 - 26.4	69.2 - 30.6
PG Grade	94 - 4	82 - 22	64 - 28

Figure 2-3 Effect of rejuvenator contents on RAP binder (Tran et al. 2012)

Zaumanis et al. (2014) evaluated six rejuvenators that include: 1) aromatic extract, 2) waste engine oil, 3) waste vegetable oil, 4) organic oil, 5) waste vegetable grease, and 6) distilled tall oil. As shown in Figure 2-4, optimum dosage rates were identified for meeting high, intermediate and low PG temperatures of the aged binder. As shown in Figure 2-5, all rejuvenators increased the penetration number of the aged binder with different amounts depending on the types and amounts of rejuvenators. They reported that the low and high PG temperatures were reduced linearly with an increased dosage rate while the penetration grew exponentially.

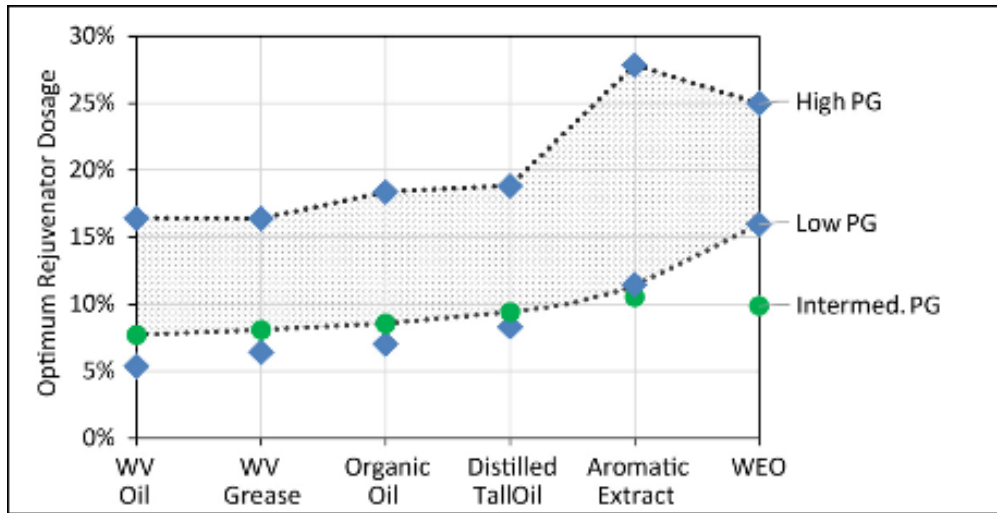


Figure 2-4 Optimum rejuvenator dosage for different rejuvenators

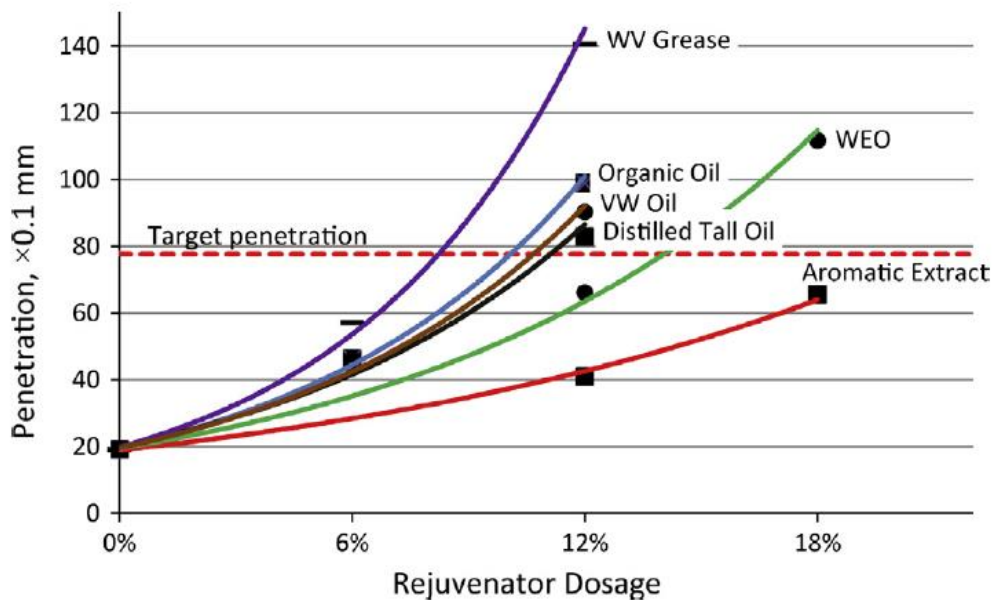


Figure 2-5 Penetration of aged binder with different rejuvenators (Zaumanis et al. 2014)

DeDene (2011) investigated the effect of waste engine oil on the properties of aged binder and confirmed the softening effect of engine oil. However, the engine oil decreased the compressive and tensile strength resulting in the increased rut depth. Hesp and Shurvell (2010) investigated the amount of waste engine oil residue in asphalt and reported that zinc and other heavy metals could be detected in asphalt using X-ray Fluorescence (XRF) technology. Studies from lab and field investigations indicated a high correlation between carbonyl content and level of aging (Ali et al. 2015; Baek et al. 2012).

In order to understand the interaction between aged asphalt and rejuvenators, nanoscopic surface properties and chemical composition of rejuvenated aged binders were assessed using atomic force microscopy (AFM) and SARA (Saturates, Aromatics, Resins, Asphaltenes) fractionation method, respectively (Yu et al. 2014). As shown in Figure 2-6, the two virgin binders displayed considerably different morphologies where virgin binder ABD exhibited a dispersed phase with flake-like structures spreading over a smooth matrix phase whereas the virgin binder AAD exhibited the elliptical domains containing “bee-structures”. Appropriate scales were chosen to better show these structures. It is interesting to note that, after aging, sizes of flake-like structures in ABD decreased whereas the sizes of bee-structures did not change. It was reported that the appearance of the “bee-structures” can be attributed to the interaction between crystallizing waxes and the remaining non-wax asphalt components.

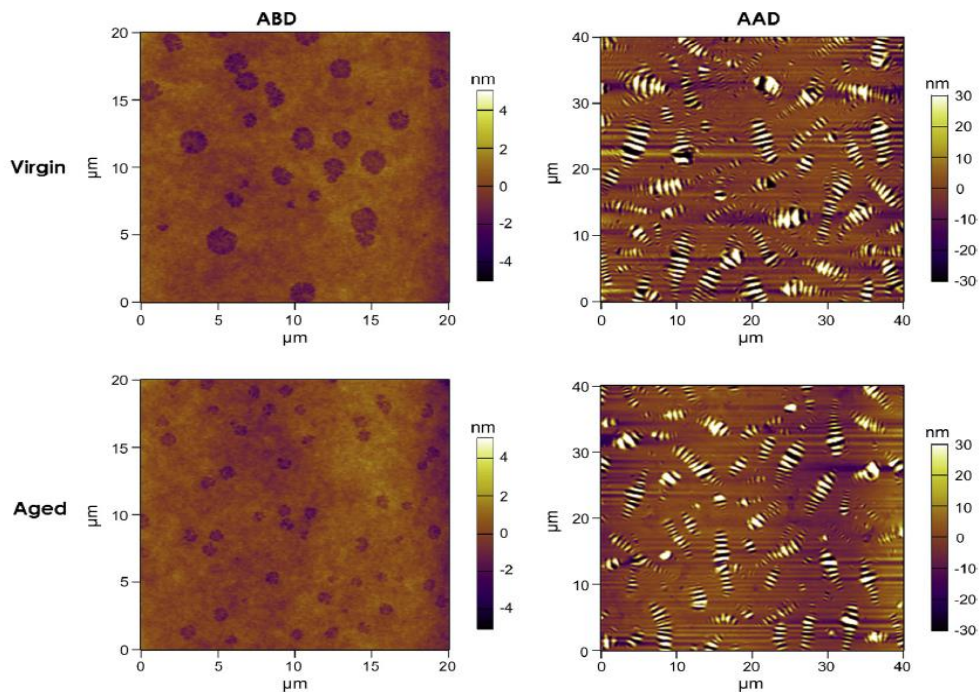


Figure 2-6 Topographic images of virgin and aged samples (Yu et al. 2014)

3 ANALYTICAL EVALUATION OF REJUVENATOR'S DIFFUSION IN HARDENED ASPHALT

Both the X-Ray Fluorescence (XRF) and the Atomic Force Microscopy (AFM) were originally considered for evaluating the chemical elements in asphalt binder. However, based on the limited successful results on the use of these technologies for determining the effects of rejuvenators on the aged binders, our research efforts were focused on the use of the Fourier Transform Infrared (FTIR) Spectroscopy. To quantify the physical properties of different asphalt binders, Cryogenic Scanning Electron Microscopy (Cryo-SEM) was also used. The Cryo module was used to decrease the sensitivity of asphalt samples to the electron beam, which can allow fracture surface of asphalt samples to be observed.

3.1 Fourier Transform Infrared (FTIR) Spectroscopy

Fourier-Transform Infrared (FTIR) Spectroscopy is commonly used to identify certain molecules or functional groups and the concentration of those molecules within a sample (Smith, 2011). The FTIR measures amounts of Infrared light that was absorbed by asphalt at each wavelength over a range of $4,000\text{ cm}^{-1}$ to 400 cm^{-1} . The asphalt would absorb different wavelengths and create a unique interferogram of reflected lights, which should be then processed using Fourier transform algorithm to derive the transmittance level for each wavelength (Sun *et al.*, 2014). FTIR spectrometers are less expensive than conventional spectrometers since producing an interferometer is easier than the fabrication of a monochromator. In addition, measurement of a single spectrum is much faster for the FTIR technique as the information at all frequencies can be collected simultaneously (Ramasamy, 2010).

To analyze the aging process of asphalt quantitatively, the peak area of oxygenated functional groups (S=O and C=O), which represents the degree of asphalt aging, can be examined (1032cm^{-1} for sulfoxide and 1699cm^{-1} for carbonyl) by measuring a coherence of electromagnetic radiation (Chen *et al.*, 2014). It can be postulated that rejuvenators would decrease these sulfoxide and carbonyl peaks (Chen *et al.*, 2014; Cong *et al.*, 2015). For this study, as shown in Figure 3-1, the following three rejuvenators were added into the aged asphalt: 1) Rejuvenator “C” which is petroleum oil with high viscosity at room temperature, 2) Rejuvenator “B” produced from refined tall oil, and 3) Rejuvenator “A” produced from vegetable oil. The source for each rejuvenator is summarized in Table 3-1.

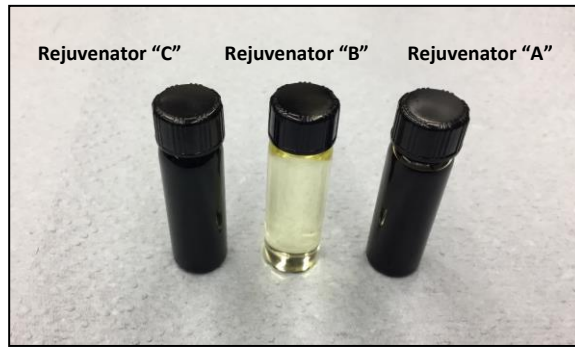


Figure 3-1 Rejuvenators used for the study

Table 3-1 Rejuvenators with their original sources

Rejuvenator	Source
Rejuvenator "C"	Extracted from petroleum oil
Rejuvenator "B"	Extracted from refined tall oil
Rejuvenator "A"	Extracted from vegetable oil

FTIR Test Procedure

To run the test using the FTIR equipment, as shown Figure 3-2, the following steps were taken:

1. Take specific amount of binder (the same for all samples) and dilute it using a solvent (Tetrahydrofuran, THF, was used for this study).
2. Shake very well to make the blend homogeneous (2-3 minutes is adequate).
3. Put salt windows (NaCl in this case) under the instrument and take the background spectrum.
4. Pour adequate amount of the diluted sample between two windows and place them under the instrument.
5. Examine the spectrum and save it.

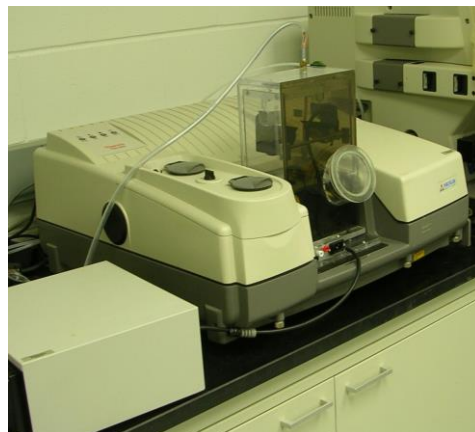


Figure 3-2 FTIR test equipment used for this study

FTIR Test Results

Two rounds of FTIR tests were performed. The first round of tests were conducted using 15% (recommended by the vendor) and 30% (double) of Rejuvenator “C” and 10% (recommended by the vendor) and 20% (double) of Rejuvenator “B”. The second round of tests were conducted using at reduced dosage rates of 8% (recommended by the vendor) and 16% (double) of Rejuvenator “C” and 5% (recommended by the vendor) and 10% (double) of Rejuvenator “B”. In addition, Rejuvenator “A” was evaluated with dosage rates of 7.5% and 15%.

First-Round Test

First, to simulate a short-term aging condition, the RTFO test (AASHTO T240-94) was performed on virgin PG 64-22 asphalt. The short-term aged asphalt was then subjected to PAV test (following AASHTO R 28) for 20 hours to simulate a long-term aging condition. The PAV-aged asphalt was then mixed with Rejuvenator “C” at two dosages rates of 15% and 30% and Rejuvenator “B” at two dosages rates of 10% and 20%. To ensure a consistent blending with the aged asphalt, the rejuvenated asphalt was agitated for 15 minutes and an oil bath was used to keep the binder temperature constant during throughout the blending process.

FTIR analysis was performed on the aged asphalt with and without the rejuvenators. Figure 3-3 shows FTIR spectra for the aged asphalt and the aged asphalt with rejuvenators. The sulfoxide (S=O) peak occurring at 1032 cm^{-1} corresponds to the oxidation of compounds containing sulfur and the carbonyl (C=O) peak at 1699 cm^{-1} corresponds to the oxidation of carbonyl compounds. The saturated C-H peak occurs at 1459 cm^{-1} . To determine the degree of oxidation, sulfoxide index (SI) and carbonyl index (CI) were calculated using Eq. 1 and Eq. 2, where a larger value indicates a higher degree of oxidation.

$$\text{Sulfoxide Index } I_{\text{s=O}} = \frac{\sum A(1032\text{cm}^{-1})}{\sum A(1459\text{cm}^{-1})} \quad (1)$$

$$\text{Carbonyl Index } I_{\text{C=O}} = \frac{\sum A(1699\text{cm}^{-1})}{\sum A(1459\text{cm}^{-1})} \quad (2)$$

where,

$\sum A(1032\text{cm}^{-1})$, $\sum A(1699\text{cm}^{-1})$ and $\sum A(1459\text{cm}^{-1})$ are absorption peak areas of sulfoxide, carbonyl and saturated C-H group, respectively.

Figure 3-4(a) shows SI values of aged asphalt and the aged asphalt rejuvenated with different amounts of Rejuvenator “C” and Rejuvenator “B”. The PAV-aged samples exhibited an increase in the SI value possibly due to a higher sulfur content in virgin asphalt. When the aged asphalt is rejuvenated, the SI value of rejuvenated asphalt is expected to decrease to the level similar to that of the unaged virgin asphalt. Figure 3-4(a) indicates that the rejuvenated asphalt samples exhibited lower SI values.

Figure 3-4(b) shows CI values of the aged asphalt and the aged asphalt rejuvenated with different amounts of Rejuvenator “C” and Rejuvenator “B”. During the aging process, the CI value is expected to increase due to the oxidation of carbon containing compounds to carbonyl containing compounds that would should the peak at 1699 cm^{-1} . While not as significant as for the case of sulfoxide formation, the mean CI value for the rejuvenated asphalt was lower than that of the aged asphalt. As shown in Figure 3-4, both rejuvenators reduced the oxidation of sulfur and carbon whereas Rejuvenator “C” reduced the oxidation of carbon more than Rejuvenator “B”.

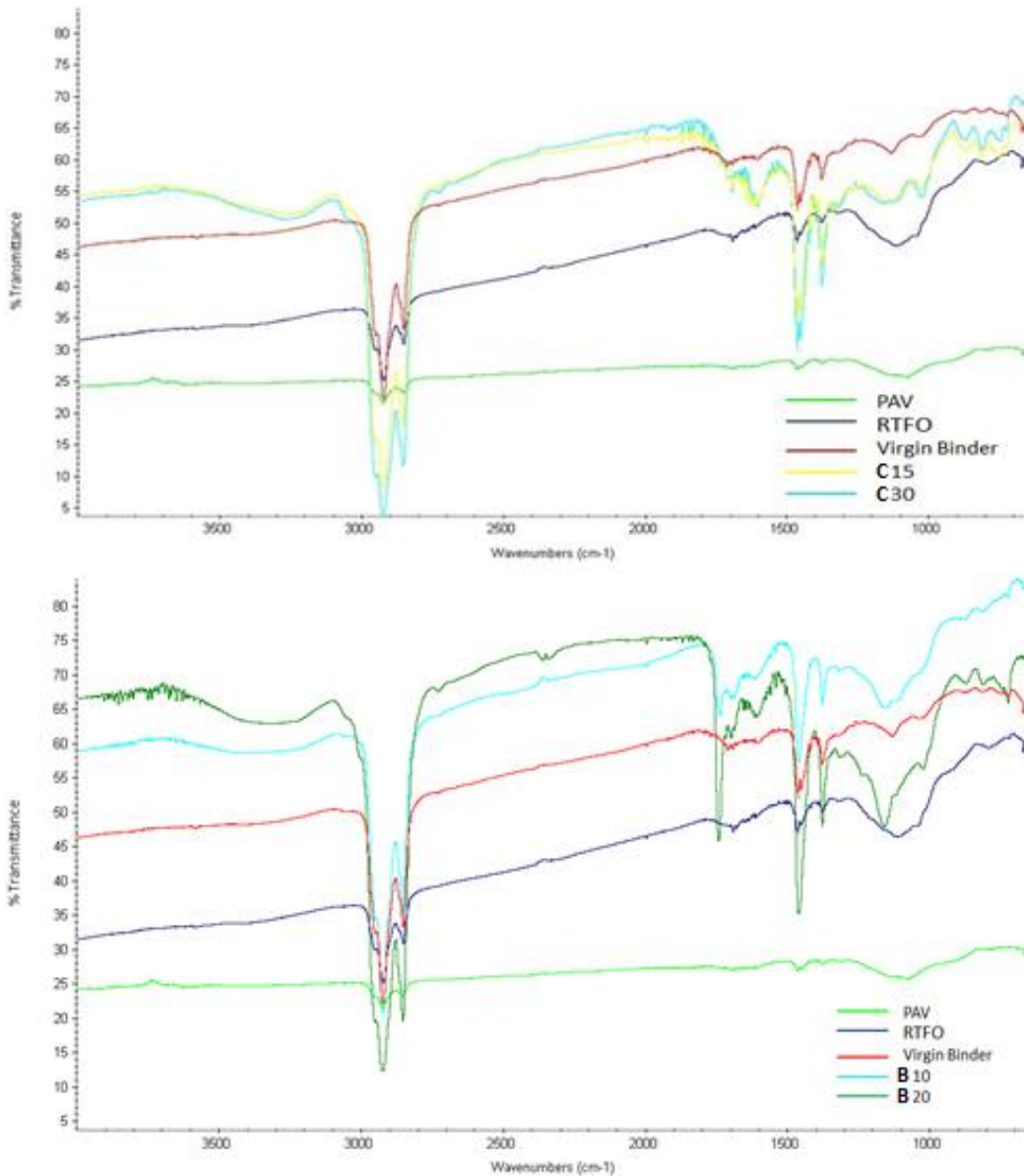


Figure 3-3 FTIR test results for aged and rejuvenated samples (i.e., C15: 15% Rejuvenator “C”; B10: 10% Rejuvenator “B”)

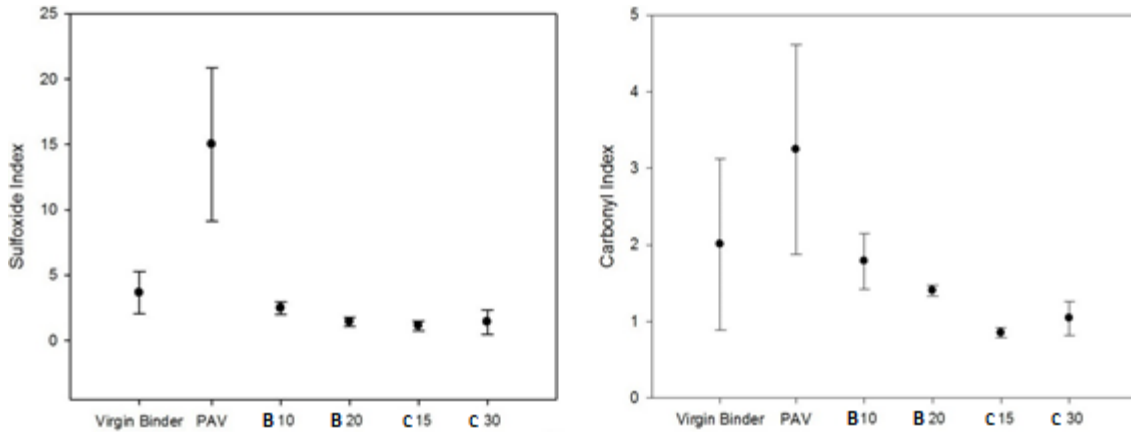


Figure 3-4 (a): Sulfoxide index; (b): Carbonyl index (i.e., C15: 15% Rejuvenator “C”; B10: 10% Rejuvenator “B”)

Second-Round Test

For the second-round test, following the recommendations from Tran et.al (2012) and Turner et.al (2015), the optimum dosages for Rejuvenator “C” and Rejuvenator “B” were lowered to 12% and 7% by weight of the aged asphalt binder, respectively. Thus, for the second-round tests, the dosage rates for these rejuvenators were decreased to 8% and 16% for Rejuvenator “C” (plus/minus 4% of the optimum rate of 12%) and 5% and 10% for Rejuvenator “B” (plus/minus 2-3% of 7%). In addition, a third Rejuvenator “A” was evaluated with two dosage rates of 7.5% and 15%.

To simulate the long-term aging of the binder, both RTFO and PAV (40-hr, double, at 100 °C under 2.1 MPa) aging procedures were adopted. In addition, the absorbance mode was selected for the second-round test so that a better visual observation can be made when considering different spectra peaks. To evaluate the repeatability of FTIR procedure, five identical

samples were tested for each binder type. FTIR spectra are shown in Figure 3-1. Figure 3-2 shows how the area under FTIR spectra are measured for each functional group can be measured by manually identifying a baseline. Table 3-2 summarizes six repeated measurements of areas under FTIR spectra of sulfoxide, carbonyl and C-H functional groups for each of eight asphalt binder types. These areas were used to compute the averages and standard deviations of sulfoxide indices and carbonyl indices of each binder type. As can be seen from Table 3-2, there exist significant differences between average values of sulfoxide and carbonyl indices among eight different asphalt binder types.

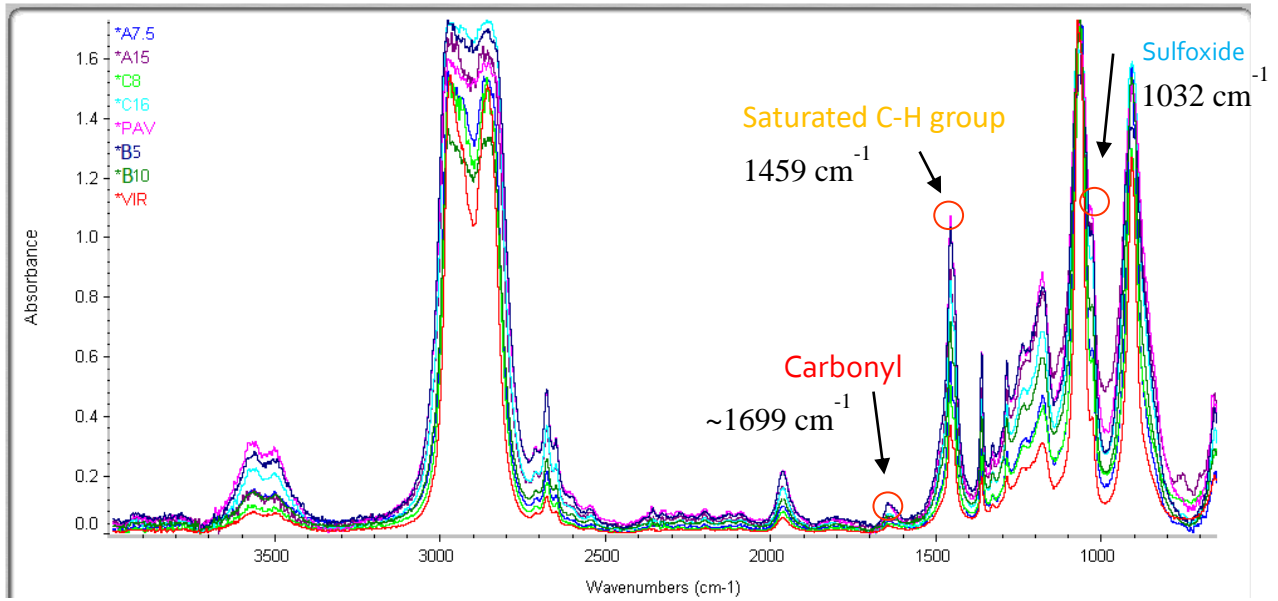


Figure 3-5 FTIR test results of aged and rejuvenated samples with rejuvenators (i.e., C8: 8% Rejuvenator “C”; B5: 5% Rejuvenator “B”; A7.5: 7.5% Rejuvenator “A”)

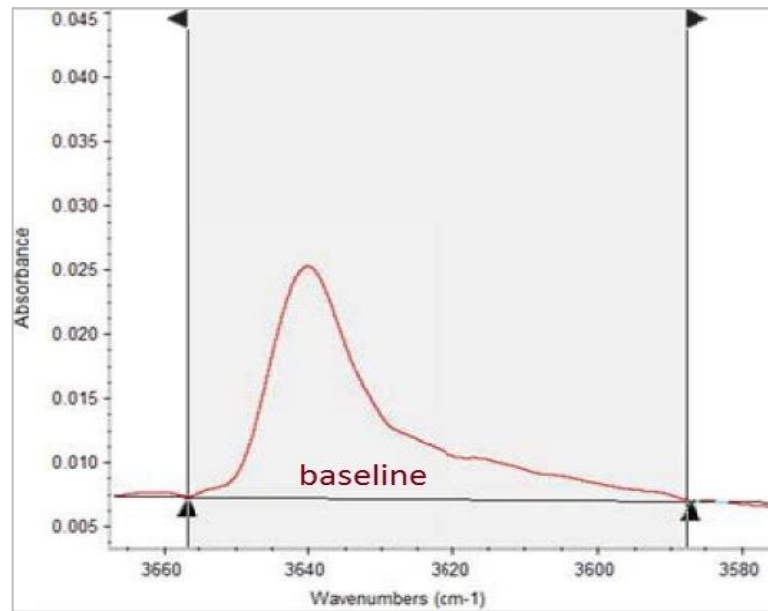


Figure 3-6 FTIR spectrum area measurement

Table 3-2 Sulfoxide and Carbonyl index values for each binder type

	C-H area	S=O area	C=O area	Sulfoxide Index	Carbonyl Index	avg. SI	avg. CI	stdev SI	stdev CI
Virgin Binder	12.25	0.821	0.668	6.70	5.45	7.03	5.40	0.612	0.425
	13.05	0.829	0.641	6.35	4.91				
	10.86	0.789	0.595	7.27	5.48				
	8.95	0.693	0.498	7.74	5.56				
	10.22	0.784	0.618	7.67	6.05				
	12.38	0.799	0.612	6.45	4.94				
PAV	20.16	1.562	1.423	7.75	7.06	8.20	7.94	1.042	0.812
	22.02	1.537	1.498	6.98	6.80				
	16.25	1.546	1.4	9.51	8.62				
	18.064	1.58	1.503	8.75	8.32				
	17.56	1.586	1.528	9.03	8.70				
	18.475	1.328	1.508	7.19	8.16				
A7.5	15.623	1.119	0.889	7.16	5.69	7.94	6.31	0.517	0.635
	14.265	1.16	0.861	8.13	6.04				
	12.956	0.982	0.825	7.58	6.37				
	11.251	0.975	0.846	8.67	7.52				
	15.515	1.236	0.936	7.97	6.03				
	14.686	1.194	0.909	8.13	6.19				
A15	17.32	1.231	1.013	7.11	5.85	7.69	5.69	0.560	0.333
	17.23	1.463	1.051	8.49	6.10				
	15.89	1.155	0.85	7.27	5.35				
	16.18	1.2	0.856	7.42	5.29				
	16.98	1.29	1.012	7.60	5.96				
	15.97	1.319	0.891	8.26	5.58				
C8	15.698	0.984	0.9325	6.27	5.94	7.39	6.57	1.049	0.722
	15.248	1.075	0.923	7.05	6.05				
	16.245	1.186	1.135	7.30	6.99				
	14.658	1.285	1.123	8.77	7.66				
	15.021	0.965	1.036	6.42	6.90				
	14.909	1.271	0.8775	8.53	5.89				
C16	17.06	1.325	0.907	7.77	5.32	7.36	5.42	0.531	0.467
	16.258	1.132	0.886	6.96	5.45				
	15.0653	1.12	0.804	7.43	5.34				
	15.135	0.984	0.828	6.50	5.47				
	17.012	1.3	0.805	7.64	4.73				
	12.4057	0.977	0.768	7.88	6.19				
B5	19.08	1.356	1.298	7.11	6.80	7.77	6.95	0.368	0.232
	16.287	1.302	1.156	7.99	7.10				
	17.064	1.321	1.212	7.74	7.10				
	15.954	1.272	1.156	7.97	7.25				
	14.846	1.208	0.989	8.14	6.66				
	16.809	1.29	1.138	7.67	6.77				
B10	15.894	1.202	1.067	7.56	6.71	7.46	5.91	0.173	0.689
	16.517	1.267	0.974	7.67	5.90				
	18.09	1.309	1.059	7.24	5.85				
	17.846	1.301	0.968	7.29	5.42				
	16.891	1.281	1.12	7.58	6.63				
	17.519	1.304	0.863	7.44	4.93				

Figure 3-7 shows the spectrum of each rejuvenator with a single dosage rate (higher one) to see the difference among rejuvenators. Since all binder types produced similar spectra, it can be observed that the chemistry of asphalt binder has not been greatly affected by rejuvenators. To confirm a chemical reaction between two materials, there should be a new peak for a certain wavenumber or a horizontal shift in spectra. A consistent vertical shift in spectra was observed with some changes in peak values which may confirm that the reaction between rejuvenators and aged binder is mostly physical rather than being chemical. However, because SI and CI values did not change linearly as the amount of a rejuvenator increased. Therefore, it can be postulated that there might be some chemical reactions between rejuvenators and the aged asphalt binder. Spectra for aged and virgin binder are very similar although chemical reactions should have occurred during the aging process.

(a) shows a plot of the SI values of eight binder types summarized in Table 3-2. As expected, the PAV-aged samples exhibited a significant increase in the SI value. The rejuvenated asphalt samples exhibited lower SI value than the PAV-aged asphalt but higher SI value than that of the virgin asphalt binder. (b) shows CI values of the same samples. As can be seen from , all rejuvenators reduced the oxidation levels of both sulfur and carbon whereas Rejuvenator “C” and Rejuvenator “A” were more effective in reducing the level of carbon oxidation than Rejuvenator “B”. Overall, the standard deviations of SI and CI values seemed to be quite large, which indicates a high variability in measurements.

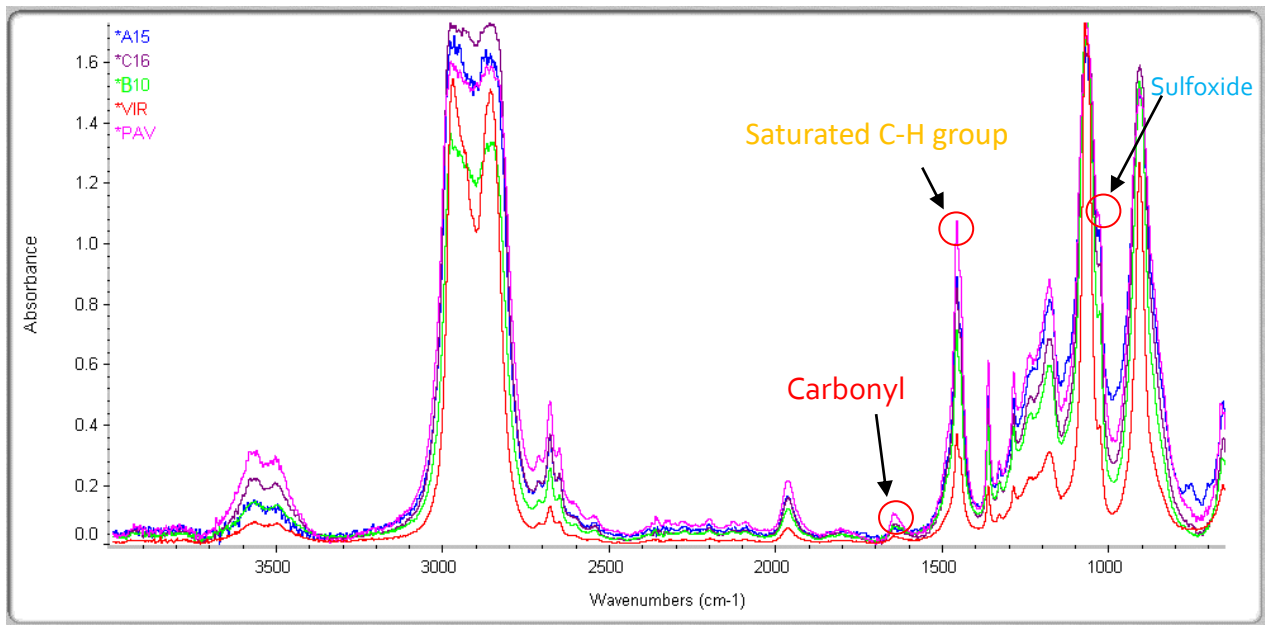
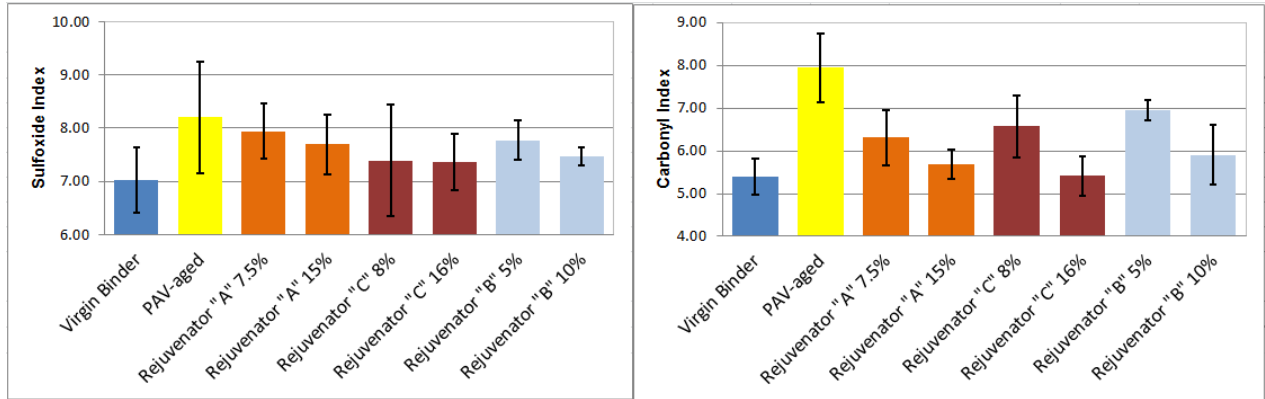


Figure 3-7 FTIR test results of the aged and rejuvenated samples for one dosage rate of rejuvenators (C16: 16% Rejuvenator “C”; B10: 10% Rejuvenator “B”; A15: 15% Rejuvenator “A”)



(a) Sulfoxide index

(b) Carbonyl index

Figure 3-8 Oxidation levels of eight different binder types

Figure 3-9 shows the FTIR test results of three rejuvenators plus virgin and PAV-aged asphalt binders. As can be seen from Figure 3-9, the spectra of two rejuvenators (Rejuvenator “B” and Rejuvenator “A”) were very similar whereas that of Rejuvenator “C” is different from them. It is interesting to note that a spectrum of virgin asphalt sample was quite different from that of PAV aged asphalt sample although their base asphalt is same.

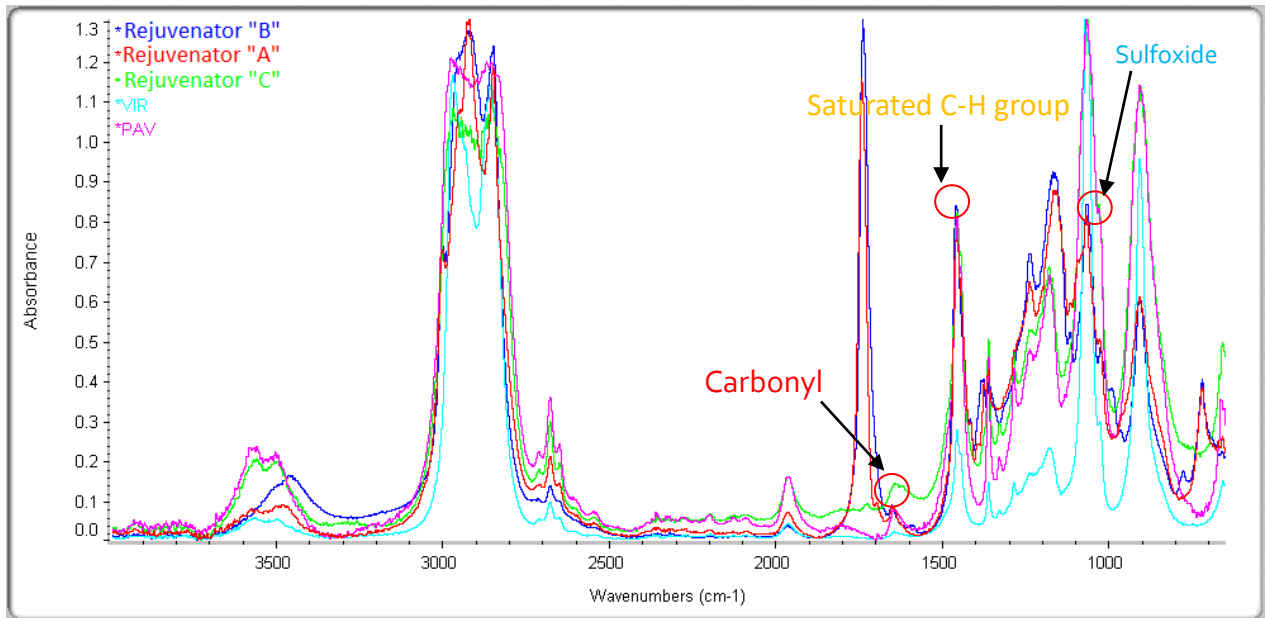


Figure 3-9 FTIR results of three rejuvenators

3.2 Cryo-Scanning Electron Microscopy

Scanning Electron Microscopy (SEM) has been used to characterize the physical properties of various types of asphalt, but it has not been successful due to a volatility of asphalt and a susceptibility to electron beam damage (Champion-Lapalu *et al.*, 2002). Cryogenic method is an appropriate tool for oily and non-conductive materials that cannot endure large amounts of energy at room temperatures and burn or deform when exposed to a beam of electrons. Therefore, the Cryo technique was adopted as an attachment to SEM to observe asphalt binder samples so that the temperature of samples can be lowered to a temperature below the glass point. Cryo-preparation enables a proper observation of microscopic properties of asphalt after being frozen using liquid nitrogen.

Cryo-SEM Sample Preparation

For preparing a Cryo asphalt sample, as shown in Figure 3-10, specific types of rivets should be used. For each asphalt type, two rivets were glued on their wider ends where asphalt is to be sandwiched between two rivets. Each asphalt sample should then be heated up and placed in a set of rivets using a syringe. Each set of rivets should be left at room temperature to cool down. All specimens were then placed in a Cryo chamber with liquid nitrogen to lower a conditioning temperature down to -165°C for about 30 minutes to make them very stiff and brittle. The shuttle and plate shown in Figure 3-10 (b) was used to keep the sample under vacuum and cryogenic conditions. A knife-shaped lever was used to hit the upper rivet of each set to make a fracture surface. To make sputter coated samples, a thin coat of gold/palladium was applied on the fracture surface of the specimens in vacuum condition using ultrapure argon gas.



(a) Sets of Rivets



(b) Shuttle and Plate

Figure 3-10 Tools used for the Cryo-SEM test

Cryo-SEM Test Results

Cryo-SEM tests were formed on PAV-aged and the rejuvenated asphalt binders. Amounts of cracks from each sample were measured by using an image processing technique. To determine the repeatability of the Cryo-SEM procedure, the same procedure was applied for the another set of samples.

First-Round Test

As the asphalt binder becomes stiffer at low temperature, the surface would develop more cracks. To show a whole sample, as shown in Figure 3-11, the Cryo-SEM images of the PAV-aged and rejuvenated asphalt specimens were magnified on a 1-mm scale. Each image includes two main circles due to the circular shape of rivets. As can be seen from Figure 3-11, the surface of the rejuvenated asphalt exhibited less amount of cracks than that of the PAV-aged asphalt.

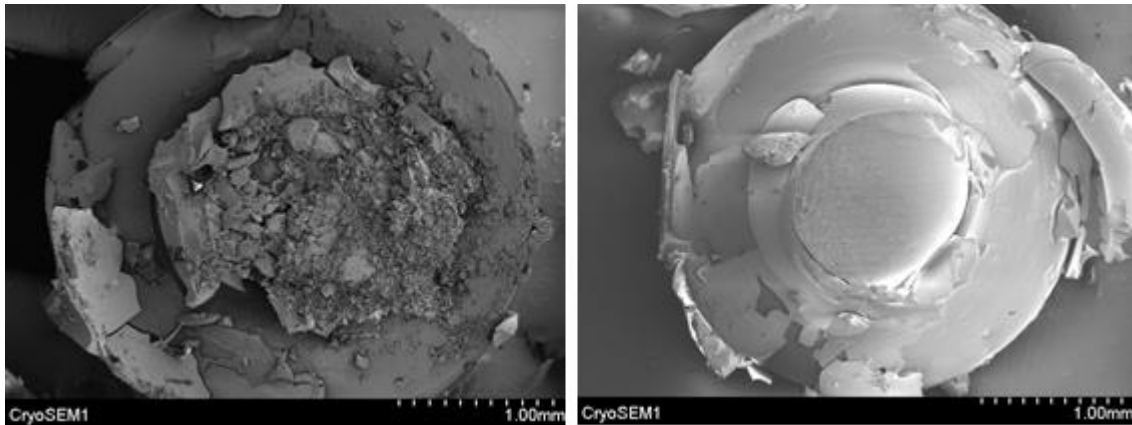
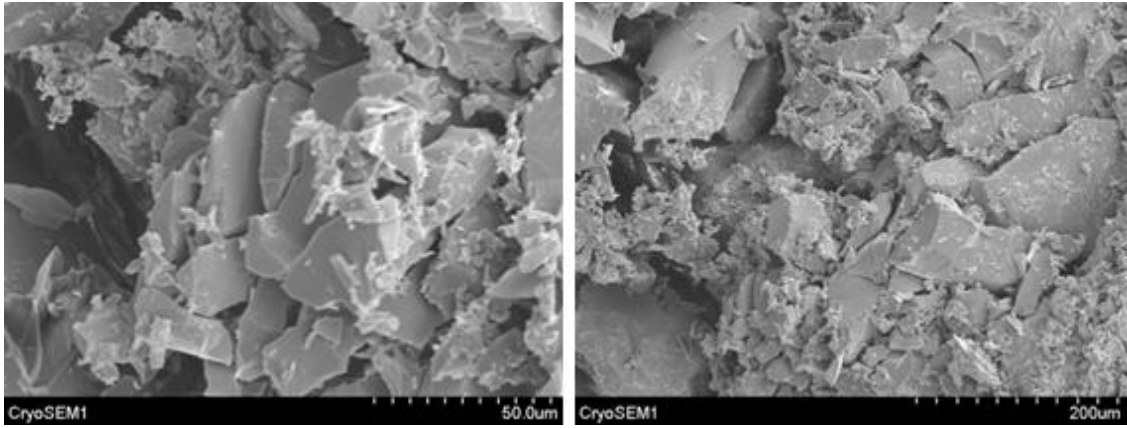
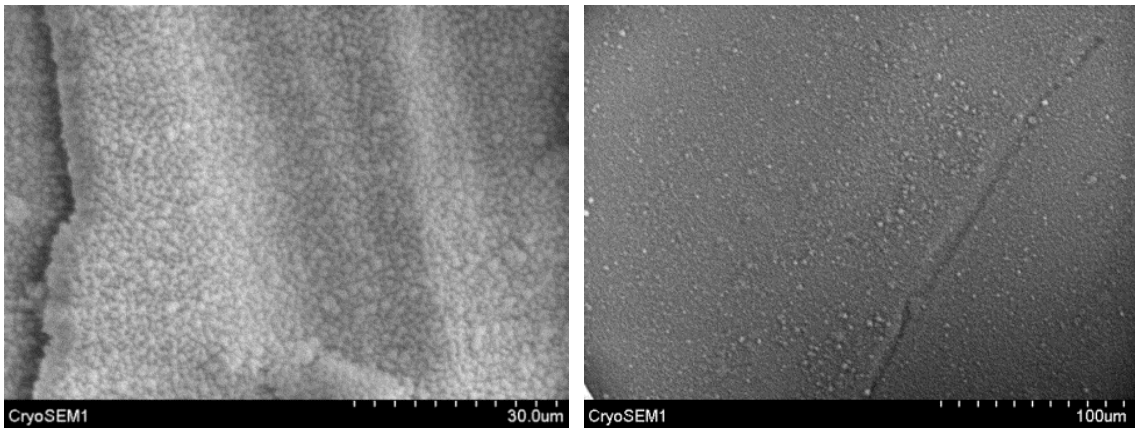


Figure 3-11 Cryo SEM images of (a): Aged and (b) 30% Rejuvenator “C”-restored asphalt

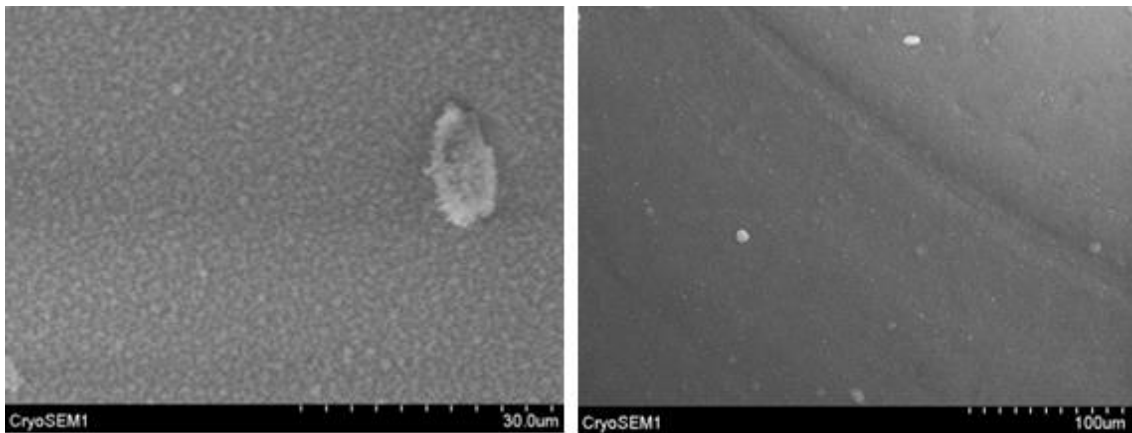
To objectively assess low-temperature characteristics of both aged and rejuvenated asphalt, the image processing technique was employed to analyze the images obtained using the Cryo-SEM. To show the fracture surface characteristics, as shown in Figure 3-12, an image with a varying magnification was captured from a different part of asphalt specimen. Figure 3-12(a) shows the aged asphalt as a control sample, where the surface is rough and fractured with more angular fragments. As shown in Figure 3-12(b) and Figure 3-12(c), 15% Rejuvenator “C” made the fracture surface of the aged asphalt smoother with some remaining minor cracks or angular fragments. As the dosage rate of Rejuvenator “C” was increased from 15% to 30%, no difference in the surface texture was observed. As shown in Figure 3-12(d), adding 10% of Rejuvenator “B” made the fracture surface slightly smoother but significant amounts of angular fragments can be observed. As shown in Figure 3-12(e), when the dosage rate of Rejuvenator “B” was increased from 10% to 20%, the fracture surface became much smoother.



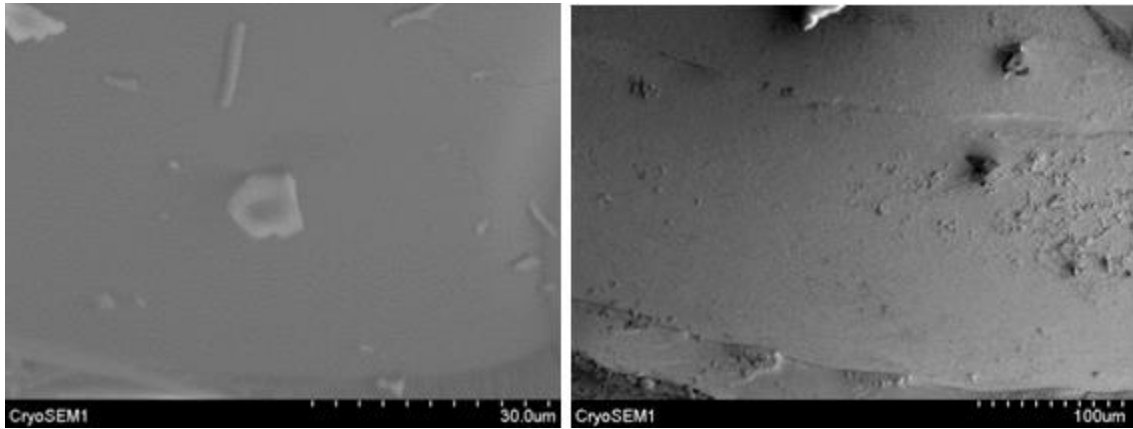
(a) Aged asphalt



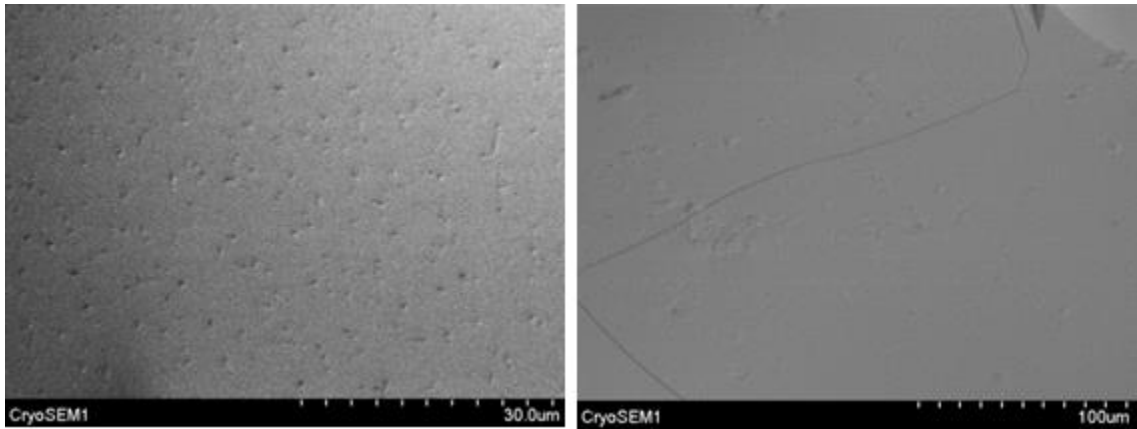
(b) Aged asphalt restored with 15% of the rejuvenator "C"



(c) Aged asphalt restored with 30% of the rejuvenator "C"



(d) Aged asphalt restored with 10% of the rejuvenator “B”



(e) Aged asphalt restored with 20% of the rejuvenator “B”

Figure 3-12 Cryo-SEM images of five asphalt samples

Crack Detection using Image Analysis

The main purpose of the image analysis is to objectively quantify the crack shape and length (Hartman and Gilchrist, 2004). Fracture models were then developed using *MATLAB* software *DIPimage toolbox* (2014b) to simulate the crack propagation. To identify an optimum algorithm to show cracks, several algorithms (Prewitt, Roberts, Canny, Zero Cross, Sobel, Laplacian of Gaussian (Log) and an algorithm developed by ImageJ v2.0.0 software which uses Canny-Deriche filtering method) were run on the same sample of Rejuvenator “C”-15% (aged asphalt restored with 15% of the rejuvenator Rejuvenator “C”). Figure 3-13 presents images processed by Canny and Log algorithms, where the image by the Canny algorithm seemed to be more representative of the original image than the Log algorithm. The steps in the Canny algorithm are presented below:

1. Smooth the input image with a Gaussian filter:

To prevent possible noise within images to be mistaken for edges, a smoothing should be run. If $f(x,y)$ denotes the image, $G_{\sigma}(x,y)$ will then be a Gaussian smoothing filter where σ would

be spread of Gaussian for controlling the degree of smoothness. The result would be an array of smoothed data (Eq. 3):

$$S(x, y) = G_{\sigma}(x, y) \otimes f(x, y) \quad (3)$$

where, $S(x,y)$ is the output of smoothed image.

2. Compute the gradient magnitude and angle images:

To generate “x” and “y” partial derivatives, $G_x(x,y)$ and $G_y(x,y)$, the gradient of the smoothed array $S(x,y)$ should be used (Eq. 4).

$$G_x(x, y) \approx [S(x, y+1) - S(x, y) + S(x+1, y+1) - S(x+1, y)] / 2 \quad (4)$$

$$G_y(x, y) \approx [S(x, y) - S(x+1, y) + S(x, y+1) - S(x+1, y+1)] / 2$$

The magnitude and orientation of the gradient can be calculated using Eq.5 and Eq.6:

$$G(x, y) = \sqrt{G_x^2(x, y) + G_y^2(x, y)} \quad (5)$$

$$\theta(x, y) = \tan^{-1} \left(\frac{G_y^2(x, y)}{G_x^2(x, y)} \right) \quad (6)$$

3. Apply non-maxima suppression (NMS) to the gradient magnitude image:

To convert the blurred edges of the generated image to sharp edges, all local maxima should be preserved while everything else is deleted. To do this, the orientation of gradient (θ) should be rounded to the nearest 45° corresponding to the use of an 8-connected neighbourhood. The edge strength of each pixel should then be compared to the edge strength of the pixel in the positive and negative gradient direction. The value of the edge strength will be preserved only if it is largest; otherwise, it should be suppressed.

4. Use double thresholding and connectivity analysis to detect the link edges:

Two threshold values should be defined in this step to be able to remove any noise. The algorithm will preserve all edges with thresholds greater than the high threshold value and remove all edge pixels below the low threshold value. Edge pixels fallen between the two defined threshold values are included only if they are connected to strong edges.

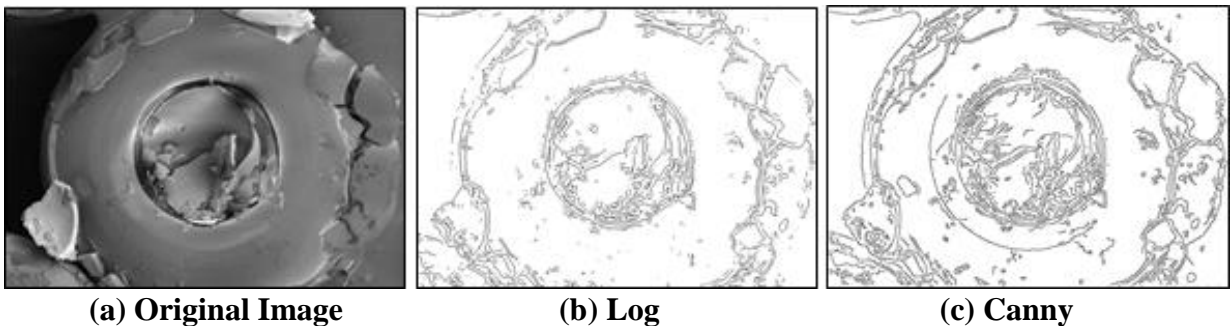
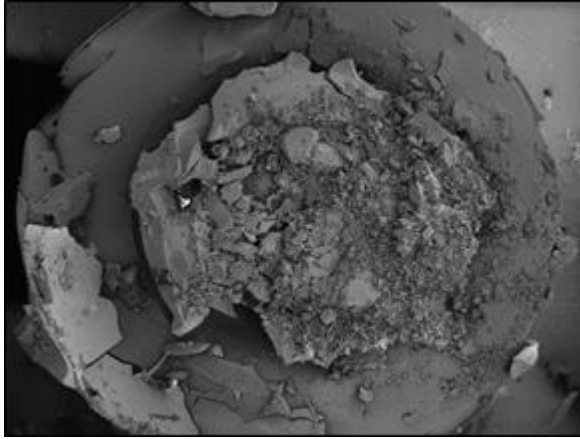
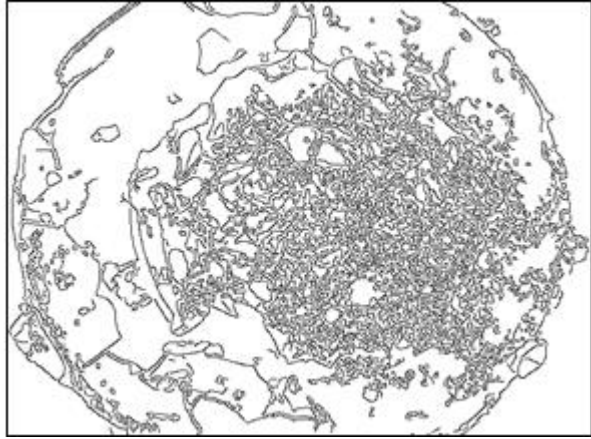


Figure 3-13 Comparison between Canny and Log methods to detect edges

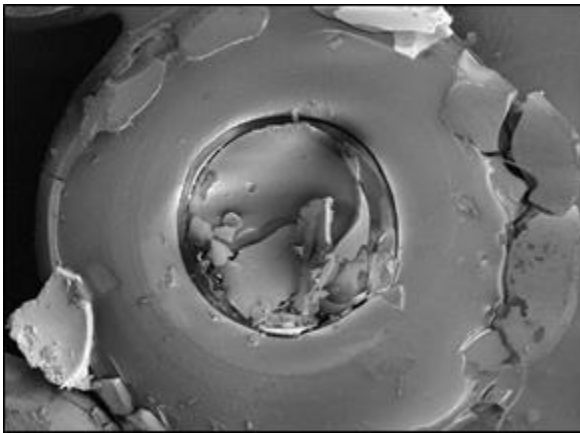
The next step is to generate binary image for other SEM images using the Canny algorithm with higher and lower thresholds. Figure 3-14 shows all original and binary images processed by the Canny algorithm.



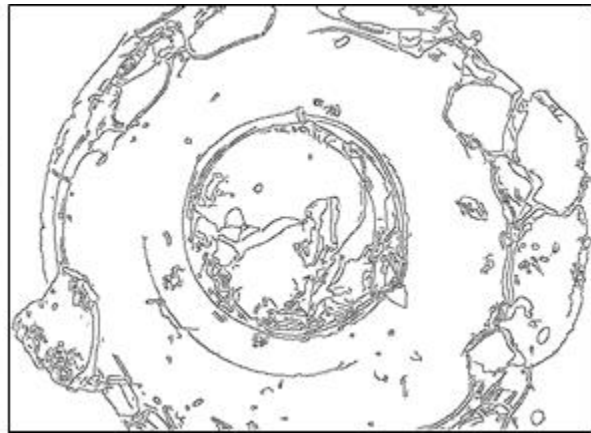
(a) PAV original image



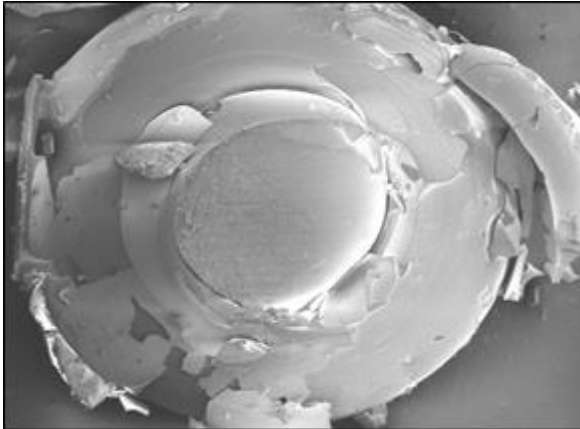
(b) PAV binary image



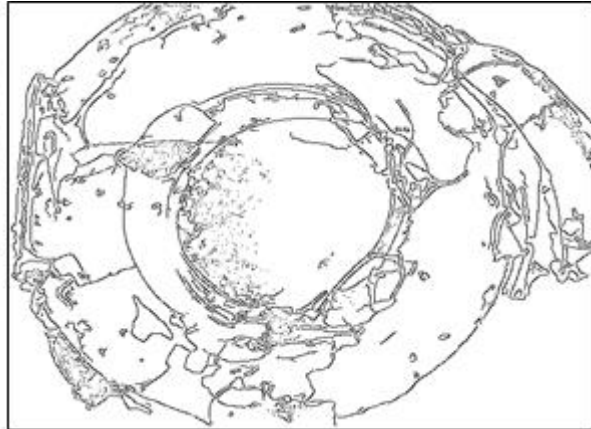
(c) Rejuvenator "C" -15% original image



(d) Rejuvenator "C" -15% binary image



(e) Rejuvenator "C" -30% original image



(f) Rejuvenator "C" -30% binary image

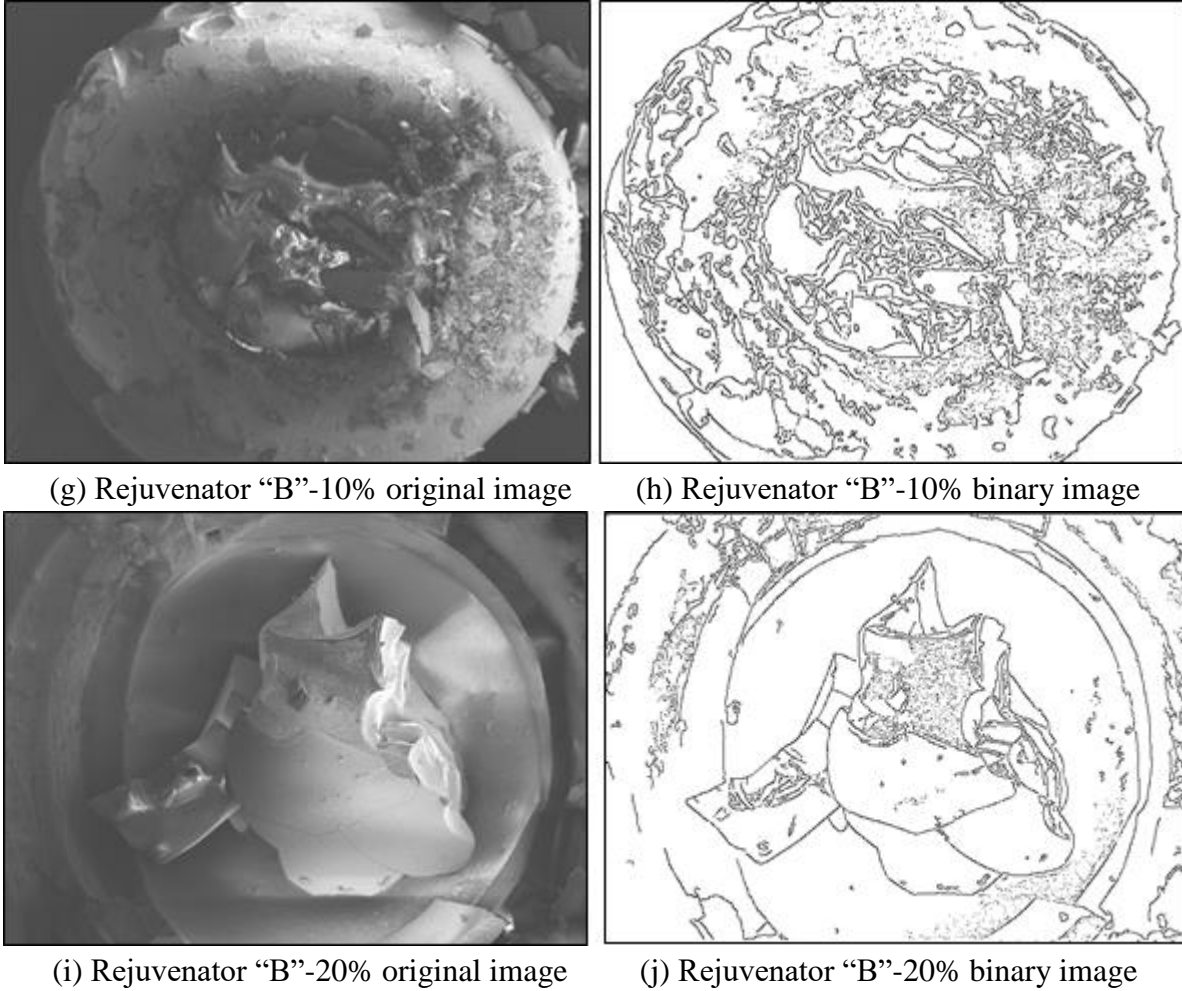


Figure 3-14 Crack detection for aged and rejuvenated asphalt

To quantify the digitally processed images, ImageTool (alpha3) software was used and amounts of black and white pixels were counted. The ratio of black to total pixels was then computed as Fracture Index (F.I.) to quantify fractured surfaces of aged and rejuvenated asphalt samples (Eq. 7).

$$\text{Fracture Index (\%)} = \frac{\text{No. of black pixels}}{\text{Total No. of pixels}} \quad (7)$$

Figure 3-15 shows F.I. values for all asphalt samples. As expected, PAV-aged asphalt exhibited the highest F.I. value. The increased dosage rate from 10% to 20% of Rejuvenator “B” decreased F.I. value. However, when the dosage rate of Rejuvenator “C” was increased from 15% to 30%, F.I. value did not change much. It can be postulated that 15% of Rejuvenator “C” is sufficient, which is equivalent to the 20% of Rejuvenator “B”. A combination of Cryo-SEM and image processing techniques can be considered as a new method to evaluate the fracture potential of the aged and the rejuvenated asphalt at low temperatures.

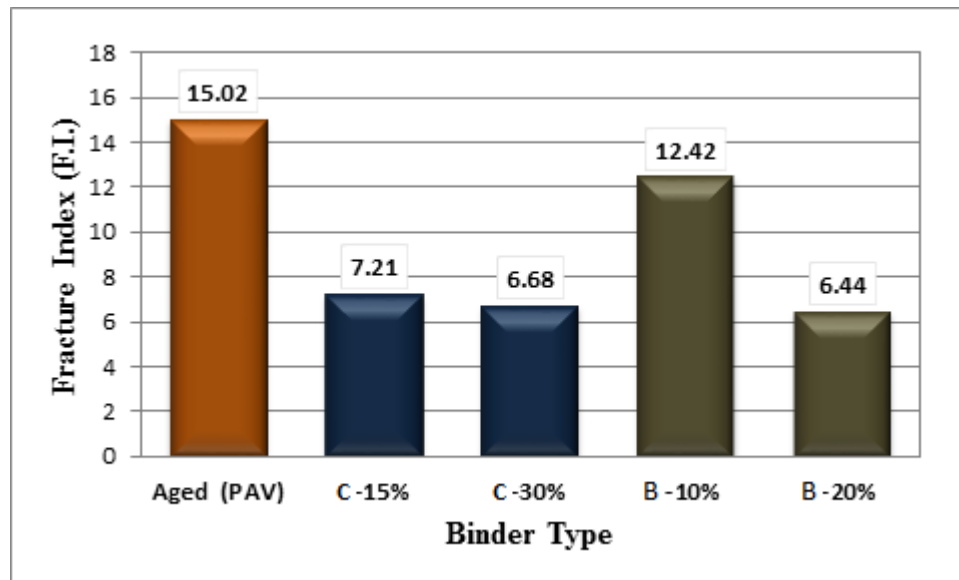
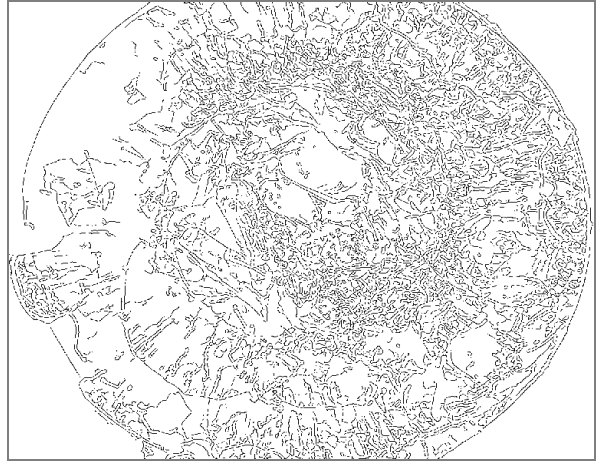
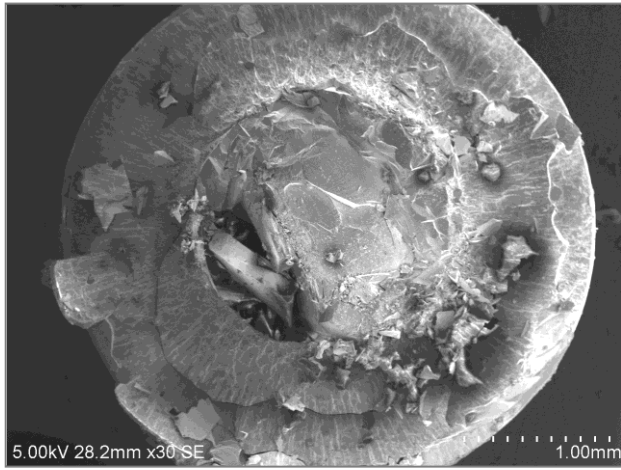


Figure 3-15 Comparative plot of Fracture Indices for various asphalt types (i.e., C-15%: 15%Rejuvenator “C”; B-10%: 10% Rejuvenator “B”)

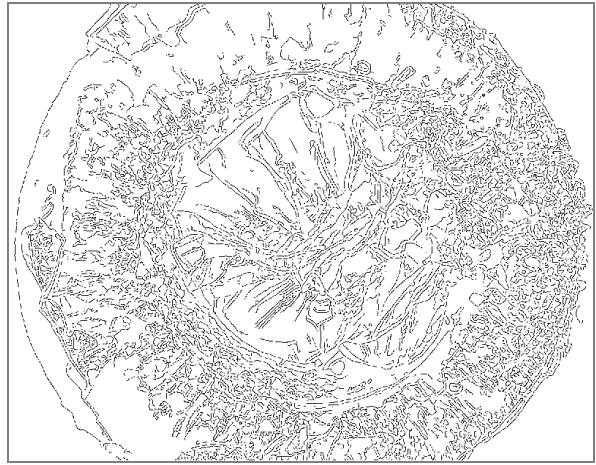
The Cryo-SEM along with image processing technique is a promising testing method to evaluate the fracture surface properties of aged and rejuvenated asphalt. The aged asphalt with rejuvenators exhibited smoother surface with less fracture than the aged asphalt without rejuvenators. The Fracture Index is presented as a parameter to rank rejuvenated asphalt in terms of low-temperature cracking susceptibility. Fracture Index values for the aged asphalt, Rejuvenator “C”-15%, Rejuvenator “C”-30%, Rejuvenator “B”-10% and Rejuvenator “B”R-20%, were calculated as 15.02, 7.21, 6.68, 12.42 and 6.44, respectively. Given the limited test results, it can be concluded that the Cryo-SEM technology is a promising method to evaluate the fracture characteristic of both aged and rejuvenated asphalt at temperatures below the glass point, which can be used to estimate the low temperature cracking potential in the field.

Second-Round Test

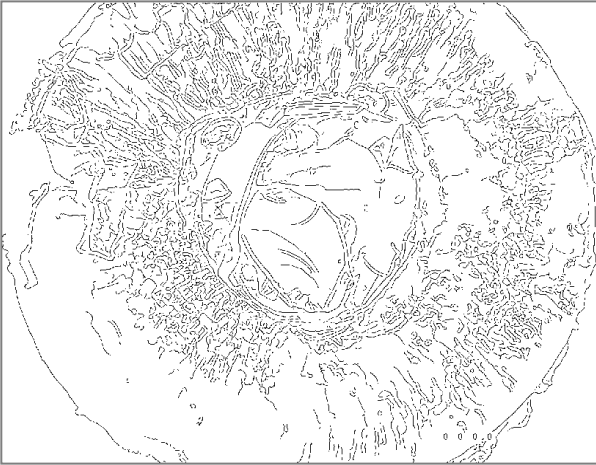
In the second-round test, two more identical samples were prepared for each binder type and the Cryo-SEM test was performed to evaluate its repeatability for evaluating the low-temperature cracking potential of the rejuvenated binders. The cryo-SEM images along with their corresponding binary crack-detected images are provided in Figure 3-16.



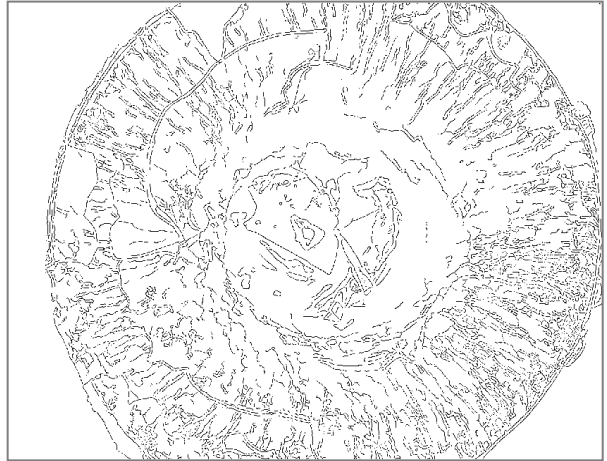
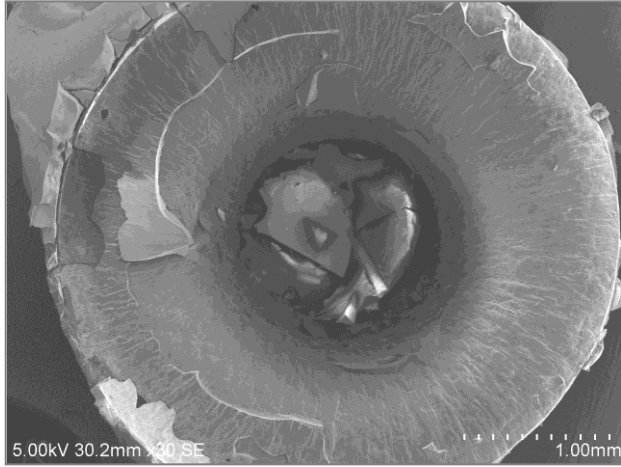
PAV Sample II



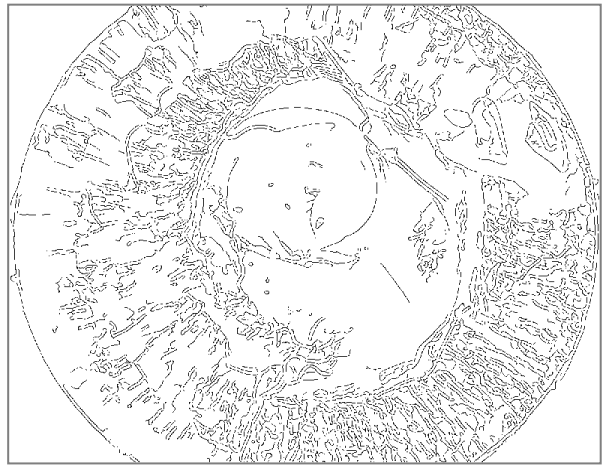
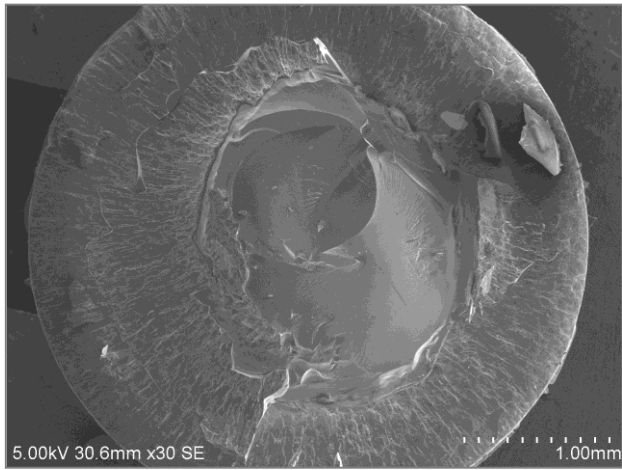
PAV Sample III



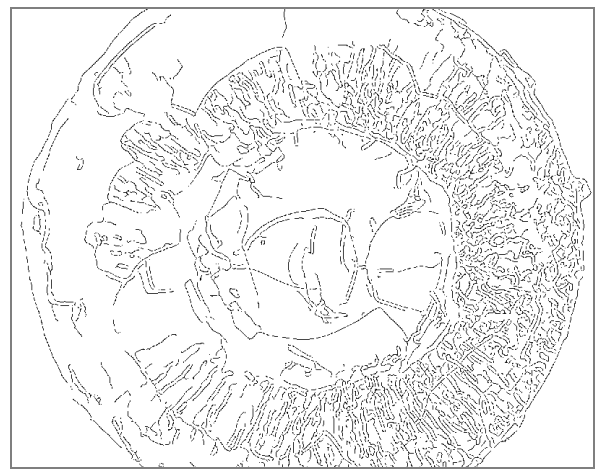
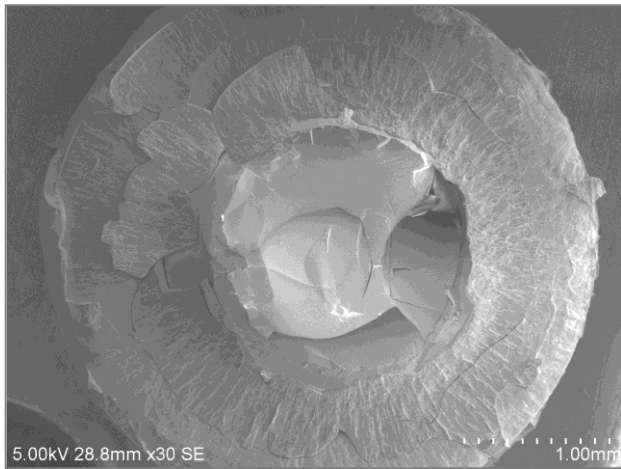
Rejuvenator "C"-15% Sample II



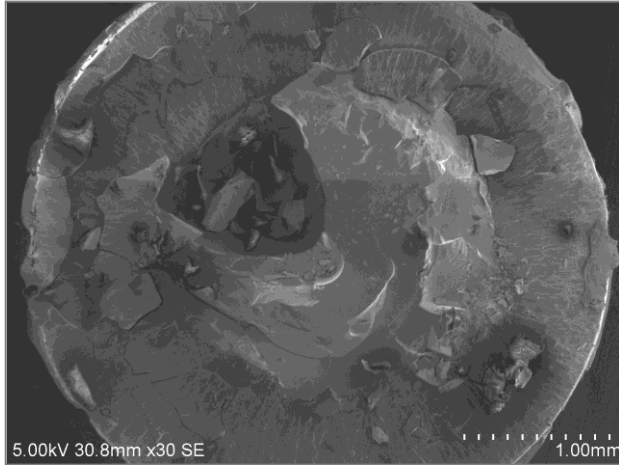
Rejuvenator "C" -15% Sample III



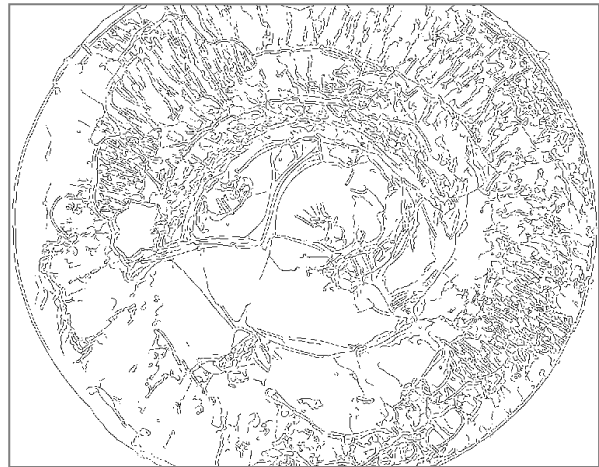
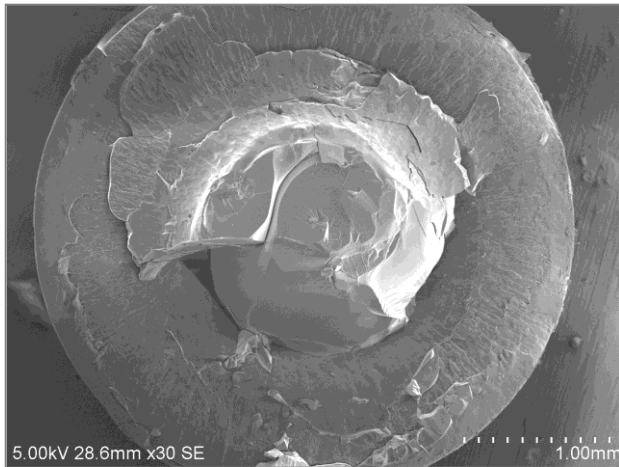
Rejuvenator "C" -30% Sample II



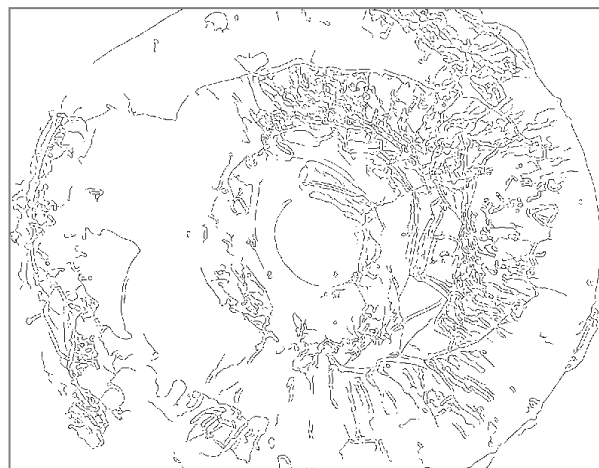
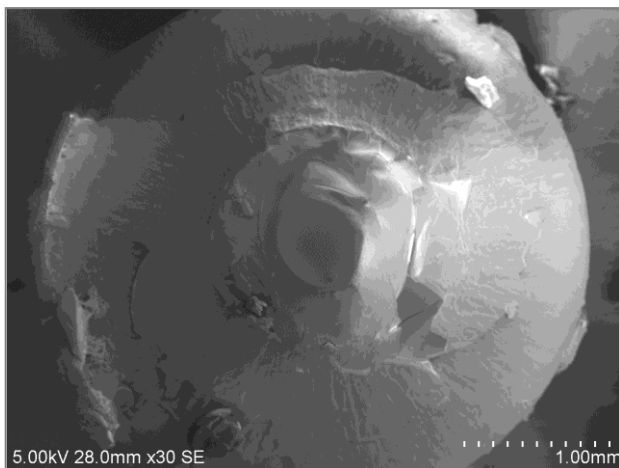
Rejuvenator "C" -30% Sample III



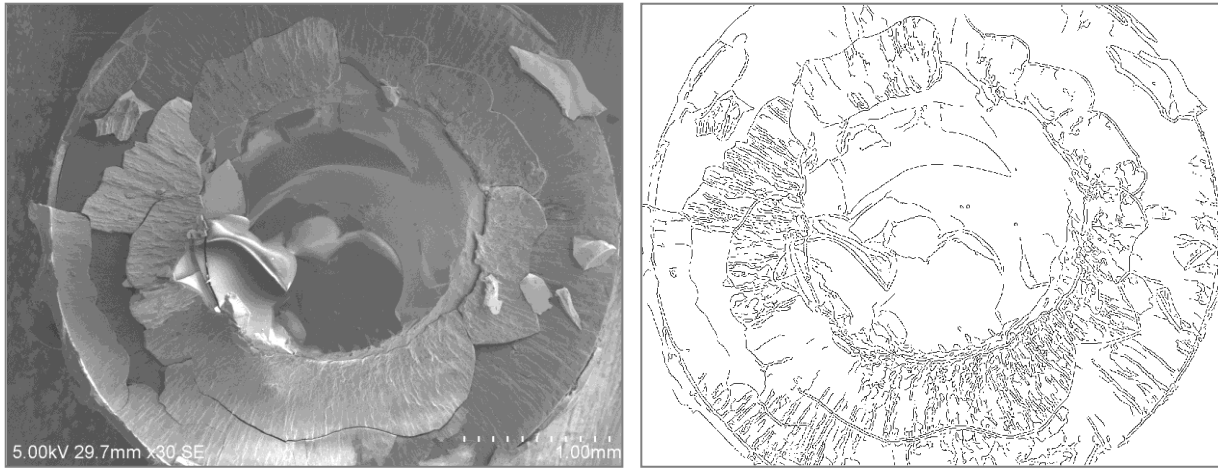
Rejuvenator "B"-10% Sample II



Rejuvenator "B" -10% Sample III



Rejuvenator "B" -20% Sample II



Rejuvenator "B" -20% Sample III

Figure 3-16 Cryo-SEM and binary crack-detected images for additional samples

Results from the second-round tests (two samples for each binder type) are plotted in Figure 3-17. As can be seen from Figure 3-17, fracture indices from the second-round test is very similar to those from the first-round test presented earlier. Figure 3-18 shows the bar charts of fracture indices from all binder samples (three samples for each binder type). The standard deviation values show that the cryo-SEM test is consistent and repeatable for evaluating the fracture surface characteristics of different types of asphalt binders (virgin, aged and rejuvenated binders).

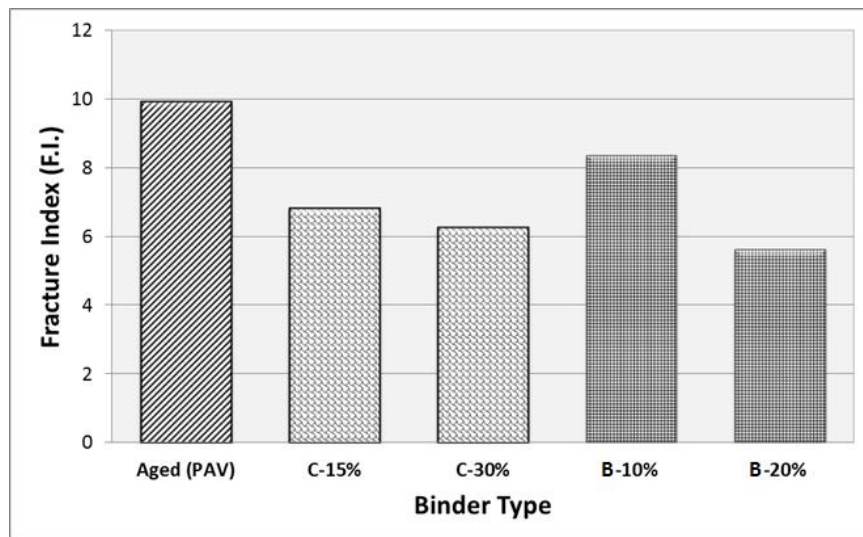


Figure 3-17 Fracture index chart for all samples from the second-round tests

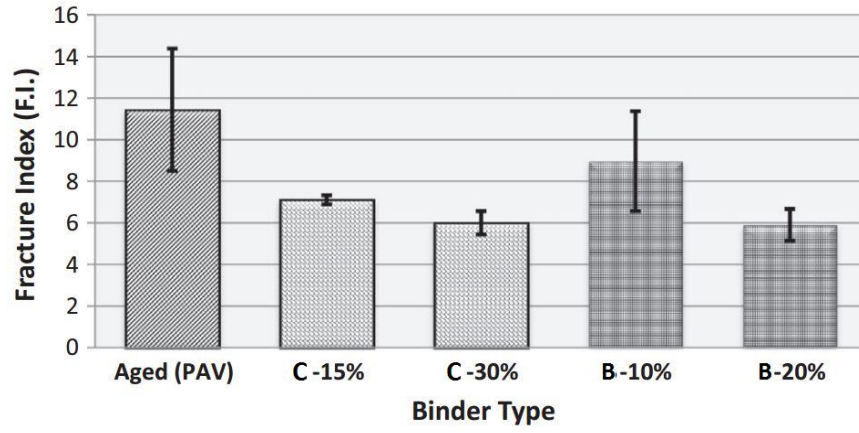


Figure 3-18 Fracture index chart for all samples from both first and second-round tests

4 RHEOLOGICAL EVALUATION OF HARDENED ASPHALT WITH VARIOUS REJUVENATORS

Superpave binder tests were performed on aged asphalt binders with and without rejuvenators. First, the PG grade of the aged asphalt was evaluated. Second, to evaluate their effects on the properties of aged asphalt binders, different types and dosage rates of the rejuvenator were added to the aged asphalt.

4.1 Dynamic Shear Rheometer (DSR) Results

To identify the high-temperature limit of PG grade of the PAV-aged asphalt and PAV-aged asphalt rejuvenated with two different dosage rates of Rejuvenator “B” RP 1000, Rejuvenator “C” and Rejuvenator “A” binders, the dynamic shear rheometer (DSR) test was performed. The DSR test results of these binder types are summarized in Table 4-1.

Table 4-1 DSR results for virgin, aged and rejuvenated binders

	dosage (% weight of binder)	G* (Kpa)	δ (degrees)	G*/sin δ	High PG Selected
PAV 40hr (PG 64-22)	-	-	-	-	>> 88
Rejuvenator “B”	5%	1.81	80.1	1.84	82
	10%	1.25	81.7	1.26	76
Rejuvenator “C”	8%	1.72	82.6	1.73	82
	16%	1.98	83.2	1.99	76
Rejuvenator “A”	7.5%	1.35	82.2	1.36	82
	15%	1.48	80.3	1.50	70

Note: The highest temperature limit for the DSR equipment was 88 °C.

As shown in Table 4-1, the high PG grade of aged binder will decrease by increasing the dosage rate of rejuvenators because rejuvenators would soften the aged binder at high temperatures. The results for 5%, 8% and 7.5% of Rejuvenator “C”, Rejuvenator “B” and Rejuvenator “A” were quite similar. However, when the dosage rate was doubled, Rejuvenator “A” significantly decreased the high-temperature limit compared to Rejuvenator “B” and Rejuvenator “C”.

4.2 Block Cracking Test Results

Block cracking can be referred to as interconnected cracks that divide the pavement up into rectangular pieces caused by an inability of asphalt binder to expand and contract with temperature cycles due to the binder aging. Glover et.al. (2005) investigated a potential correlation between binder ductility and DSR properties. To simulate ductility at 15 °C at a rate of 1 cm/min, the DSR test should be performed at 15 °C and a frequency of 0.005 rad/s. However, the frequency 0.005 would make the DSR test very time-consuming. Thus, a new testing condition of temperature 44.7 °C and frequency 10 rad/s was proposed while using a division coefficient of 2000 for conversion. The following test procedure with G-R parameter thresholds was adopted for this study.

Test Procedure:

- Texas A&M method (Glover et.al, 2005)
- Dynamic Shear Rheometer (DSR) was used.
- 25 mm parallel plates
- 1 mm gap between plates
- Temperature was set at 44.7 C
- Frequency was set at 10 rad/s

G-R Parameter Thresholds:

- G-R parameter = $\frac{G^* \cos^2 \delta}{\sin \delta}$
- G-R parameter < 180 KPa → No Block Cracking
- G-R parameter > 180 KPa and < 450 KPa → Damage Zone
- G-R parameter > 450 KPa → Block Cracking

The above test procedure was applied on virgin asphalt, PAV-aged asphalt and PAV-aged asphalt rejuvenated by Rejuvenator “C”, Rejuvenator “B”, and Rejuvenator “A”. The test results of PAV-aged asphalt rejuvenated by Rejuvenator “C”, Rejuvenator “B”, and Rejuvenator “A” are plotted in Figure 4-1, Figure 4-2 and Figure 4-3, respectively. All test results are plotted in Figure 4-4.

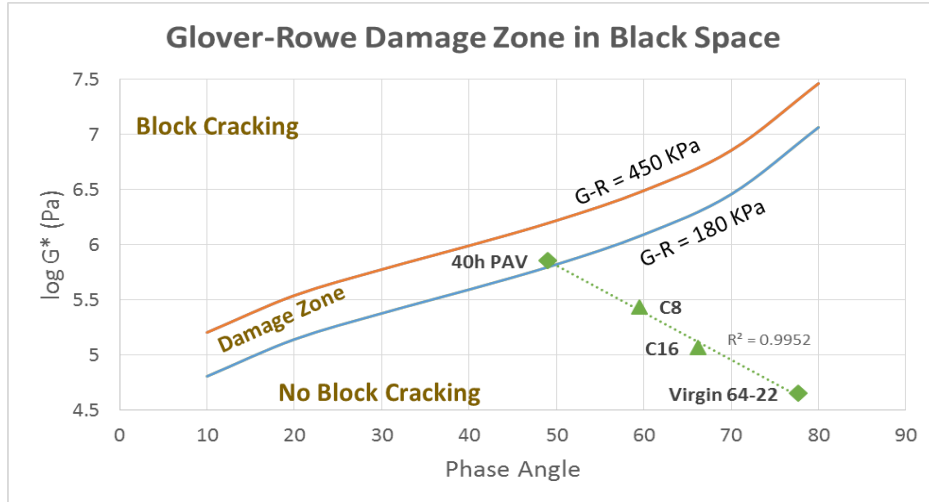


Figure 4-1 G-R Parameter for virgin, aged and rejuvenated binder with Rejuvenator “C”

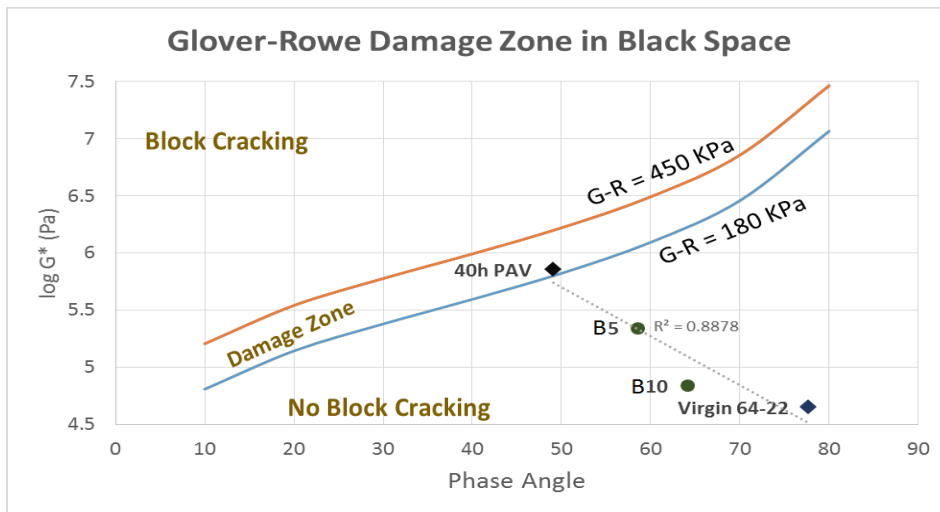


Figure 4-2 G-R Parameter for virgin, aged and rejuvenated binder with Rejuvenator “B”

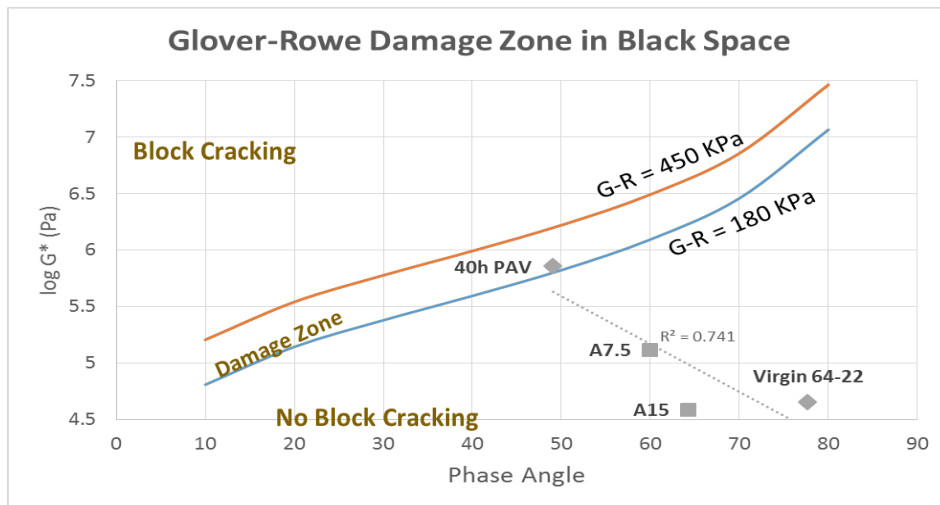


Figure 4-3 G-R Parameter for virgin, aged and rejuvenated binder with Rejuvenator “A”

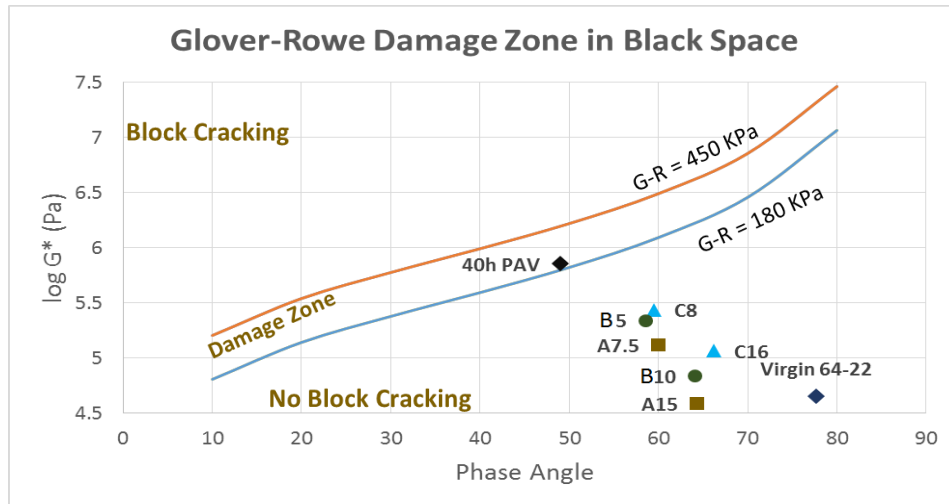


Figure 4-4 Comparative chart of G-R parameter for virgin, aged and all rejuvenated binders

Based on the results shown in Figure 4-4, rejuvenators were effective in reducing the potential of block cracking. However, none of the rejuvenators could lower the block cracking potential to the level of the virgin binder. The only sample which is in the damage zone is the 40-hr PAV aged binder. A linear trend line was also added to Figure 4-1 to Figure 4-3 to evaluate any possible linear correlation between the G-R parameter of binders with and without rejuvenator. As can be seen from these figures, there were significant correlations among virgin asphalt, rejuvenated asphalt binders and PAV-aged asphalt, and the highest correlation was asphalt binders rejuvenated with Rejuvenator “C” followed by Rejuvenator “B” and Rejuvenator “A”. Overall, based on the G-R parameter plots, Rejuvenator “A” showed a better performance followed by Rejuvenator “B” and Rejuvenator “C”.

4.3 Statistical Relationship between G-R Values and Carbonyl Index

Since G-R value and carbonyl index are both related to aging phenomenon of asphalt binders, it is suspected that there could be a possible correlation between G-R values and carbonyl indices. As can be seen in Figure 4-5, a significant correlation was observed between carbonyl indices and G-R values. Thus, it can be concluded that carbonyl index can be used to evaluate the degree of aging of asphalt binders with various rejuvenators. Sulfoxide index values were also plotted against G-R parameter values but, as can be seen from Figure 4-6, these two parameters did not correlate well. It can be concluded that sulfoxide index may not represent the degree of oxidation of asphalt binder well.

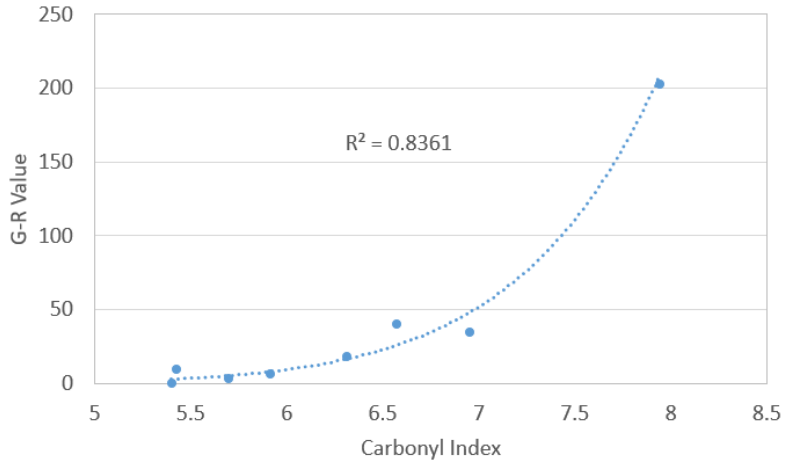


Figure 4-5 Relationship between G-R values and Carbonyl indexes

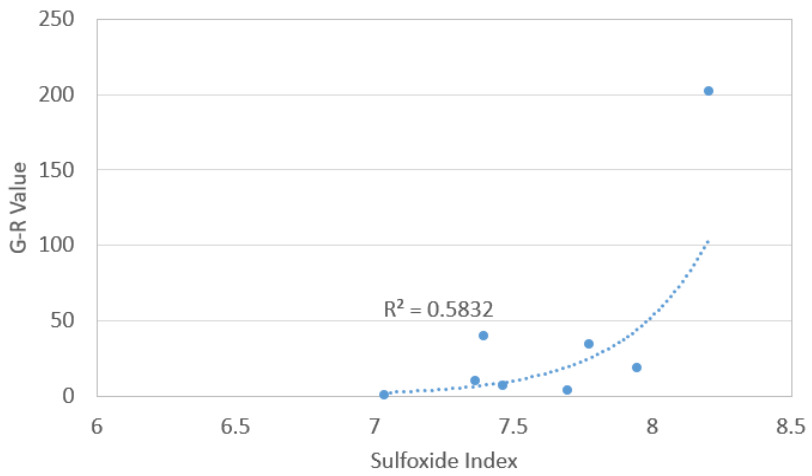


Figure 4-6 Relationship between G-R values and Sulfoxide indexes

4.4 Bending Beam Rheometer (BBR) Results

To evaluate the low temperature properties of various asphalt binders, the bending beam rheometer (BBR) test, following AASHTO T 313, was performed on virgin asphalt, 40-hrs PAV-aged asphalt and rejuvenated asphalt binders. The main objective of the BBR test was to identify each rejuvenator's optimum dosage rate that can bring the low-temperature PG grade of PAV-aged binder to that of virgin asphalt. Two different dosage rates were selected for each rejuvenator and the test was performed at two different temperatures. Three samples were prepared for each binder type and the average values of m-value and stiffness are presented in Table 4-2 and Table 4-3, respectively.

Table 4-2 Average m-values for virgin, aged and rejuvenated binders

	-22	-28	-34	m-value low PG
PAV	0.304	0.247		-22.4
7.5% Rejuvenator "A"	0.317	0.271		-24.2
15% Rejuvenator "A"		0.330	0.301	-34.2
5% Rejuvenator "B"	0.286	0.266		-17.8
10% Rejuvenator "B"		0.313	0.280	-30.4
8% Rejuvenator "C"	0.265	0.233		-15.4
16% Rejuvenator "C"		0.256	0.209	-22.4

Table 4-3 Average stiffnesses for virgin, aged and rejuvenated binders

	-22	-28	-34	Stiffness low PG	Delta Tc
PAV	205	446		-24.9	-2.5
7.5% Rejuvenator "A"	115	243		-29.7	-5.5
15% Rejuvenator "A"		103	199	-37.7	-3.5
5% Rejuvenator "B"	148	284		-28.5	-10.7
10% Rejuvenator "B"		152	313	-33.6	-3.3
8% Rejuvenator "C"	251	449		-23.8	-8.4
16% Rejuvenator "C"		370	808	-26.4	-4.0

To identify the optimum dosage of each rejuvenator, a linear regression technique was used. For example, for 5% rejuvenator "B" binder, the BBR test was performed at two different temperatures (-22°C and -28°C) to measure stiffness and m-value. As shown in Figure 4-7, a linear regression equation correlating between the test temperatures and m-values was developed to identify the temperature (-17.8°C) at which the m-value becomes 0.3. The same procedure was used for the correlation between the temperature and stiffness to find the temperature (-30.4°C) at which the stiffness becomes 300 MPa. A higher temperature of -17.8 °C between these two temperatures (-17.8°C and -30.4°C) should be selected as a PG grade temperature. The same

procedure was used for 10% rejuvenator “B” and a temperature -30.4 °C was selected as a PG grade temperature. To identify the optimum dosage for -22°C PG grade temperature of a virgin binder, a linear relationship between the PG grade temperatures of -17.8°C and -30.4 °C and corresponding rejuvenator dosages of 5% and 10% was developed. As can be seen from Figure 4-8, the optimum dosage of 6.9% was selected for the rejuvenator “B”.

Based on the BBR test results, an optimum dosage of each rejuvenator was identified and summarized in Table 4.4. The optimum dosage rates of Rejuvenator “B” and Rejuvenator “A” were similar as 6.9% and 6.2%, respectively, whereas that of Rejuvenator “C” was significantly higher at 16.0%.

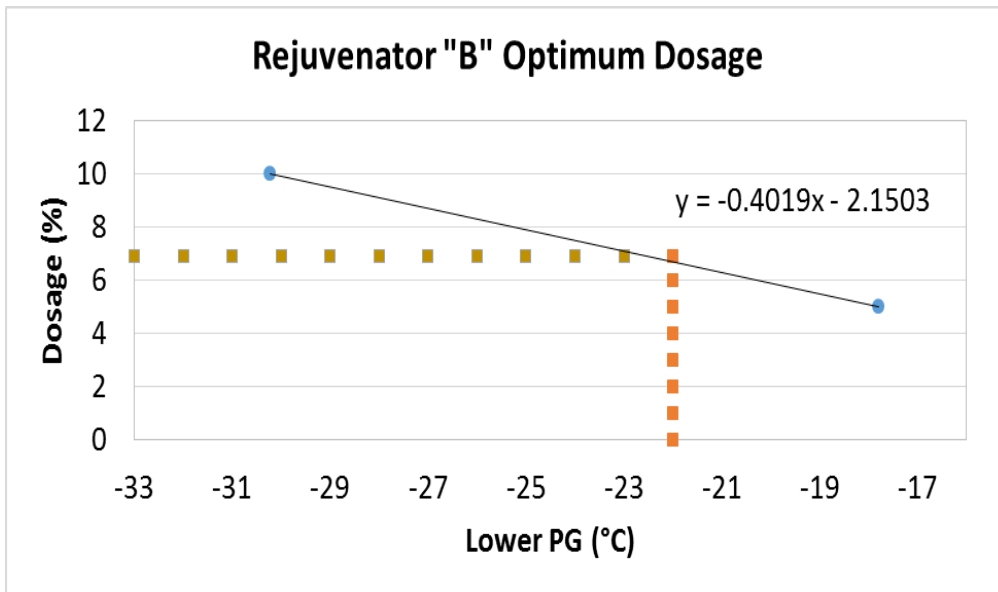


Figure 4-9 Determining optimum dosage of rejuvenator "B"

Table 4-4 Optimum Dosages for virgin, aged and rejuvenated binders

	Dosage	Lower PG	OPT. DOSAGE
PAV Binder (40-hrs)		-22.42	
Rejuvenator "A"	7.5	-24.12	6.2
	15	-34.31	
Rejuvenator "B"	5	-17.79	6.9
	10	-30.23	
Rejuvenator "C"	8	-15.53	16.0
	16	-22.43	

5 EVALUATION OF HIGH-RAP MIXTURES WITH VARIOUS REJUVENATORS

5.1 Mix Design

Two asphalt mixtures with 27.6% and 70% RAP (by binder replacement) were prepared using PG 64-22 binder. Figure 5-1 and Figure 5-2 show RAP material gradation, virgin aggregate gradation and final gradation for the asphalt mixtures with 27.6% and 70% RAP materials, respectively. Virgin aggregate gradation was selected such that the final gradation falls into the desired Superpave gradation limits. For each mixture, a total of five specimens were prepared, which include one virgin mixture, a control RAP mixture and three RAP mixture with a rejuvenator at an optimum dosage rate. Table 5-1 shows volumetric parameters for each asphalt mixture with 27.6% and 70% RAP. As can be seen from Table 5-1, it was more difficult to meet all the Superpave mix design requirements as more RAP materials were added in the asphalt mixtures.

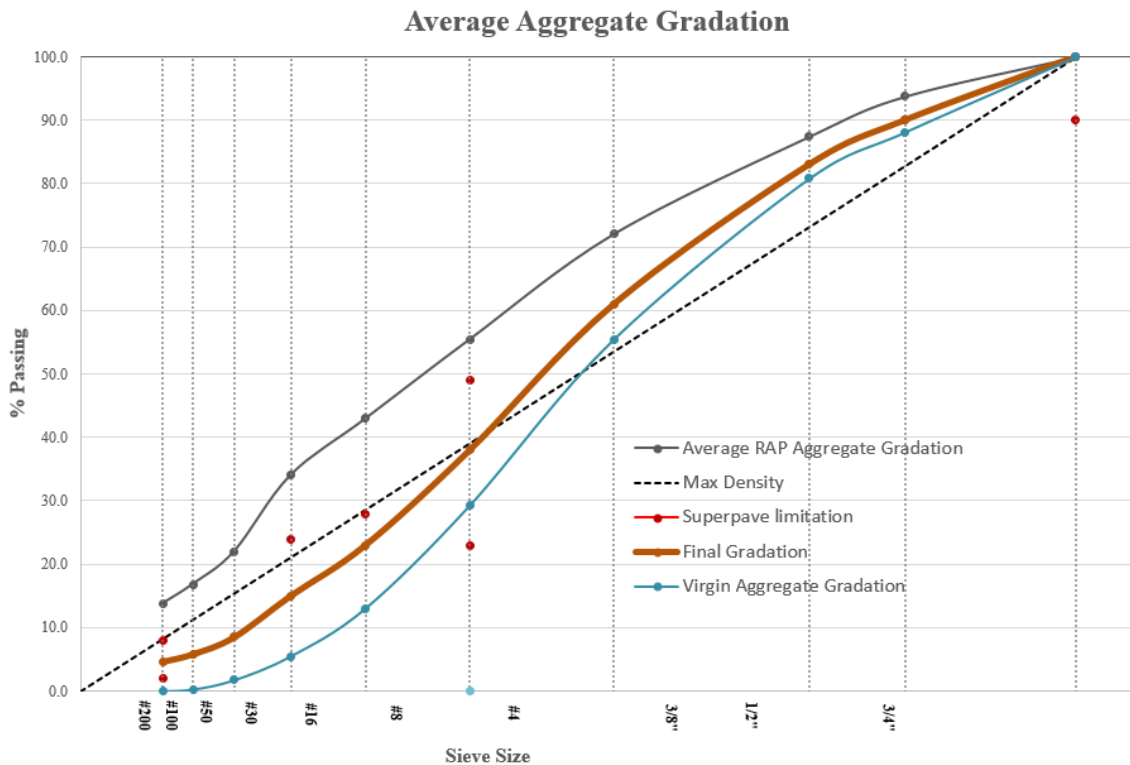


Figure 5-1 Gradation for 27.6% RAP-included mixture

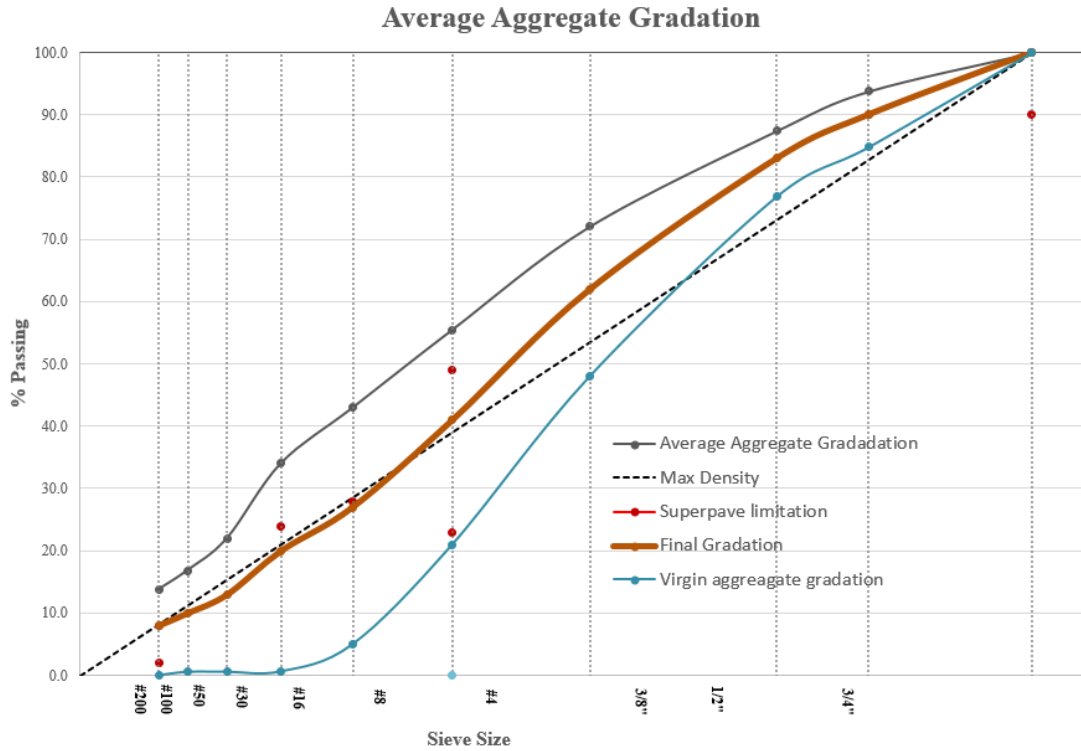


Figure 5-2 Gradation for 70% RAP-included mixture

Table 5-1 Volumetric Mix Design Results

	27.6% RAP Mixture	70.0% RAP Mixture	Requirements
Gsb RAP	2.619	2.619	
Gsb Virgin Aggregate	2.625	2.625	
Gsb Total	2.623	2.622	
Optimum binder content (%)	5.56	3.93	
Gmm @ opt. binder	2.430	2.471	
Gmb @ opt. binder	2.333	2.372	
VMA	16.00	13.12	Min. 14
VFA	75	70	70-80
Film Thickness	12.63	6.39	8-13
Air Void (%)	4.00	4.00	4.00

5.2 Disk-shaped Compact Tension (DCT) Test

To evaluate the effects of rejuvenators on the low-temperature cracking performance, DCT tests were conducted on high-RAP mixtures following ASTM D7313. The first-round test was performed on 100% RAP mixtures with a fixed amount of rejuvenator of 10%. The second-round

test was performed on 27.6% and 70% RAP mixtures with an optimum dosage rate for each rejuvenator.

First Round Test

The DCT test was performed to evaluate the effect of different rejuvenators on 100% RAP mixtures. The RAP materials were collected from highway 1, Iowa City, Iowa and the RAP material gradation is presented in Figure 5-3. To evaluate the relative effect, a uniform dosage rate of 10% of each rejuvenator was added to 100% RAP mixtures (by weight of RAP binder). The DCT test was then performed on rejuvenated 100% RAP mixtures at -12 °C, which is 10 °C higher than the low PG grade temperature of asphalt binder used for this study. Two duplicate samples were tested for each mixture type and if the results varied much, a third sample was also tested. The results of fracture energy and load-displacement plot are shown in Figure 5-4. Based on the test results, all rejuvenators except Rejuvenator “C” significantly increased the fracture energy of 100% RAP mixtures.

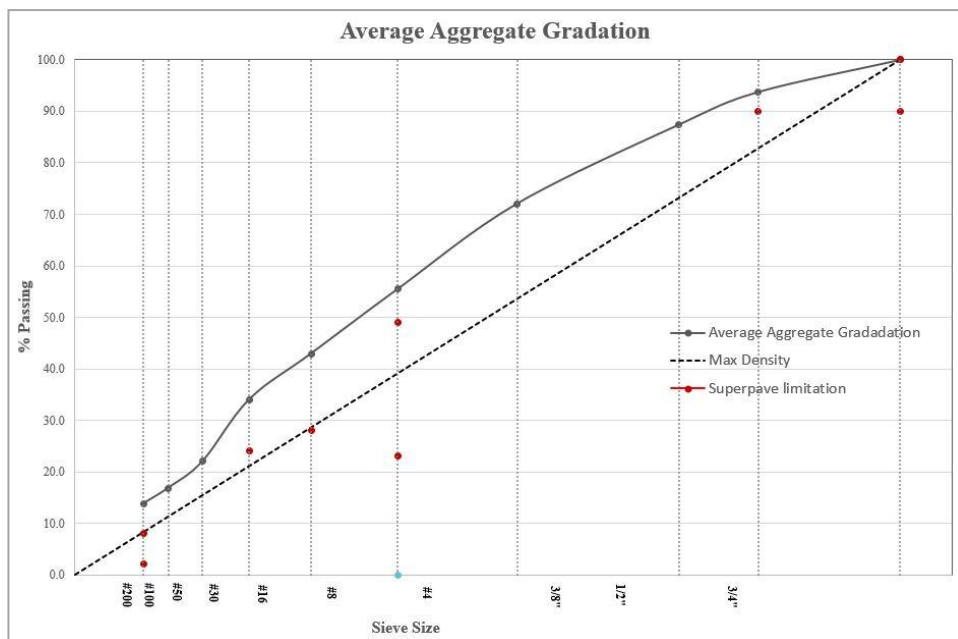


Figure 5-3 RAP materials gradation

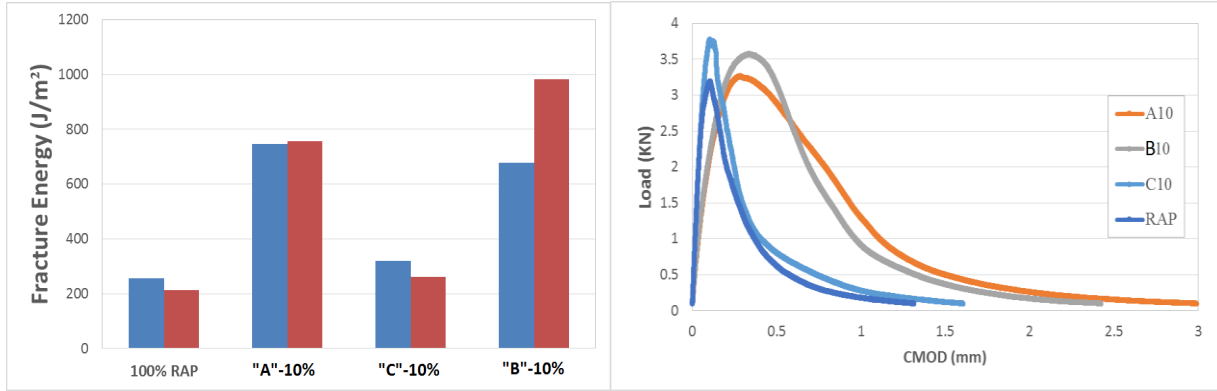


Figure 5-4 DCT test results

Second Round Test

The rejuvenated specimens for DCT test were compacted at optimum rejuvenator dosage obtained from the BBR test discussed in the previous section. Specimens were compacted at 4% air void and three samples were prepared for each mixture type. A long-term aging process was performed on them in an oven at 85 °C for 120 hours. It should be noted that some samples were cracked immediately after the initial loading and the results from these samples were discarded. Figure 5-5 shows a bar chart of fracture energy values and a plot of load versus the crack opening of samples with 27.6% RAP materials. As can be seen from Figure 5-5 , Rejuvenator “B” and Rejuvenator “A” significantly increased a fracture energy of the mixtures with the aged asphalt even slightly higher than that of virgin asphalt. However, Rejuvenator “C” decreased a fracture energy of the aged binder mixtures. DCT test result of each specimen can be found from Appendix A.

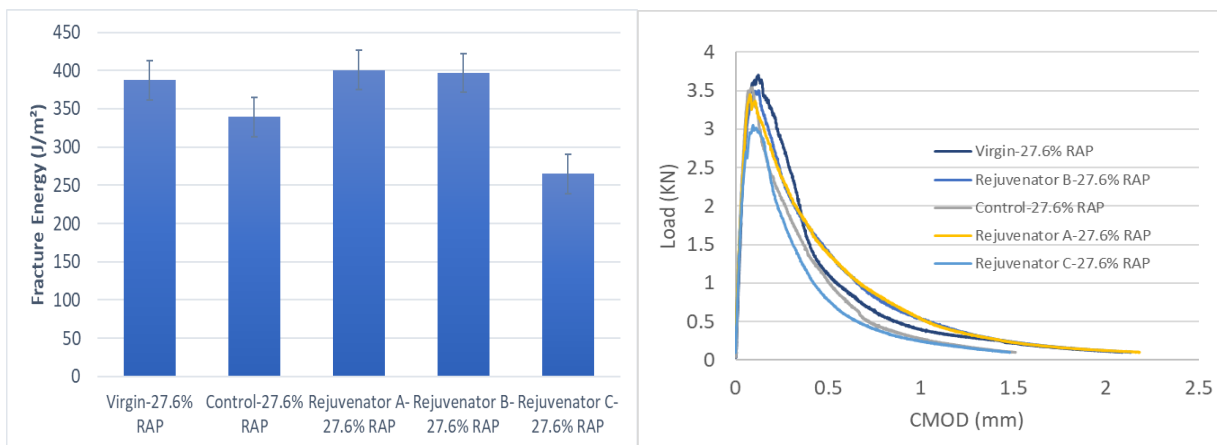


Figure 5-5 DCT results for 27.6% RAP lab-compacted mixtures

Figure 5-6 shows a bar chart of fracture energy values and a plot of load versus the crack opening of samples with 70% RAP materials. The fracture energy of mixtures of aged binder is very similar to that of mixtures of virgin binder. As can be seen from Figure 5-6, Rejuvenator “B” and Rejuvenator “A” slightly increased a fracture energy but Rejuvenator “C” decreased a fracture

energy of the aged binder mixtures. It should be noted that the Rejuvenator “C” sample was tested a few months after the sample was compacted at the laboratory. The DCT test result of individual specimen can be found from Appendix A.

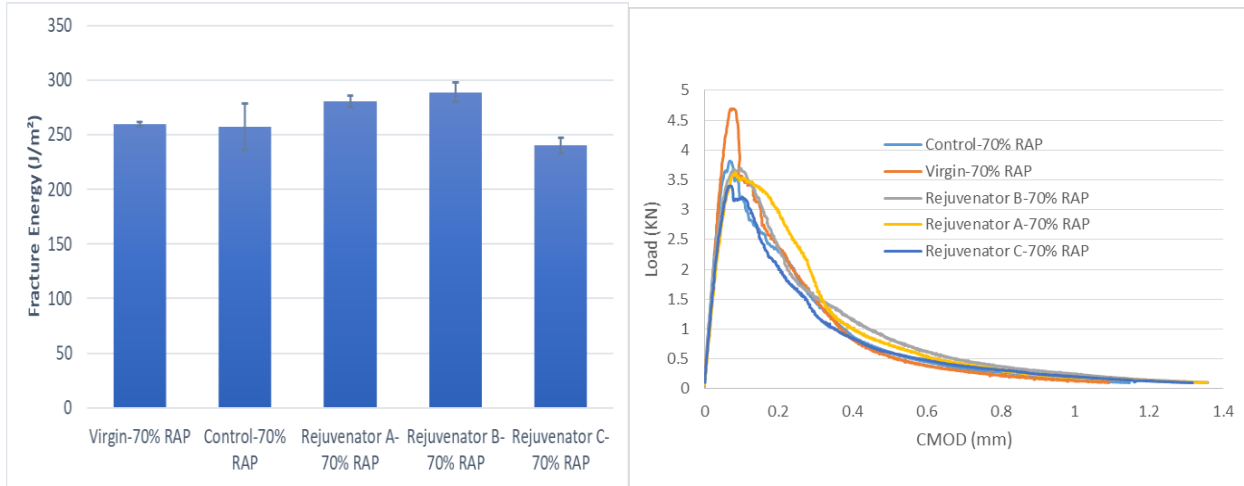


Figure 5-6 DCT results for 70% RAP lab-compacted mixtures

6 CONSTRUCTION OF TEST SECTION AND TESTING OF FIELD SAMPLES

To evaluate field performance of high RAP mixtures with and without a rejuvenator, two test sections were constructed in the field in August and November 2017. The field loose mixtures and cores were tested using HWT, DCT testing equipment.

6.1 Test Section in Crawford County

As shown in Figure 6-1 and 6-2, on August 28, 2017, County Highway M-64 project was constructed in Crawford County, Iowa (near Vail & Westside) between O & N avenues by Omni Engineering Company and Jebro Inc. supplied PG 58-28S binder. Two different mixtures with 30% RAP were obtained: one without any rejuvenator (as control mixture) and the other one with rejuvenator “D” (9.2% by RAP binder weight, 2.2% by total binder weight, or 0.123% by total mix weight). Both DCT and HWT tests were performed on laboratory compacted loose pictures from the field and the DCT test was performed on the 5-cm thick cores. Aggregate gradation and volumetric mix design parameters are presented in Table 6-1 and Table 6-2, respectively. The target and actual mix design parameters are summarized in Table 6-3. As can be seen in Table 6-3, binder grade did not comply with the specification.

Table 6-1 Crawford County Highway M-64 Project Mixture Gradation

Job Mix Formula - Combined Gradation (Sieve Size in.)										
1"	3/4"	1/2"	3/8"	#4	#8	#16	#30	#50	#100	#200
					Upper Tolerance					
100	100	100	93	66	50		25			5
100	100	94	86	59	45	32	21	8.8	4.2	3.0
100	100	87	79	52	40		17			1.0
					Lower Tolerance					

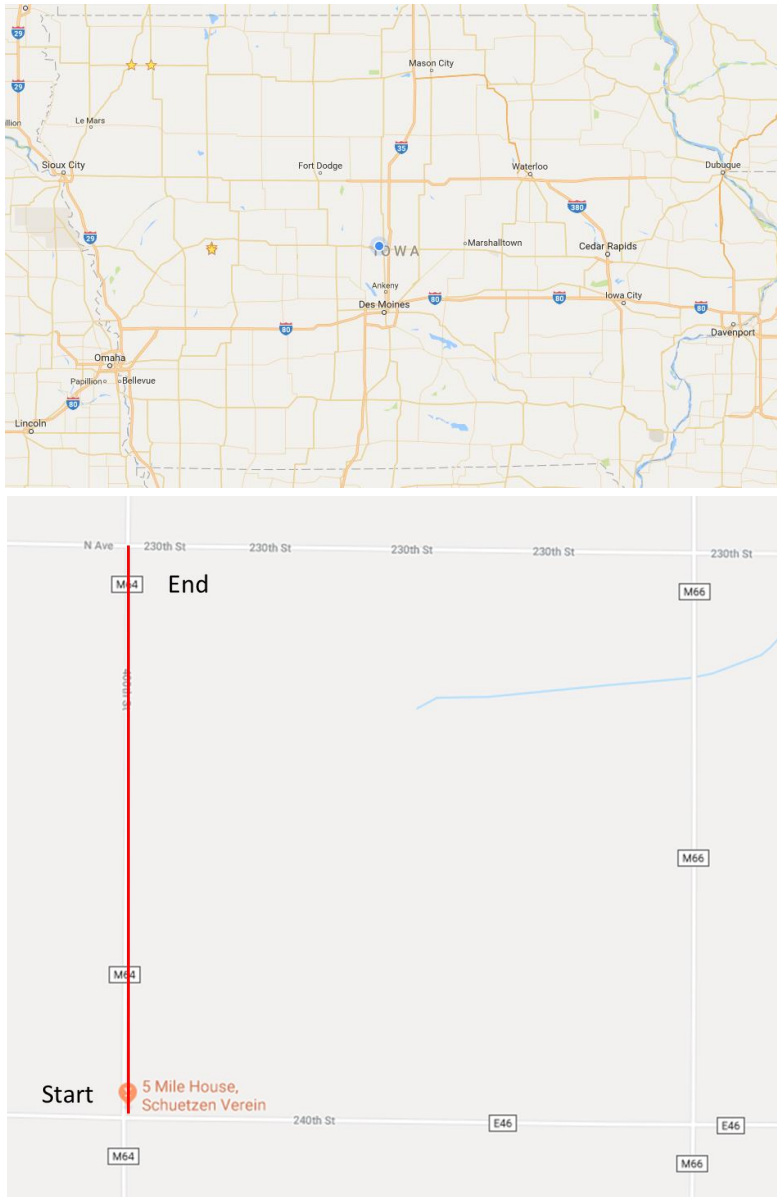


Figure 6-1 Layout of test section in Crawford County

Table 6-2 Crawford County Highway M-64 Project Mix Design Data

Asphalt Binder Source and Grade:	Jebro, Inc.(Sioux City, IA)				
Adjust grade to PG 52-34S	Gyratory Data				
% Asphalt Binder	5.00	5.54	5.56	5.80	6.00
Gmb @ N-Des.	2.323	2.355	2.355	2.357	2.365
Max. Sp.Gr. (Gmm)	2.462	2.454	2.453	2.444	2.435
% Gmm @ N- Initial	88.8	90.6	90.7	91.4	91.5
%Gmm @ N-Max					
% Air Voids	5.6	4.0	4.0	3.6	2.9
% VMA	14.5	13.8	13.8	13.9	13.8
% VFA	61.0	70.7	71.0	74.5	79.2
Film Thickness	9.36	10.17	10.21	10.81	11.41
Filler Bit. Ratio	0.77	0.70	0.70	0.66	0.63
Gse	2.656	2.671	2.670	2.670	2.667
Pbe	3.92	4.26	4.28	4.53	4.78
Pba	1.14	1.36	1.35	1.35	1.30
% New Asphalt Binder	70.7	73.7	73.8	74.9	75.8
Combined Gb @ 25°C	1.0300	1.0300	1.0300	1.0300	1.0300



Figure 6-2 Rejuvenator “D” test section in Crawford County

Table 6-3 Target vs. Actual Design Parameters of Crawford County Project

BINDER					
	Target	Actual	Spec	Comply?	
% Added Binder	4.10	4.35	N/A		
% Total Binder	5.60	5.76	5.30-5.90	Yes	
% RAP	30.00	29.13%	≤100%	Yes	
% RAS					
% Binder Replacement	26.04%	24.51%	≤ 30%	Yes	
PG Grade	58-28S		52-34S	No	
Binder replacement exceeded. Binder grade does not comply.					
Gb:	1.03151	Gsb:	2.580	Pbe (%):	4.67

6.1.1 HWT Test Results of Lab-compacted Field Mixtures

For HWT test, loose mixtures were collected from the field and compacted at the laboratory at 6% air void. It should be noted that the number of gyrations needed to compact samples was higher than normal (typically 150±20). Figure 6-3 shows the HWT results of the control and rejuvenator “D” mixtures from M-64 in Crawford county.

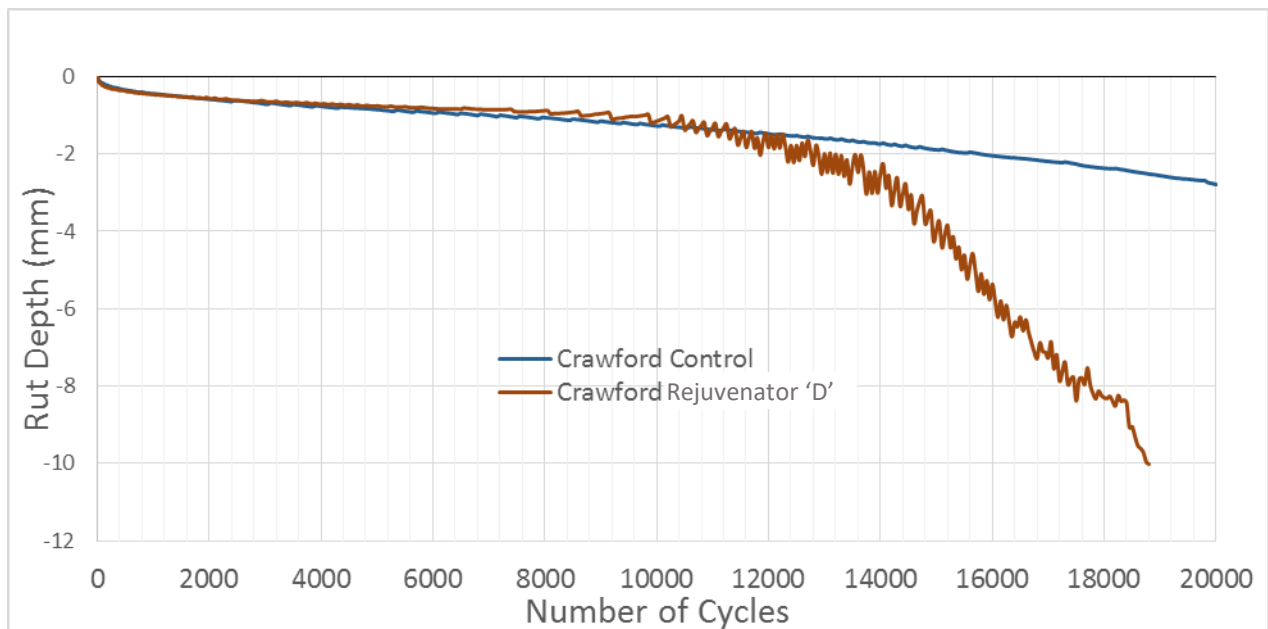


Figure 6-3 HWT Results for Crawford Control vs. Rejuvenator “D” Mixture

As can be seen from Figure 6-3, the control mixture exhibited a better performance than the rejuvenator “D” mixture. The stripping inflection point was identified at 13,120 cycles for the

rejuvenator “D” mixture which is acceptable for “S” (standard) level of traffic (see Table 6-4) whereas the control mixtures performed very well with a stripping inflection point greater than 20,000 cycles.

Table 6-4 Minimum Stripping Inflection Point (Iowa DOT)

Traffic Designation	SIP, Number of Passes ^{1, 2}
S	10,000
H, V	14,000

6.1.2 DCT Test Results of Cores and Lab-compacted Field Samples

DCT test was performed on the laboratory compacted loose mixtures from the field at 4% air voids and 5-cm thick cores collected from the test section. DCT test was performed at -18 °C since the PG grade of a virgin asphalt binder was 58-28S. As shown in Figure 6-4, both mixtures exhibited the nearly identical performance indicating that rejuvenator “D” did not improve the low-temperature cracking resistance of the control mixture.

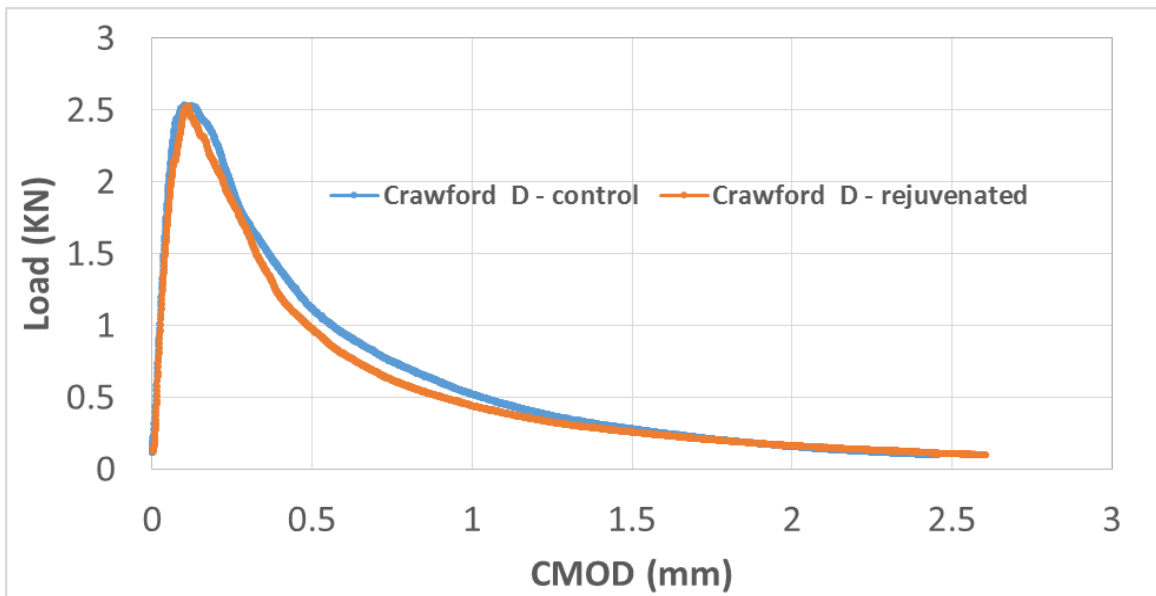


Figure 6-4 DCT Results for Crawford County

6.1.3 Beam Fatigue Test for Crawford Mixtures

Beam Fatigue test was performed on control and rejuvenator “D” mixtures from test section in Crawford county and the results are summarized in Table 6-5. Two identical samples were tested for each set and an average value is reported in Table 6-5. Based on the fatigue test results, it can be concluded that rejuvenator “D” improved fatigue cracking resistance at every strain level while showing the higher dissipated energy values.

Table 6-5 Beam Fatigue Results for Crawford County Project

Group	Air Void	Microstrain	N _f	Cumulative Dissipated Energy (MJ/m ³)
Control Mixture	6.5±0.5	900	6210	13.99
	6.5±0.5	700	24310	34.82
	6.5±0.5	500	78180	66.47
	6.5±0.5	300	923355	278.70
Rejuvenator “D” Mixture	6.5±0.5	900	53760	61.40
	6.5±0.5	700	139360	97.34
	6.5±0.5	500	471150	244.12
	6.5±0.5	300	1872170	541.75

6.2 Test Section in O’Brien County

Another test section was constructed on November 15th to 17th on State Highway 18 in O’Brien County, Iowa, located in the east of Sheldon towards Sanborn. The test section is about 7 miles long and constructed by Omni Engineering company. The control mix used quartzite aggregates and polymer modified asphalt with 30% RAP. Virgin asphalt binder supplied by Jebro Inc. was PG 58-34H and two different rejuvenators were used for this project: rejuvenator “D” (at 3.6% of virgin binder weight) and Rejuvenator “B” (at 3% of virgin binder weight). Aggregate gradation and mix design information for rejuvenator “D” control mixtures are presented in Table 6-6 and Table 6-7, respectively. Aggregate gradation and mix design information for rejuvenator “D” mixtures are presented in Table 6-8 and

Table 6-9, respectively. Gradation and mix design information of Rejuvenator “B” control mixtures are presented Table 6-10 and Table 6-11, respectively. Gradation and mix design information of rejuvenated “B” mixtures are presented in Table 6-12 and Table 6-13.

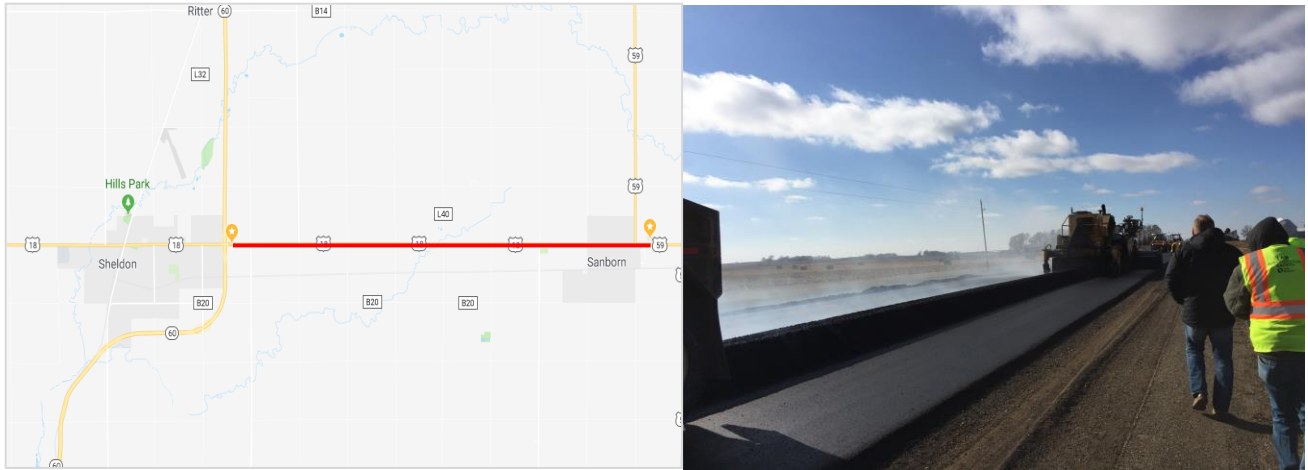


Figure 6-5 Test section in O'Brien County

Table 6-6 Aggregate Gradation for rejuvenator "D" Control Mixtures

GRADATION (%Passing)						<input type="checkbox"/> Use DOT
Sieve	Specs	11-15CF1			Avg	District
1 in.	100	100.0			100.0	
3/4 in.	100	100.0			100.0	
1/2 in.	90-100(97)	98.0			98.0	
3/8 in.	83-97(90)	90.0			90.0	
* #4	64-78(71)	72.0			72.0	
* Dev	± 7.0	1.0			1.0	
*#8	38-48(43)	42.0			42.0	
*Dev	± 5.0	-1.0			-1.0	
#16		27.0			27.0	
*#30	15-23(19)	20.0			20.0	
* Dev	± 4.0	1.0			1.0	
#50		11.0			11.0	
#100		6.0			6.0	
*#200	2.4-6.4(4.4)	4.4			4.4	
*Dev	± 2.0	0			0	
Gradation Compliance?		Yes			Yes	
DBR	Sugg 0.6 - 1.4	0.80			0.80	
% +4 Type 4		87.7			87.7	
% +4 Type 3					0.0	
(+4/-4) Type 2		87.7/61.4			87.7/61.4	

Table 6-7 Target vs. Actual Design Parameters for Control Mixtures

BINDER					
	Target	Actual	Spec	Comply?	
% Added Binder	5.00	5.33	N/A		
% Total Binder	5.85	6.12	5.55-6.15	Yes	
% RAP	18.00	16.56%	≤100%	Yes	
% RAS					
% Binder Replacement	14.68%	12.86%	≤ 30%	Yes	
PG Grade	58-34H		58-34H	Yes	
Gb:	1.02738	Gsb:	2.631	Pbe (%):	5.52

Table 6-8 Aggregate Gradation for rejuvenator “D” Mixtures

GRADATION (%Passing)						<input type="checkbox"/> Use DOT
Sieve	Specs	EMS11-15CF1			Avg	District
1 in.	100	100.0			100.0	
3/4 in.	100	100.0			100.0	
1/2 in.	88-100(95)	96.0			96.0	
3/8 in.	78-92(85)	88.0			88.0	
* #4	54-68(61)	64.0			64.0	
* Dev	± 7.0	3.0			3.0	
*#8	31-41(36)	38.0			38.0	
*Dev	± 5.0	2.0			2.0	
#16		25.0			25.0	
*#30	12-20(16)	18.0			18.0	
* Dev	± 4.0	2.0			2.0	
#50		11.0			11.0	
#100		6.3			6.3	
*#200	2.3-6.3(4.3)	4.8			4.8	
*Dev	± 2.0	0.5			0.5	
Gradation Compliance?		Yes			Yes	
DBR	Sugg 0.6 - 1.4	1.00			1.00	
% +4 Type 4		88.2			88.2	
% +4 Type 3					0.0	
(+4/-4) Type 2		88.2/50.2			88.2/50.2	

Table 6-9 Target vs. Actual Design Parameters for rejuvenator “D” Mixtures

BINDER				
	Target	Actual	Spec	Comply?
% Added Binder	3.60	3.84	N/A	
% Total Binder	5.05	5.24	4.75-5.35	Yes
% RAP	30.00	28.92%	≤100%	Yes
% RAS				
% Binder Replacement	28.75%	26.64%	≤ 30%	Yes
PG Grade	58-34H		52-40H	No
Binder replacement exceeded. Binder grade does not comply.				
Gb:	1.02780	Gsb:	2.629	Pbe (%): 4.80

Table 6-10 Aggregate Gradation for Rejuvenator “B” Control Mixtures

GRADATION (%Passing)						<input type="checkbox"/> Use DOT
Sieve	Specs	11-17CF1			Avg	District
1 in.	100	100.0			100.0	
3/4 in.	100	100.0			100.0	
1/2 in.	90-100(97)	97.0			97.0	
3/8 in.	83-97(90)	91.0			91.0	
* #4	64-78(71)	72.0			72.0	
* Dev	± 7.0	1.0			1.0	
*#8	38-48(43)	44.0			44.0	
*Dev	± 5.0	1.0			1.0	
#16		29.0			29.0	
*#30	15-23(19)	21.0			21.0	
* Dev	± 4.0	2.0			2.0	
#50		13.0			13.0	
#100		7.1			7.1	
*#200	2.4-6.4(4.4)	5.1			5.1	
*Dev	± 2.0	0.7			0.7	
Gradation Compliance?		Yes			Yes	
DBR	Sugg 0.6 - 1.4	0.94			0.94	
% +4 Type 4		88.1			88.1	
% +4 Type 3					0.0	
(+4/-4) Type 2		88.1/61.6			88.1/61.6	

Table 6-11 Target vs. Actual Design Parameters for Control Mixtures (November 17th, 2017)

BINDER					
	Target	Actual	Spec	Comply?	
% Added Binder	5.00	5.26	N/A		
% Total Binder	5.85	6.03	5.55-6.15	Yes	
% RAP	18.00	16.19%	≤100%	Yes	
% RAS					
% Binder Replacement	14.68%	12.77%	≤ 30%	Yes	
PG Grade	58-34H		58-34H	Yes	
Gb:	1.02738	Gsb:	2.632	Pbe (%):	5.44

Table 6-12 Aggregate Gradation for Rejuvenator “B” Mixtures

GRADATION (%Passing)						<input type="checkbox"/> Use DOT
Sieve	Specs	SR11-17CF1			Avg	District
1 in.	100	100.0			100.0	
3/4 in.	100	100.0			100.0	
1/2 in.	88-100(95)	96.0			96.0	
3/8 in.	78-92(85)	87.0			87.0	
* #4	54-68(61)	64.0			64.0	
* Dev	± 7.0	3.0			3.0	
*#8	31-41(36)	37.0			37.0	
*Dev	± 5.0	1.0			1.0	
#16		25.0			25.0	
*#30	12-20(16)	18.0			18.0	
* Dev	± 4.0	2.0			2.0	
#50		11.0			11.0	
#100		6.5			6.5	
*#200	2.3-6.3(4.3)	5.0			5.0	
*Dev	± 2.0	0.7			0.7	
Gradation Compliance?		Yes			Yes	
DBR	Sugg 0.6 - 1.4	1.04			1.04	
% +4 Type 4		87.8			87.8	
% +4 Type 3					0.0	
(+4/-4) Type 2		87.8/50.0			87.8/50.0	

Table 6-13 Target vs. Actual Design Parameters for Rejuvenator “B” Mixtures

BINDER				
	Target	Actual	Spec	Comply?
% Added Binder	3.60	3.88	N/A	
% Total Binder	5.05	5.29	4.75-5.35	Yes
% RAP	30.00	29.24%	≤100%	Yes
% RAS				
% Binder Replacement	28.75%	26.67%	≤ 30%	Yes
PG Grade	58-34H		52-40H	No
Binder replacement exceeded. Binder grade does not comply.				
Gb:	1.02780	Gsb:	2.629	Pbe (%): 4.81

Table 6-14 shows the field density measured from each test section. The density of Rejuvenator “B” mixture section was very low. Since Rejuvenator “B” mixture did not meet air void requirements, the contractor ended up with 5.4% pay penalty. However, Rejuvenator “B” control section constructed on November 17th met required air voids to achieve 0.8% pay bonus. Rejuvenator “D” trial section achieved a target density and received a full pay like control section built on November 15th.

Table 6-14 Density Results for Rejuvenator “D” and “B” field mixtures

Test Section	Rejuvenator “D” Control Mixtures	Rejuvenator “D” Rejuvenated Mixtures	Rejuvenator “B” Control Mixtures	Rejuvenator “B” Rejuvenated Mixtures
RAP (%)	18	30	18	30
Density (%)	93.6	93.7	92.95	93.48

6.2.1 HWT Test Results of Lab-compacted Field Mixtures

For HWT test, loose mixtures were collected from the field and compacted at the laboratory at 6±0.5% air void. It should be noted that the number of gyrations needed to compact samples was higher than normal (typically 150±20). HWT test results of samples from the control section and Rejuvenator “B” section are plotted in Figure 6-6 and Figure 6-7, respectively. The Rejuvenator “B” mixtures performed better than the control mixtures with stripping point of 14,433 compared to 11,400. As shown in Figure 6-8, the stripping was observed from the HWT specimens after the failure, which could be attributed to the quartzite aggregates with smooth surface.

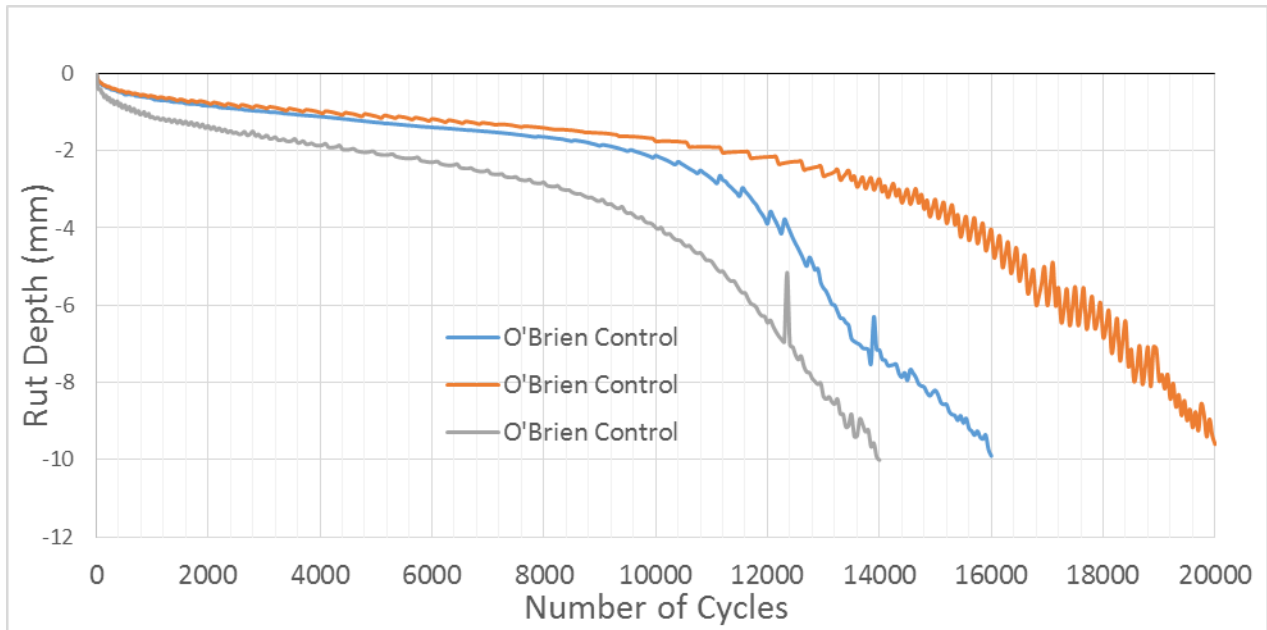


Figure 6-6 HWT Results for O'Brien Rejuvenator "B" Control Mixture

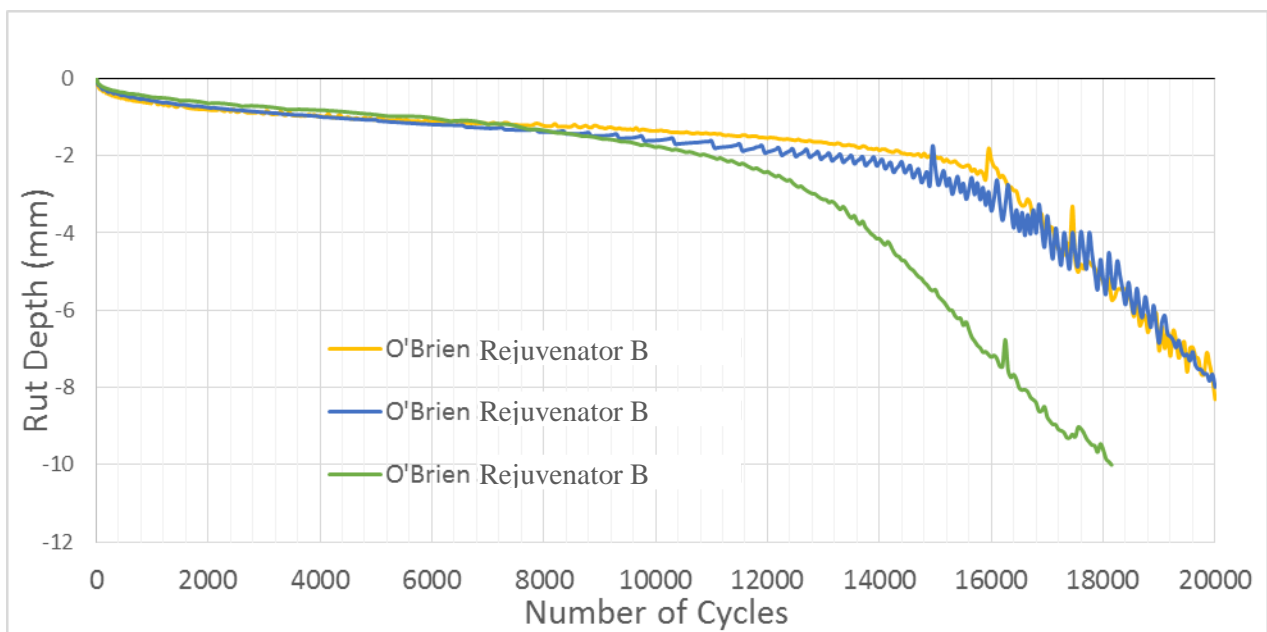


Figure 6-7 HWT Results for O'Brien Rejuvenator "B" Mixture



Figure 6-8 Stripping observed after HWT test

6.2.2 DCT Test Results of Cores

To evaluate the low-temperature cracking resistance, DCT test was performed on the cores of four different mixtures collected from the field test sections. DCT test was performed at the temperature which is 10 °C higher than the low-temperature limit of PG grade of virgin binder. DCT test results of Rejuvenator “D” and “B” mixtures are presented in Figure 6-9 and Figure 6-10, respectively. Rejuvenator “D” specimen exhibited both higher peak strength and higher residual strength whereas Rejuvenator “B” contributed lower peak strength but a higher residual strength. As shown in Figure 6-11, the cores collected from the field had variable thicknesses, slightly higher or lower than the standard dimension of 50 mm as a test specimen. It should be noted that some samples exhibited non-uniform thickness.

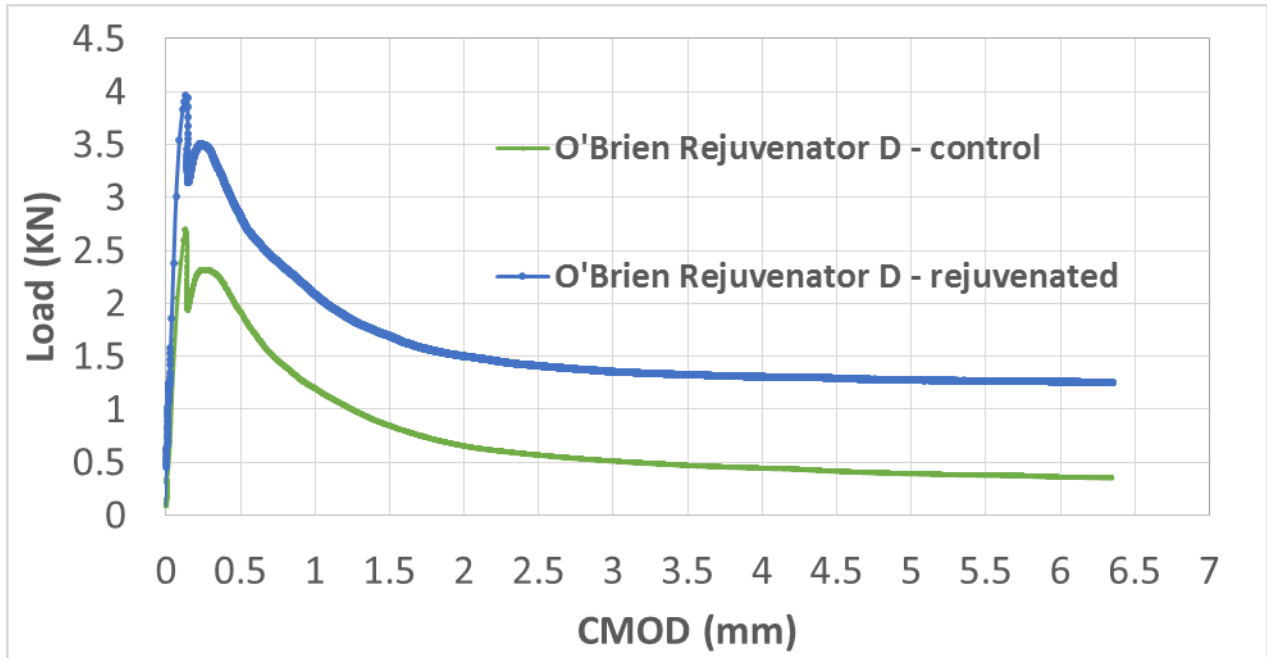


Figure 6-9 DCT Results for Rejuvenator “D” Mixtures

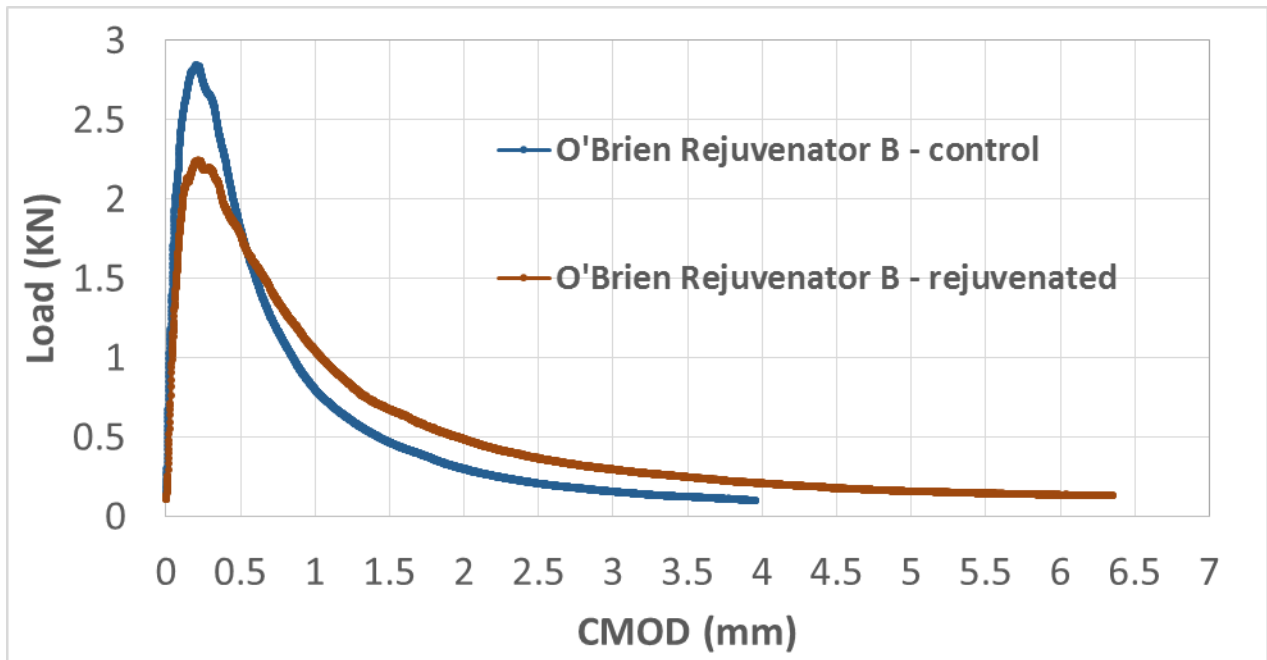


Figure 6-10 DCT Results for Rejuvenator “B” Mixtures



Figure 6-11 Difference in lab samples and field cores thicknesses

6.2.3 DCT Test Results of Lab-compacted Field Samples

To prepare DCT test specimens, loose mixtures were collected from the test section and brought to the laboratory for compaction. As shown in Figure 6-132, Rejuvenator “B” rejuvenated mixtures exhibited a lower peak strength but a higher residual strength resulting in a higher energy value which indicates a greater resistance to low temperature cracking compared to control mixtures. It should be noted that the control mixtures had 18% RAP whereas the rejuvenated mixtures had 30% RAP materials.

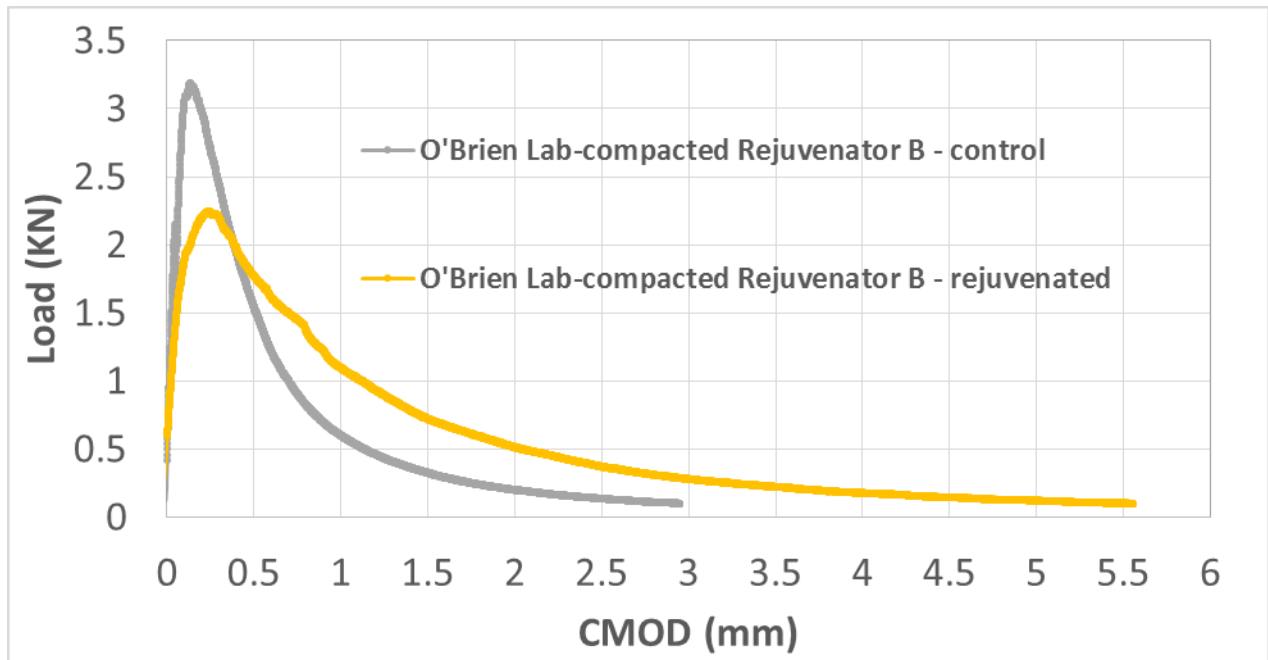


Figure 6-12 DCT Results for Rejuvenator “B” Lab-compacted Field Samples

As shown in Figure 6-13, both rejuvenators were effective in improving low temperature cracking performance of high RAP mixtures. It should be noted that the fracture energy values of Rejuvenator “B” control mixtures was different from those of rejuvenator “D” control mixtures because actual mix designs were different. Rejuvenator “B” control mixtures had higher air voids with different aggregate gradations than rejuvenator “D” control mixtures.

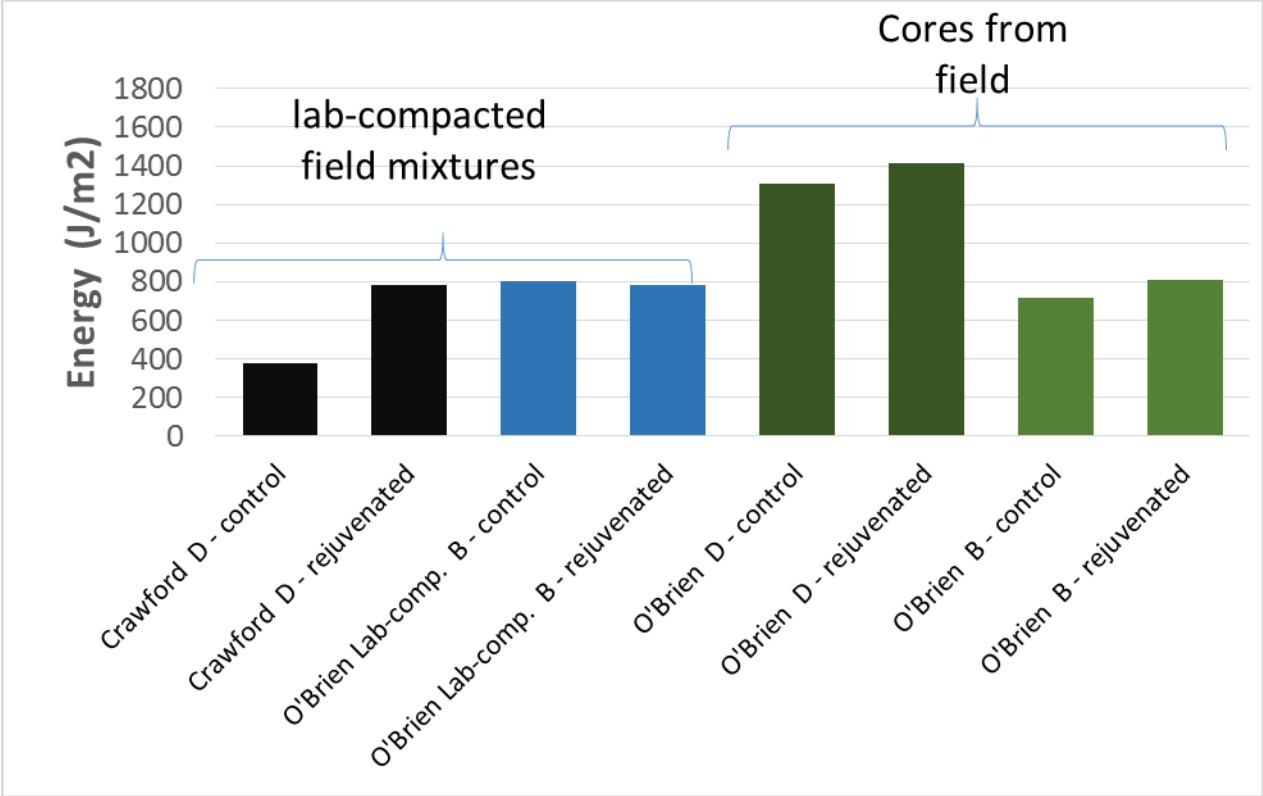


Figure 6-13 Energy Values for All Cores and Lab-compacted Samples

7 SUMMARY AND CONCLUSION

In this study, the following tasks have been performed: 1) evaluate the effectiveness of various rejuvenators to soften aged binders by employing analytical technologies to examine different rejuvenators in the laboratory-aged asphalt, 2) perform rheological binder tests to determine the effects of rejuvenators on aged binder properties, 3) perform mechanistic mixture tests such as Hamburg Wheel Tracking (HWT) and Disc-shaped Compact Test (DCT) to assess the effect of rejuvenators on high RAP mixtures, 4) build test sections with selected rejuvenators and 5) perform laboratory tests of loose mixtures and cores obtained from the field.

The effects of different rejuvenators were evaluated through applying each of them to aged asphalt binder and high-RAP mixtures. Four different rejuvenators of Rejuvenator “C”, Rejuvenator “B”, Rejuvenator “A” and Rejuvenator “D” were evaluated. The optimum dosage rate of each rejuvenator was identified using the Bending beam Rheometer (BBR) test for Rejuvenator “C”, Rejuvenator “B”, Rejuvenator “A”, Rejuvenator “D” at 6.2%, 6.9%, 16% and 3% by weight of aged binder. The m-value was more critical for all binder types than Stiffness values.

Fourier Transform Infrared (FTIR) test indicated all rejuvenators were effective in decreasing the aging level of hardened asphalt binder. Although neither spectrum peak shifting nor new peak was observed after adding rejuvenators to the aged asphalt binder, the Sulfoxide and Carbonyl indexes did not change linearly when the amount of rejuvenator was increased linearly. Therefore, it can be postulated that some chemical reaction might have occurred between rejuvenators and the aged asphalt binder.

Cryo-SEM technology was then utilized to measure cracking developed on the surfaces of both aged and rejuvenated asphalt binders when the temperature was lowered to -165 °C for 30 minutes. Significantly less cracking was observed from the surface of rejuvenated asphalt compared to that of aged asphalt cracking. The fracture index was developed as a measure to quantify the extent of cracking developed on the surface of the aged asphalt binders, which confirmed that rejuvenators improved a resistance to low-temperature cracking.

Based on DSR test, all rejuvenators lowered both PG high-temperature and low-temperature limits. G-R parameter was calculated to determine the effect of rejuvenators in lowering the stiffness of the aged asphalt binder. The aged binder showed the higher G-R value indicating a high level of aging whereas rejuvenated asphalt binders exhibited G-R values between the aged asphalt and virgin asphalt. Overall, all rejuvenators lowered the aging level at different extents but did not bring its properties to those of the original virgin binder. A significant correlation was observed between carbonyl indices and G-R values.

To evaluate the low-temperature cracking potential, DCT test was performed on the laboratory high-RAP mixtures with 27.6% and 70% of RAP materials by binder replacement. The DCT test was performed on mixtures with virgin asphalt, aged asphalt and rejuvenated asphalt

binders. DCT results confirmed that some rejuvenators at optimum dosage rates improved the low-temperature cracking characteristics of high-RAP without rejuvenators. Overall, based on the laboratory test results, it can also be concluded that Rejuvenator “B” and Rejuvenator “A” performed better than Rejuvenator “C” at their optimum dosage rates.

A test section using rejuvenator “D” was successfully constructed in Crawford County and another test section using both Rejuvenator “B” and “D” was constructed in O’Brien Country in Iowa. Loose field mixtures were compacted at the laboratory for both DCT and HWT tests. Based on the DCT test results, it was concluded that high-RAP mixtures with rejuvenators were more resistant to a low-temperature cracking. However, based on HWT test results, rejuvenators did not improve the moisture susceptibility and rutting potential with some samples exhibiting stripping conditions.

This study identified the analytical method to find the most appropriate rejuvenators for Iowa’s high RAP mixtures, which are resistant to both low temperature cracking and rutting while improving environment conditions and reducing the production cost. It is expected that the outcome of this research would help pavement engineers specify the most appropriate rejuvenator for the given condition by understanding complex chemical and physical interactions between aged binder and rejuvenators.

For the next phase, current research findings should be expanded to cover not only high binder replacement but also the aggregate replacement. For the next phase study, it is recommended and unanimously approved by the TAC to perform the following tasks:

1. Collect Recycled Asphalt Materials (RAM) from across the state to use for determining limits of multiple rejuvenators for a wide variety of mix designs.
2. Evaluate different equipment/methods for fractionating RAP materials and adding rejuvenators.
3. Apply FTIR for evaluating rejuvenators and DCT and HWT tests for RAM contents with various rejuvenators.
4. Build test sections using high RAM contents and fractionated RAP materials with various rejuvenators.
5. Monitor conditions of both existing and future test sections with high RAM contents and fractionated RAP materials.
6. Evaluate long-term oven aging of both laboratory and field rejuvenated high RAM mixtures.
7. Develop specifications for evaluating rejuvenators and high RAM contents and fractionated RAP materials.

8 REFERENCES

- ASTM 4887 (2016), Standard Practice for Preparation of Viscosity Blends for Hot Recycled Asphalt Materials.
- ASTM 4552 (2016), Standard Practice for Classifying Hot-Mix Recycling Agents.
- AASHTO, R30. (2002). Standard Practice for Mixture Conditioning of Hot Mix Asphalt.
- Ali, H., & Mohammadafzali, M. (2015). Long-Term Aging of Recycled Binders.
- Baek, C., Underwood, B., & Kim, Y. (2012). Effects of oxidative aging on asphalt mixture properties. *Transportation Research Record: Journal of the Transportation Research Board*, (2296), 77-85.
- Bell, C. A., Wieder, A. J., and Fellin, M. J. (1994). Laboratory Aging of Asphalt-Aggregate Mixtures:Field Validation. SHRP-A-390, Strategic Highway Research Program, National Research Council. Washington, D.C.
- Bloomquist, D., G. Diamond, M. Oden, B. Ruth and M. Tia (1993). Engineering and Environmental Aspects of Recycled Materials for Highway Construction. Final Report.
- Carpenter, S. H. and J. R. Wolosick (1980). "Modifier influence in the characterization of hot-mix recycled material." *Transportation research record*(777).
- City of Columbus (2006), Supplemental specification 1540: asphalt rejuvenating agent.
- Corbett, L. W. (1975). "Reaction variables in the air blowing of asphalt." *Industrial & Engineering Chemistry Process Design and Development* 14(2): 181-187.
- DeDene, C. D. (2011). "Investigation of using waste engine oil blended with reclaimed asphalt materials to improve pavement recyclability."
- Feng, Z., X. Chen and B. Zhou (2011). "A new approach for evaluating rejuvenator diffusing into aged bitumen." *Journal of Wuhan University of Technology-Mater. Sci. Ed.* 26(1): 43-46.
- García, Á., E. Schlangen, M. van de Ven and G. Sierra-Beltrán (2010). "Preparation of capsules containing rejuvenators for their use in asphalt concrete." *Journal of hazardous materials* 184(1): 603-611.
- Haghshenas, Hamzeh; Nabizadeh, Hesanaddin; Kim, Yong-Rak; and Santosh, Kommidi, "Research on High-RAP Asphalt Mixtures with Rejuvenators and WMA Additives" (2016).Nebraska Department of Transportation Research Reports.
- Hachiya, Y., Nomura, K., and Chen, J. (2003). Accelerated Aging Test for Asphalt Concretes. Zurich: 6th RILEM Symposium PTEBM.
- Hesp, S. A. and H. F. Shurvell (2010). "X-ray fluorescence detection of waste engine oil residue in asphalt and its effect on cracking in service." *International Journal of Pavement Engineering* 11(6): 541-553.
- Im, S., F. Zhou, R. Lee and T. Scullion (2014). "Impacts of rejuvenators on performance and engineering properties of asphalt mixtures containing recycled materials." *Construction and Building Materials* 53: 596-603.

- Karlsson, R. and U. Isacson (2003). "Application of FTIR-ATR to characterization of bitumen rejuvenator diffusion." *Journal of Materials in Civil Engineering* 15(2): 157-165.
- Mallick, R. B., K. A. O'Sullivan, M. Tao and R. Frank (2010). Why Not Use Rejuvenator for 100% RAP Recycling? Transportation research board 89th annual meeting.
- Mogawer, W., Booshehrian, A., Vahidi, S., & Austerman, A. (2013). Evaluating the effect of rejuvenators on the degree of blending and performance of high RAP, RAS, RAP/RAS mixtures (Tech.)
- Mollenhauer, K., and Mouillet, V. (2011). Re-road – End of Life Strategies of Asphalt Pavements. European Commission DG Research.
- NAPA (2017) Asphalt Pavement Industry Survey on Recycled Materials and Warm-Mix Asphalt Usage 2016, Information Series 138.
- Nicholls, C. (2006). Analysis of Available Data for Validation of Bitumen Tests. Forum of European National Highway Research Laboratories, ed. Cliff Nicholls, TRL. UK: Report on Phase 1 of the BiTVal Project, Forum of European National Highway Research Laboratories.
- NCAT (2014). "NCAT Researchers Explore Multiple Uses of Rejuvenators." National Center for Asphalt Technology, Auburn, AL
- Oliver, J. W. (1974). "Diffusion of oils in asphalts." *Industrial & Engineering Chemistry Product Research and Development* 13(1): 65-70.
- Partl, M. N., Bahia, H. U., Canestrari, F., De la Roche, C., Di Benedetto, H., Piber, H., and Sybilski, D. (2013). Advances in Interlaboratory Testing and Evaluation of Bituminous Materials. RILEM. RILEM.
- Petersen, J. C. (1984). "Chemical composition of asphalt as related to asphalt durability: state of the art." *Transportation research record*(999).
- Ramasamy, N. B. (2010). Effect of polyphosphoric acid on aging characteristics of PG 64-22 asphalt binder. University of North Texas.
- Reed, J. (2010). Evaluation of the Effects of Aging on Asphalt Rubber Pavements. Masters Thesis, PhD Dissertation., Arizona State University.
- Roque, R., B. Birgisson, C. Drakos and B. Dietrich (2004). "Development and field evaluation of energy-based criteria for top-down cracking performance of hot mix asphalt (with discussion)." *Journal of the Association of Asphalt Paving Technologists* 73.
- Shen, J., S. Amirkhani and B. Tang (2007). "Effects of rejuvenator on performance-based properties of rejuvenated asphalt binder and mixtures." *Construction and Building Materials* 21(5): 958-964.
- Shirodkar, P., Y. Mehta, A. Nolan, K. Sonpal, A. Norton, C. Tomlinson, E. Dubois, P. Sullivan and R. Sauber (2011). "A study to determine the degree of partial blending of reclaimed asphalt pavement (RAP) binder for high RAP hot mix asphalt." *Construction and Building Materials* 25(1): 150-155.
- Smith, Brian C. (2011) *Fundamentals of Fourier Transform Infrared Spectroscopy*, Second Edition, CRC Press, Taylor & Francis Group, Boca Raton, Florida.

- TRAP, N., R. C. West, B. Powell and A. N. Kvasnak (2009). "Evaluation of AASHTO rut test procedure using the asphalt pavement analyzer." *Journal of the Association of Asphalt Paving Technologists* 78.
- Tran, N., A. Taylor and R. Willis (2012). "Effect of rejuvenator on performance properties of HMA mixtures with high RAP and RAS contents." Auburn, AL: National Center for Asphalt Technology.
- Turner, P., Taylor, A., & Tran, P. N. (2015). Laboratory evaluation of REJUVENATOR "B"™ RP 1000 rejuvenator.
- Van den Bergh, W. (2009). The Development of an Artificially Aged Asphalt Mixture (in Dutch): Artificial Aged Asphalt mixture. Gent, Belgium: In: Belgian Road Congress.
- Wilson, A., G. Fuchs, C. ScRAPoncin, D. Martin and J. Planche (2000). "Localization of the polymer phase in bitumen/polymer blends by field emission cryo-scanning electron microscopy." *Energy & fuels* 14(3): 575-584.
- Yu, X., M. Zaumanis, S. dos Santos and L. D. Poulikakos (2014). "Rheological, microscopic, and chemical characterization of the rejuvenating effect on asphalt binders." *Fuel* 135: 162-171.
- Zaumanis, M., R. B. Mallick and R. Frank (2014). "100% Recycled hot mix asphalt: a review and analysis." *Resources, Conservation and Recycling*.
- Zaumanis, M., R. B. Mallick and R. Frank (2014). "Determining optimum rejuvenator dose for asphalt recycling based on Superpave performance grade specifications." *Construction and Building Materials* 69: 159-166.
- Zaumanis, M., R. B. Mallick, L. Poulikakos and R. Frank (2014). "Influence of six rejuvenators on the performance properties of Reclaimed Asphalt Pavement (RAP) binder and 100% recycled asphalt mixtures." *Construction and Building Materials* 71: 538-550.
- Zhu, C. (2015). Evaluation of Thermal Oxidative Aging Effect on the Rheological Performance of Modified Asphalt Binders (Doctoral dissertation, University of Nevada, Reno).

APPENDIX A: DCT RESULTS FOR LAB-PRODUCED SAMPLES

Figure A-1: DCT Results for 27.6% RAP Mixtures

Mixture Type	Fracture Energy (J/m ²)	avg. Energy (J/m ²)
Virgin	377	387.7
	372	
	414	
Control	336	339.7
	321	
	362	
Rejuvenator A	437	400.5
	357	
	457	
	351	
Rejuvenator B	329	397.0
	436	
	455	
	368	
Rejuvenator C	265	265.0

Figure A-2: DCT Results for 70% RAP Mixtures

Mixture Type	Fracture Energy (J/m ²)	avg. Energy (J/m ²)
Virgin	261	259.5
	258	
Control	272	257.0
	242	
Rejuvenator A	284	280.5
	277	
Rejuvenator B	295	289.0
	283	
Rejuvenator C	245	240.0
	235	